# IDENTIFICATION AND CHARACTERIZATION OF NOVEL REGULATORS OF ADIPOGENESIS

By

Schantel A. Hayes

A DISSERTATION

Submitted to
Michigan State University
In partial fulfillment of the requirements
For the degree of

DOCTOR OF PHILOSOPHY

Pathology

2011

ABSTRACT

IDENTIFCATION AND CHARACTERIZATION OF NOVEL REGULATORS OF ADIPOGENESIS

By

Schantel A. Hayes

Adipocytes are highly specialized cells that are central to the control of energy balance and lipid homeostasis. Obesity, the excess accumulation of adipose tissue, is a risk factor for type 2 diabetes, cardiovascular disease, hypertension and cancer. With global rates of obesity on the rise, it is important to study adipocyte biology and function to gain insight to the molecular basis of these metabolic diseases. There have been many significant advances in the study of adipocyte biology with the discovery of transcription factors, coactivators and growth factors that are involved in adipocyte differentiation. PPARγ is considered to be the master regulator of the terminal differentiation phase of adipogenesis and functions in concert with members of the CCAT/enhancer binding protein (C/EBP) family and Kruppel like factor family in a transcriptional cascade. Although much is known about the molecular mechanisms regulating the late phase of adipocyte differentiation, little is known about the transcriptional regulation of the early phase (determination) of adipogenesis as well as intracellular signaling pathways that are involved in this regulatory process. In our studies, we demonstrated that ZNF638, a transcription factor involved in the early phase of adipogenesis, is essential for adipocyte differentiation in vivo. In this study, we generated mice with adipose specific knockdown of ZNF638 (Fat-ZNF638-KD) by cre-lox interference. Fat-ZNF638-KD mice were smaller, weighed less and had a significant reduction of adipose tissue in all depots. Furthermore, mice were resistant to diet induced obesity that was potentiated by a higher metabolic rate and greater lean mass when compared to controls. mRNA expression levels of key adipogenic genes were reduced in the visceral depot of Fat-ZNF638-KD mice. We also demonstrated that nuclear matrix coactivator 1

(NMC1), a novel isoform of ZNF638, interacts with Smad4-interacting factor 1 (SMIF). SMIF, an activator of TGFβ signaling, was found to be highly regulated during adipocyte differentiation and to physically interact and repress the transcriptional activity of PPARγ. Lastly, we demonstrated that fat specific ablation of Serum Glucocorticoid Inducible Kinase 1 (SGK1), an AKC kinase involved in the early phase of adipocyte differentiation, results in sexual dimorphism. Our study showed that female mice have an increased fat mass, a decrease lean mass, increased visceral and inguinal adiposity and a trend for insulin resistance. Male mice were indistinguishable from their wild type littermate controls. These data show that our laboratory has identified and confirmed in vitro two novel regulators. We have also identified one potential regulator of adipocyte differentiation.

# ACKNOWLEDGEMENTS

I would like to first thank God who is my refuge and strength, an ever-present help in trouble (Psalm 46:1). Through His boundless grace, He continuously shows me that I can do all things through Him that strengthens me (Philipians 4:13). I would like to first acknowledge that my dissertation research funding was provided through the Intramural Research Programs of the National Institutes of Diabetes and Digestive and Kidney Diseases and the Center for Cancer Research, National Cancer Institute, Bethesda, MD. I was supported on an Intramural Research Training Award as a Molecular Pathology Fellow in the Comparative Biomedical Scientist Training Program, a component of the National Institutes of Health Graduate Partnership Program, in partnership with Michigan State University. I would like to thank everyone who has had a part in the development of this dissertation work including Matti Kiupel, my committee chair at Michigan State University, my principal investigator, Elisabetta Mueller from the Genetics of Development and Disease Branch at the National Institute of Diabetes, Digestive and Kidney Diseases, my committee members Mark R. Simpson from the Comparative Molecular Pathology Unit at the National Cancer Institute, Ingeborg Langohr and James Wagner at Michigan State University. A special thanks to my fellow laboratory members at the National Institute of Diabetes, Digestive and Kidney Diseases who were instrumental in my introduction to laboratory bench work and my education in molecular biology. I would like to thank my family and friends for their support and I would eminently like to express my gratitude to my parents, Mr. & Mrs. Hayes, my sister, Sonya Hayes and my fiancé Tariiq Walton for their unwavering support and confidence in my success.

TABLE OF CONTENTS

LIST OF TABLES

LIST OF FIGURES

# INTRODUCTION

**Abstract:** Mesenchymal stem cell differentiation is governed by tightly controlled gene expression and transcriptional events driven by a sequence of transcription factors that lead to the development of muscle, bone, cartilage, and adipose tissue. Zinc finger (ZF) transcription factors have been shown to be fundamental transcriptional regulators of the development and differentiation of bone, muscle, central nervous system and crucial in regulating adipocyte development. The nuclear receptor peroxisome proliferator-activated receptor γ (PPARγ) was the first ZF transcription factor shown to be a central regulator of adipocyte differentiation by controlling a transcriptional cascade that includes the CCAT/enhancer binding protein alpha (C/EBPα), a member of a family of basic leucine zipper transcription factors. Recently, a growing number of ZF containing molecules have been shown to be involved in various stages of adipocyte differentiation. Here we review the ZF transcription factors that have been shown to play a role as regulators of adipose tissue development.

## I. Adipose Tissue

Obesity can be defined as a prolonged imbalance between the levels of energy intake and expenditure where the excess is stored as body lipids. Over the last three decades, obesity has become a global pandemic with the highest incidence primarily within industrialized nations and the prevalence in underdeveloped countries on the rise (Dixon J 2010). Almost 30% of the United States adult population is considered obese with a body max index (BMI) of 30 or greater (Dixon J 2010). The determinants of obesity are poorly defined and appear to be multifactorial. Current trends in overweight/obesity have been described to be largely attributable to

environmental influences that promote excessive food intake and decreased physical activity however other factors such as genetics and socioeconomic status have been implicated (French S) (Bell C). Excess weight is associated with an increased incidence of chronic diseases such as cardiovascular disease, type 2 diabetes mellitus, hypertension, stroke, dyslipidemia, osteoarthritis and cancer (Calle E) (Must A).

With the surge of obesity and associated co-morbidities, the adipocyte has garnered much attention with pivotal discoveries in the mid to late 1990s. The discovery of leptin and subsequent revelations of other adipocyte derived proteins (adipokines) critical for regulating metabolism in health and disease and the characterization of the transcriptional regulator of adipocyte differentiation, PPARγ, in 1994, led to a better understanding of adipocyte physiology (Galic S 2010 and Tontonoz 1994).

**White and Brown Adipose Tissues**

In mammals there are two types of fat depots: white and brown. Adipocytes in white adipose tissue (WAT) are the primary site of triglyceride storage and those in brown adipose tissue (BAT), regulate energy expenditure. In rodents, BAT is first identifiable as early as embryonic day 14.5, mostly concentrated in the intrascapular region and it remains abundant throughout the neonatal period when non-shivering thermogenesis is needed. With aging, the intrascapular BAT depot gradually involutes. Brown adipocytes can also be found in other areas, including near the hilus of the kidney, in the periaortal region, in the mediastinun and intermixed with white adipocytes. Morphologically, BAT can be distinguished from WAT by small intracytoplasmic lipid droplets, centralized hyperchromatic nuclei, rich vascularization and abundant mitochondrial density. WAT appears at the latest stages of embryonic development with

maturation occurring postnatally, when energy storage is most needed. WAT is dispersed throughout the body with two principle depots: subcutaneous and several visceral depots located within the thorax (mediastinal) and abdomen (omental, mesenteric, perirenal, epididymal, parametrial) (Cinti S 2009). In mature white adipocytes, the cytoplasm is primarily occupied by lipid with only a thin rim of visible cytoplasm and eccentrically placed nuclei.

Many genes are differentially expressed in mature brown and white adipocytes. With the exception of uncoupling protein-1 (UCP-1) and cell death-inducing DFF45-like effector A (Cidea), most differentially expressed genes show only relative differences between the two adipose cell types. UCP-1 is a membranous mitochondrial carrier protein that is expressed exclusively in the brown adipose tissue and is generally accepted to be the defining marker of brown fat (Klaus S 1991). UCP-1 functions by uncoupling electron transport from ATP production, allowing energy to be dissipated as heat (Klaus S 1991) (Cannon B 2004). Cidea is highly expressed in BAT where it interacts with and inhibits UCP-1 activity (Zhou Z 2003). Other genes are selectively expressed in the brown fat and therefore not limited to adipose tissue. The nuclear coactivator peroxisome proliferator-activated receptor gamma coactivator alpha (PGC1-α), originally cloned from BAT cells as a cold inducible coactivator of PPARγ, is responsible for regulating mitochondrial biogenesis and thermogenesis in most cell types including brown fat cells and skeletal muscle. PRD1-BF-1-RIZ2 homologous domain containing protein-16 (PRDM16), first identified at a chromosomal breakpoint in myeloid leukemia, was recently found to activate a broad program of brown fat differentiation when expressed in white preadipocytes or in white fat depots *in vivo* (Seale P). Cold-inducible glycoprotein of 30KDa (Cig30) a transmembrane glycoprotein expressed only in the BAT and liver, is involved in pathways responsible for brown fat hyperplasia after cold exposure (Tvrdik P). Peroxisome

proliferator-activated receptor alpha (PPARα), a ligand activated transcription factor that is most expressed in tissues with high rates of fatty acid oxidation and perioxisomal metabolism, mediates gene upregulation of UCP1 and coordinates activation of lipid oxidation and thermogenic activity in BAT (Barbera M). All of these genes are preferentially expressed in BAT whereas, leptin an adipokine involved in satiety, thermogenesis and fatty acid oxidation, is produced primarily by white adipocytes (Ahima R 2006). Nuclear corepressor, RIP140, and matrix protein fibrillin-1 are also more highly expressed in WAT than BAT (Gesta S 2007).

**White and Brown Fat Differentiation**

Adipose tissue, similar to bone and muscle tissue, is generally considered to develop from a pluripotent mesenchymal/mesodermal stem cell but the precise mesenchymal stem cell lineages that produce white and brown adipocytes are not well known. It has been recently shown that brown adipocytes are developmentally closer to skeletal muscle than to white adipose cells. Notably, genetic mapping experiments indicate that brown adipocytes in the intrascapular region and skeletal muscle arise from cells that express Myc5, a gene that was previously assumed to be almost exclusively expressed in committed skeletal muscle precursors (Seale P). Similarly, global gene expression analyses show that brown but not white adipocyte precursors endogenously share a common early transcriptional program with skeletal muscle, which is then suppressed early during differentiation (Timmons J). Nevertheless, WAT and BAT share many common features including a conserved proliferator-activated receptor gamma (PPARγ) driven transcriptional program. Mice with adipose-specific deletion of PPARγ display marked reduction in both WAT and BAT (He W 2003). Indeed PPARγ is necessary for BAT and WAT development but this factor alone is not sufficient to drive mesenchymal cells into adipose tissue.

PGC-1α is expressed early in brown adipogenesis and ectopic expression is sufficient to promote several aspects of BAT differentiation including the induction of UCP1 gene expression. PGC1-α is also rapidly and highly induced by cold exposure and turns on several key components of the adaptive thermogenic program in brown fat including fatty acid oxidation and mitochondrial biogenesis through coactivation of transcription factors such as PPARs and nuclear respiratory factor 1, NRF1 (Uldry M 2006). Mice deficient in PGC-1α are cold sensitive with low expression of UCP-1 and have morphologically abnormal BAT (Lin J 2004). Interestingly, although loss of PGC-1α in brown fat cells in culture leads to reduced induction of thermogenic genes, PGC1-/- brown fat preadipocytes differentiate normally, suggesting that PGC1α is important for the thermogenic function of brown fat but is dispensable for the differentiation of brown fat cells (Uldry M 2006). Recently, PRDM16 was found to be the master regulator of brown adipocyte formation and essential to induce expression of genes associated with mitochondrial biogenesis and oxidative phosphorylation. Forced expression of PRDM16 in white adipocyte cells line or WAT *in vivo* activates a brown fat phenotype and the induction of PGC1-α, UCP1 and type 2 deiodinase expression (Seale P 2007). Depletion of PRDM16 in primary brown fat precursors ablates these brown adipocyte characteristics (Seale P 2007). PRDM16 functions through its interactions with either PGC-1α/β or C-terminal binding proteins (CtBPs), to activate brown genes or to suppress white gene expression respectively (Kajimura S 2008). Consequently, PRDM16 was found to interact with a variety of DNA binding transcription factors such as PPARγ, PPARα and members of the CCAT/enhancer binding protein family (C/EBPs) (Kajimura S 2008).

A number of transcription factors have been shown to govern the differentiation of the more extensively studied white adipocyte. These include PPARγ and members of the CCAT/enhancer

binding protein family such as C/EBPα, C/EBPβ and C/EBPδ. The transcriptional control of white adipocyte differentiation will be discussed in detail later in the text.

**Plasticity of Adipose Tissue**

Although plasticity of WAT and BAT has been reported, it remains a controversial issue. In rodents and humans, BAT depots are replaced by WAT during aging (Gesta S 2007). In conditions of a positive energy balance such as those observed during a high fat diet, brown adipocytes in obese animals gradually change to cells similar in morphology to white adipocytes including the transformation of the lipid depot from multilocular to unilocular (Cinti S 2009). Conversely, brown adipocytes are observed in classical white adipose depots after cold acclimatization or after the administration of hormonal and/or pharmacological treatments such as $\beta_3$ adrenoceptor agonist, retinoic acid and thiazolidinediones (Cinti S 2009) (Gesta S 2007) (Barbatelli G 2010).

Several theories have been postulated to explain the phenomena of white adipose tissue converting into brown. It has been suggested that the brown fat observed where white cells are normally present could be due to either newly formed brown adipocytes derived from existing stem cells resident in the tissue, from migrating stem cells, from the trandifferentiation of white adipocytes or from the combination of these phenomena (Cinti S 2009) (Gesta S 2007). Many researchers support the former theory suggesting that conversion of white into brown is due to recruitment and differentiation of mesechymal progenitor cells or brown adipocytes within the white adipose tissue (Gesta S 2007). Indeed, the stromovascular fraction of white adipose tissue is a heterogeneous population that contains pluripotent cells capable of differentiation into multiple lineages, including cells of mesodermal origin (adipocytes, osteoblasts, chondrocytes,

myocytes) and endothelial cells (Planat-Benard V 2004) (Fraser J 2006). A growing body of evidence suggests that, if needed, brown adipose tissue can increase at the expense of white through trandifferentiation. It was recently shown that after cold acclimatization and $\beta_3$ adrenoceptor agonist treatment, new adipocytes morphologically similar to brown adipocytes which are UCP1 positive are formed in the absence of cell proliferation (Barbatelli G 2010).

**WAT Differentiation**

A large number of studies on the transcriptional regulation of white adipocyte differentiation have been performed *in vitro* by using preadipocyte cell lines (3T3-L1 and 3T3-F442A cells) or cultured preadipocytes isolated from the stromal-vascular fraction of dissociated fat pads. The most extensively characterized are 3T3-L1 and 3T3-F442A cell lines, which were isolated from non-clonal Swiss 3T3 cells derived from disaggregated 17 to 19 day mouse embryos. These cells are already committed to the adipocytic lineage (Rosen E 2000). When treated with a pro-differentiation cocktail containing fetal bovine serum (FBS), dexamethasone, isobutlmethylxanthine and insulin, these cells undergo differentiation into mature adipocytes over a 4-6 day period (Rosen E 2000) (Farmer 2006). C3H 10T1/2 cells, derived from 14 to 17 day old mouse embryos, display fibroblastic morphology in cell culture and are functionally similar to mesenchymal stem cells. Inhibiting methylation with 5-azacytidine in C3H10T ½ cells produces cells that exhibit stable morphological and biochemical features of muscle, adipose, bone, or cartilage cells (Reznikoff K 1973) (Penny D 1989). Less commonly used, Ob17 cells were generated from adipose precursors present in the epididymal fat pads of genetically obese (*ob/ob)* adult mice (Gregoire F 1998). In addition to these models, embryonic

stem cells (ES) cells have been shown to differentiate into mature adipocytes in vitro (Gregoire F 1998).

Despite the many insights gleaned from data obtained *in vitro*, it is important to keep in mind the inherent difference with *in vivo* adipocyte differentiation. Preadipocyte cell lines differentiate almost exclusively into white adipocytes so they are not a valid model of brown adipose tissue differentiation. Moreover, these cells grow in monolayers on plastic dishes and therefore exist out of their natural context of extracellular matrix and supporting structures. With the aforementioned caveats, the recent production of animal models with altered expression of key transcription factors for fat cell development has provided essential support for current *in vitro* models of adipogenesis. Of these, transgenic mice established that express cre recombinase under the control the adipose-specific fatty acid binding protein 4 (FABP4)/aP2 enhancer/promoter have been the most insightful. Since its discovery, the aP2 promoter has been used by hundreds of laboratories to construct transgenes that have largely fat specific-expression.

Concertedly, *in vitro* and *in vivo* data has shown that white adipocyte differentiation occurs in two phases: the early, or determination, phase which involves the commitment of pluripotent mesenchymal stem cells to the adipocyte lineage and the late, or terminal differentiation, phase, which involves the maturation of pre-adipocytes into fully differentiated adipocytes, performing functions necessary for lipid metabolism and transport, insulin sensitivity and the secretion of adipocyte specific proteins such as adipokines (Rosen and MacDougald 2006). Countless transcription factors have been shown to control the differentiation of white adipocytes in both early and late phases of the adipogenic process, including members of the zinc finger transcription factor family such as PPARγ, Kruppel Like Factors (KLFs), GATA 2 and GATA 3.

We will discuss below our current knowledge of how zinc finger transcription factors contribute to white adipose tissue differentiation.

## II. Zinc Finger Transcription Factors in Adipogenesis

### Zinc Finger Transcription Factors

Zinc finger proteins form one of the most prevalent structural families in eukaryotes, comprising approximately 2% of the proteins encoded by the human genome (Matthews JM and Sunde M, 2002). The zinc finger domain that characterizes these factors was first identified in the protein transcription factor IIIA from *Xenopus laevis* oocytes (Miller J et al. 1985). The term "zinc finger" applies to a rather diverse set of protein motifs that have in common the property of binding zinc ions in order to stabilize the structure of a small, autonomously folded protein domain (Klug A and Schwabe J 1995). Distinct classes or motifs of zinc fingers differ largely by function, as well as the identity and spacing of their zinc-binding residues. There are currently at least 14 different well-characterized motifs (Matthews JM and Sunde M, 2002). These classes have a variety of different roles within the cell, but they share the common feature of being able to mediate the interaction of proteins with DNA, RNA, other proteins or lipids. Many proteins contain multiple zinc fingers, often belonging to different classes, as well as a variety of other protein domains (Matthews JM and Sunde M, 2002). Some of the better-characterized motifs based on their structural and functional characteristics include the classical $C_2H_2$- ZnF motif, the GATA-type ZnF motif, the LIM-type ZnF motif and the zinc ribbon type ZnF motif.

The $C_2H_2$ or "classical" zinc finger is the most common type of zinc finger present in ZF proteins and contains the consensus sequence (F/Y)-X-C-$X_{2-5}$-C-$X_3$(F/Y)-$X_5$-Ψ-$X_2$-H-$X_{3-4}$-H, were X is any amino acid and Ψ is the hydrophobic residue (Brayer K and Segal D 2008). The

$C_2H_2$ motifs were initially identified in the DNA-binding domains of transcription factors however they are now recognized to bind bind RNA and protein in addition to DNA (Brayer K and Segal D 2008).

The GATA type zinc fingers are specifically found in the DNA binding domain of GATA transcription factors and comprised of one or two zinc binding modules containing four cysteines embedded in the sequence Cys-$X_2$-Cys-$X_{17/18}$-Cys-$X_2$-Cys and an adjacent basic region (Gronenborn A). This motif is involved in binding the specific (A/T)GATA(A/G) DNA sequence . The GATA type motif can also function in protein-protein interactions.

The LIM-type zinc finger is composed of two sequential zinc-binding motifs (CCHC/CCCZ) and is found in many proteins such as homeodomain transcription factors, kinases and adapters. The LIM-type zinc finger motif acts primarily to mediate protein-protein interaction and as scaffold in the formation of transcriptional complexes (Matthews et al 2009).

The zinc ribbon type zinc finger motif is composed of three-stranded antiparallel β sheets and two zinc knuckles (Cys-X4-Cys and Cys-X2-Cys) (Filhol O et al and Krishna S et al 2003). This motif has been sub-classified into families due to significant sequence and structural variability: classical, adenovirus DNA-binding protein, B-box, Rubredoxin and Rubredoxin-like domains. The classical zinc ribbon family includes domains from proteins involved in translation/transcription machinery such as the transcription elongation factor SII, the transcription initiation factor TFIIB.

## Zinc fingers TF contributing to early phases of adipocyte differentiation

### Zfp423

Zfp423 is a ZF TF containing 30 $C_2H_2$ type zinc fingers initially shown to be implicated in the development of the cerebellum, olfactory neuronal cells and pre-B lymphocytes in the rat as a transcriptional partner of Olf-1/EBF (Tsai R et al 1997, Cheng L et al 2007). It has recently been shown to be a regulator of preadipocyte commitment (Gupta R et al 2010). Gain of function experiments in NIH 3T3 fibroblasts show that Zfp423 can activates PPARγ expression in undifferentiated cells and potentiates adipocyte differentiation, while its ShRNA-mediated knockdown in 3T3-L1 cells greatly reduces adipocyte differentiation and PPARγ1 and PPARγ2 expression. Zfp423-/- MEF cells show fewer lipid-laden adipocytes when compared to differentiated cultures from wild type controls and Zfp423 -/- mouse embryos have impaired white adipocyte differentiation in the subcutaneous tissue (Gupta R et al 2010).

Zfp423 also contains a BMP signaling module formed by two clusters of fingers that bind to SMAD1 in response to BMP2 (Hata A et al 2000).

### ZNF638

ZNF638 is a ZF transcription factor that contains two $C_2H_2$ type zinc fingers motifs and a splicing motif (RS motif), three RNA binding domains (RRM) (Matsushima, Ohshima et al. 1996) (Warder and Keherly 2003). ZNF638 was initially cloned in 1996 and subsequently shown to be expressed during mouse brain development (Inagaki H et al 1996,Gray, Fu et al. 2004), but no clear function had been associated with this TF. Our laboratory has recently identified ZNF638 as a critical regulator of adipocyte differentiation. The expression of ZNF638

occurs prior to the expression of PPARγ and concomitant with the expression of early regulators, C/EBPβ and C/EBPδ. ZNF638 physically interacts with C/EBPβ and C/EBPδ and transcriptionally activates PPARγ (Meruvu et al. unpulished data). When ZNF638 is ectopically expressed in uncommitted mesenchymal cells it promotes adipogenesis with increased expression of adipocyte specific genes such as PPARγ and aP2 while its knockdown inhibits adipocyte differentiation and decreases the expression of adipocyte specific genes (Meruvu et al. unpulished data). Adipose-specific knockdown of ZNF638 using cre-loxP induced RNA interference in vivo results in marked reduction of subcutaneous, visceral and peri-gondal adipocyte depots. Mice weighed significantly less than wild type controls and are resistant to diet induced obesity. Adipocyte size is reduced in all three depots and the number of multilocular adipocytes is increased in the visceral depot. mRNA expression levels of key adipocyte genes involved in differentiation, (PPARγ and C/EBPα), lipid storage and metabolism (adiponectin, leptin, perilipin) are down regulated in the visceral depot (Hayes et al unpublished data).

**Kruppel Like Factors (KLFs)**

To date seventeen KLFs have been identified in the human genome. The defining feature of KLFs is a highly conserved DNA binding domain at the carboxyl or C terminus that contains three classical zinc fingers (Bieker J 2001). The zinc fingers enable KLFs to bind to similar DNA sequences which consist of CACCC or related GC-rich elements (Bieker J 2001 and Pearson et al 2008). Outside of the zinc fingers, domains amongst family members are highly variable and are involved in gene activation, repression or both as well as in protein-protein interactions (Bieker J 2001). The KLFs regulate many biological processes, including proliferation, apoptosis, differentiation and development (Person R et al. 2008 and Haldar SM et al 2007).

Eight members of mammalian KLFs have been identified as key components of the transcriptional network integral for adipocyte differentiation.

**KLF15** was the first KLF described to be involved in adipocyte differentiation. KLF 15 is markedly up-regulated during the differentiation of 3T3-L1 preadipocytes into adipocytes and acts synergistically with C/EBPα to increase the activity of the PPAR$\gamma_2$ promoter (Mori T et al 2005). KLF15 also induces the expression of glucose transporter 4 (GLUT4), the main effecter of insulin-stimulated glucose transport (Gray S et al 2002).

**KLF5** is induced in the early stages of adipocyte differentiation by C/EBPβ and C/EBPδ and act in concert with the CEBPs to activate the PPAR$\gamma_2$ promoter (Oishi Y 2005). Neonatal heterozygous knockout mice exhibit a marked deficiency in white adipose tissue development. KLF5 +/- weighed significantly less than the wild type mice and intrascapular and dorsal white adipose tissue contained numerous small cells that had little to no lipid however, by 4 weeks knockout mice weighed similar to and had comparable adipocyte morphology to the wild type mouse (Oishi Y et al 2005).

**KLF6** promotes adipocyte differentiation in 3T3-L1 cells by transcriptionally repressing Delta-like 1/preadipocyte factor-1 (DLK1/PREF-1), a gene encoding an epidermal growth factor-like homeotic transmembrane protein that inhibits adipocyte differentiation. Repression of DLK1 requires HDAC3 deacetylase activity, which is recruited to the endogenous DKL1 promoter where it interacts with KLF6. Silencing of KLF6 in 3T3-L1 cells reduces adipocyte differentiation however, forced expression is not sufficient to promote adipocyte differentiation (Li D 2005).

**KLF4** is specifically activated early in 3T3-L1 differentiation by IBMX, one of the components of the standard adipogenic induction cocktail and an inducer of cAMP. KLF4

knockdown cell lines show a marked decrease in adipogenesis and reduced expression of adipocyte markers including C/EBPβ suggesting that KLF4 is an upstream transcriptional regulator of C/EBPβ. KLF4 binds to the C/EBPβ promoter and together with Krox20 cooperatively transactivates the C/EBPβ promoter. C/EBPβ knockdown increases levels of KLF4 suggesting that C/EBPβ normally suppresses KLF4 expression via a tightly controlled negative feedback loop (Birsoy K et al 2008).

**KLF9** is the most recent KLF found to promote adipogenesis (Pei H et al 2010). KLF9 is upregulated at day 4 of 3T3-L1 cells differentiation. Overexpression of KLF9 in 3T3-L1 cells does not upregulate the expression of C/EBPα or PPARγ. However, knockdown by siRNA suppresses adipocyte differentiation and inhibits mRNA expression levels of late adipogenic genes PPARγ, C/EBPα, and aP2. KLF9 binds to the proximal promoter of PPARγ2 and acts in concert with C/EBPα to tranactivate the PPARγ2 promoter.

Interestingly, although the majority of the KLFs so far implicated in adipogenesis are positive regulators of adipogenesis, KLF 2, KLF7 and KLF3 perform an inhibitory function.

**KLF2** is expressed in preadipocytes and expression is markedly reduced in mature adipocytes. Overexpression in 3T3-L1 cells markedly inhibits lipid accumulation and potently inhibits PPARγ. Upstream regulators of adipogenesis, C/EBPβ and C/EBPδ were unaffected however, C/EBPα and SREBP1e/ADD1 (adipocyte determination and differentiation factor-1/sterol regulatory element-binding protein-1), factors involved in positive feedback loop with PPARγ, were also significantly reduced. An examination of the PPARγ promoter revealed the presence of a single consensus Kruppel binding site in which KLF2 is able to bind (Banerjee S et al 2003). Wu and colleagues demonstrated through the generation of KLF2 tet-responsive 3T3-

L1 cells, KLF2 prevents preadipocyte differentiation partially via the restoration of Delta-like 1/preadipocyte factor-1 (DLK1/PREF-1) (Wu J et al 2005).

**KLF7** has also been implicated as a negative regulator of adipogenesis. Over-expression of KLF7 in preadipocytes results in the inhibition of adipogenesis in 3T3-L1 cells (Kanazawa A et al 2005). KLF7 also plays an important role in the pathogenesis of type 2 diabetes. Over-expression of KLF7 regulates adipokine gene expression in human adipocytes and inhibits glucose-induced insulin secretion in pancreatic β-cells (Kawamura Y et al 2006).

**KLF3** is expressed most prominently at day 0 in the 3T3-L1 system and levels dramatically decrease as proadipogenic genes increase during differentiation. Forced expression of KLF3 in 3T3-L1 cells blocks adipogenesis by recruiting C-terminal binding protein (CtBP) corepressors (Turner and Crossley 1998) to the C/EBPα promoter. KLF3 knockout mice are smaller, have less white adipose tissue and their fat pads contain smaller and fewer adipocytes (Sue N et al 2008).

**Specificity Protein 1 (SP1)**

Sp1 is a ubiquitous protein that has three $Cys_2His_2$ zinc finger motifs that recognize and specifically bind to GC-rich sites (Kaczynski J et al 2003). Sp1 has been shown to activate or repress numerous genes implicated in a variety of cellular process such as cell growth, differentiation, angiogenesis and immune response (Tan N et al 2009). In adipogenesis, Sp1 has been shown to exert a repressive effect on C/EBPα prior to the induction of differentiation. Sp1 represses C/EBPα transcription by binding to the GC box at the 5 prime end of the C/EBPα regulatory unit in the C/EBPα promoter and this competitive binding prevents the transactivation by C/EBPβ and C/EBPδ (Tang QQ et al 1999).

**Early Growth Response (Egr)**

Four early growth response proteins have been described in the literature. Two early growth factor proteins, Egr1 and Egr2, are implicated in adipogenesis. Early Growth Response proteins possess highly homologous DNA-binding domains composed of three $Cys_2$-$His_2$ fingers that regulate transcription of their target genes through specific binding to a GC-rich region (Swirnoff and Milbrandt 1995).

**Krox20/Egr2** is induced early in 3T3-L1 cell differentiation and appears to be the earliest inductive factor expressed during adipogenesis (Gonzalez F 2005). Chen et al show that over-expression of Krox20 in both 3T3-L1 preadipocytes and multipotent NIH3T3 cells stimulate adipogenesis by transactivating the C/EBPβ promoter and increasing C/EBPβ gene expression. Conversely, RNAi-mediated knockdown of Krox20 reduced adipogenesis in 3T3-L1 cells (Chen Z et al 2008). Knockdown of C/EBPβ diminished but did not completely block Krox20's proadipogenic effect indicating that it may stimulate adipogensis via a C/EBPβ independent pathway (Chen Z et al 2008).

Krox24/Egr1 acts as a negative regulator of 3T3-L1 differentiation. The addition of the differentiation cocktail, MDI, in 3T3-L1, rapidly induces Krox 24 by 1 hour followed by a drastic decrease to near undetectable levels on days 2 and 3. Sustained expression of Krox24 reduces preadipocyte differentiation and the expression of proadipogenic factors such as PPARγ, C/EBPα, and aP2. Knockdown of Krox24 potentiates adipogenesis particularly in the absence of IBMX from the differentiation cocktail however; there was no correlation between IBMX and Krox24 expression and no effect on CREB, a known target of IBMX. While mRNA levels of both PPARγ, C/EBPα were modulated during alterations of Krox24, there is no evidence in

promoter-reporter assays that Egr1 can modulate either one of these proadipogenic genes (Boyle KB et al 2009).

**GATA-2 and GATA-3**

GATA binding proteins have been implicated in regulating the onset of cardiac myocyte differentiation (Zhao R et al. 2008) and to osteoblast differentiation and bone formation (Nakashima K et al 2002).

**GATA-2 and GATA-3** are down regulated during differentiation of 3T3-L1 and 3T3-442A preadipocytes. Forced expression of both transcription factors inhibits adipogenesis and decreases expression levels of PPARγ, Glut4, and aP2. GATA-2 and GATA-3 bind directly to two sites on the proximal PPARγ promoter and negatively regulate its basal transcriptional activity (Tong Q et al 2000). GATA factors can also form complexes with C/EBPα and C/EBPβ that appear to be critical for the ability of these transcription factors to inhibit adipogenesis. Mutations in the interaction domain on GATA-2 that bind to C/EBPα abolish the ability of GATA-2 to suppress adipocyte differentiation (Tong Q et al 2005).

**Monocyte Chemotactic Protein-1 induced protein (MCPIP)**

Monocyte chemotactic protein-1 induced protein (MCPIP) is induced by the binding of monocyte chemotactic protein-1 (MCP-1) to C-C chemokine receptor 2 (CCR2). MCPIP has been shown to promote angiogenesis and the activation of macrophages. In 3T3-L1 cells, MCPIP is produced with the addition of adipogenic cocktail, MDI, prior to the induction of early adipogenic factors of the C/EBP family. Treatment of 3T3-L1 with MCP-1 or forced expression of MCPIP can induce adipocyte differentiation in the absence of standard induction media, MDI.

Inteerstingly, Younce and colleagues demonstrated that MCPIP can induce adipogenesis even in the absence of PPARγ by showing that PPARγ -/- mouse embryonic fibroblasts that constitutively express MCPIP can induce the expression of C/EBP β, C/EBPδ and C/EBPα and lead to adipocyte differentiation (Younce C et al 2009).

**ETO/MTG**

Eight-twenty-one (ETO also known as MTG8, myeloid tumor gene), contains two MYND domains. ETO frequently fuses with acute myeloid leukemia-1 (AML-1) to form a chimeric protein associated with acute myeloid leukemia. The MYND domain of ETO has been reported to act as a powerful corepressor by recruiting co-repressors N-CoR and mSin3 to suppress transcription (Lutterbach B et al 1998). ETO/MTG is highly expressed in confluent cultures of 3T3-L1 and 3T3-F442 cells and upon hormonal stimulation rapidly decreases. Constitutive ETO expression severely impairs lipid accumulation during adipocyte differentiation and markedly inhibits the expression of C/EBPα. Other key adipogenic genes such as aP2, PPARγ, and Glut4 (a C/EBPα target) are also diminished. Gel shift and ChIP data indicate that ETO inhibits the binding of C/EBPβ to the CEBPα promoter therefore, preventing the transactivaion of the C/EBPα promoter (Rochfor J et al 2004).

**HZF (haematopoietic zinc finger)**

HZF contains three $C_2H_2$ type zinc fingers that can potentially act as DNA binding motifs. HZF is required for megakaryocyte development and can modulate p53 tranactivation functions in regulating cell fate decisions in response to genotoxic stress (Kimura Y et al 2002 and Das S et al 2007). HZF is induced early in differentiation of preadiocytes and highly expressed in

mouse adipose tissue. shRNA mediated knockdown of HZF in 3T3-L1 cells inhibits adipocyte differentiation and significantly impairs C/EBPα induction due to reduced translation of its mRNA. HZF modulates C/EBPα induction by binding through its zinc finger domains to a specific sequence within the 3prime untranslated region of C/EBPα to enhance its translation. HZF -/- mice exhibit no defects in adipose tissue development however; HZF null mice have functional disregulation of adipose tissue that leads to glucose intolerance and insulin resistance when compared to the wild type controls (Kawagishi H. et al 2008).

## Zinc fingers contributing to late phases of differentiation

### Peroxisome Proliferator-activated Receptor γ (PPARγ)

Peroxisome proliferator-activated receptor γ (PPARγ) is considered to be the master regulator of adipocyte differentiation and is required for the differentiation of this tissue in vivo and in vitro (Rosen, Sarraf et al. 1999). PPARγ has two isoforms, PPARγ1 and PPARγ2 : although PPARγ2 expression is restricted primarily to adipose tissue, both are required for adipogenesis (Mueller E et al. 2002). Forced expression of PPARγ in various fibroblastic cell lines is sufficient to induce adipogenesis (Tontonoz P et al 1994) and in vivo studies have demonstrated that PPARγ is essential for efficient adipogenesis. PPARγ null embryos die in utero due to placental defects and myocardial thinning however, a tetraploid rescued mutant surviving to term was deficient in brown and fat adipose tissue and had hepatic steatosis (Barak et al 1999). More recently, several mouse models have been developed using the cre-lox system and selective disruption of the PPARγ2 isoform to circumvent the lethality observed in PPARγ null mice. Adipose specific PPARγ mice knockout mice have substantial fat cell loss, are insulin resistant,

and have hepatic steatosis (He et al 2003). Similar to PPARγ fat specific mice, PPARγ2 null mice have an overall reduction in white adipose tissue (Zhang J et al 2004).

PPARγ is a ligand activated transcription factor that belongs to the family of nuclear hormone receptors and the PPAR subfamily. PPARγ regulates gene expression by forming an obligate heterodimer with retinoid X receptor α (RXRα) to bind to peroxisome proliferator response elements, a DNA specific sequence present in the promoter regions of PPAR-regulated genes. This binding enables subsequent recruitment of a multi-subunit protein complex consisting of coactivators or corepressors that modify chromatin and contact the basal transcriptional machinery. Unliganded PPAR:RXRα dimer is bound to DNA and recruits corepressors such as the Nuclear receptor Corepressor (NCor) and the Silencing Mediator of Retinoid and Thyroid hormone receptor (SMRT) (Yu and Reddy 2007). Ncor and SMRT, in turn recruits a complex with histone deacetylase enzymatic activity to repress transcription of target genes (Yu, Markan et al. 2005). Alternatively, binding of a ligand to PPARγ results in the dissociation of corepressor protein complexes, followed by an orchestrated recruitment of several transcriptional coactivators. Some of these coactivators are responsible for the modification of histones and chromatin structure to open up DNA for transcription, while others provide linkage to the core basal transcriptional machinery (Yu and Reddy 2007). Steroid Receptor Coactivator (SRC-1/P160), of CREB cyclic-AMP response element binding protein-binding protein (CBP) and of adenovirus E1A-associated (p300) are coactivators that remodel the chromatin structure via their intrinsic histone acetyltransferase (HAT) or methyltransferase activitiy. A second group of coactivators form a multisubunit coactivator complex, called TRAP/DRIP/ARC/PRIC/ Mediator complex that consists of 15-30 proteins. These proteins serve as protein docking platform or molecular bridges to transfer the upstream signal of nuclear receptor specific gene activation to

the basal transcriptional apparatus (Yu and Reddy 2007). Ligands for PPARγ include naturally occurring fatty acids and the thiazolidinedione class (TZD) of antidiabetic drugs (Tontonoz and Spiegelman 2008).

**Slug (SNAI2)**

Slug is a member of the Snail family of zinc finger transcription factors that are composed of a highly conserved carboxy-terminal region, which contains from four to six zinc fingers. The $C_2H_2$ fingers function as sequence-specific DNA binding motifs. Snail transcription factors share an evolutionary conserved role in mesoderm formation, cell-signal cascade, and formation of appendages, cell division and survival (Nieto MA 2002). Slug triggers epithelial-mesenchymal transitions and controls many developmental processes.

Slug is expressed in human white adipocytes and its expression is tightly regulated during the differentiation of 3T3-L1 cells. Slug deficient mice weigh less, have less white adipose tissue and are resistant to diet induced obesity when compared to wild type mice. Conversely, mice carrying a tetracycline-responsive Slug transgene (Combi-Slug) exhibit an increase in weight and white adipose tissue mass. Slug deficient mouse embryonic fibroblasts (MEFs) show a reduced capacity to differentiate into adipocytes while Combi-Slug MEFs have marked lipid accumulation. PPARγ expression in both in vitro and in vivo systems is altered by differential histone deacetylase recruitment to the PPARγ promoter (Perez-Mancera P et al 2007).

**Schunurri-2**

Schunurri is a large transcription factor that contains three $C_2H_2$ zinc finger domains and one $C_2HC$ domain that is required for signaling through Decapentaplegic, the Drosophila homolog of

BMP, via interactions with Mad/Medea transcription factors (Aora et al 1995, Grieder et al 1995, Dai H et al 2000). Schnurri-2, a mammalian ortholog, is required for T cell development, is critical in locomotion and anxiety like behavior and is a novel regulator of adult bone remodeling (Takagi et al 2001, Takagi et al 2006 and Saita Y et al 2007).

Shn-2 -/- mice are smaller, weigh less and have a marked reduction in adipose tissue mass and adipocyte size when compared to their wild type littermate controls. Shn-2 -/- mice also have increased glucose tolerance and insulin sensitivity. Shn-2 -/- MEFs have significantly less adipocyte differentiation and have reduced mRNA levels of C/EBPα, C/EBPβ, and PPARγ. Based on luciferase reporter and gel shift mobility assays, Schurri-2 inters the nucleus after BMP-2 stimulation and binds directly to Smads 1/4 and C/EBPα which then act synergistically to transactivate the PPARγ promoter (Jin W et al 2006).

**SIRT1**

SIRT 1 is the mammalian orthologue to the yeast SIR2 gene. Sirt1 is an NAD dependent deacetylase that is involved in a variety of biological functions such as aging, mitochondrial biogenesis, cell survival and cell death (Haigis M and Sinclair D 2010).

It has been shown that Sirt1 acts as a negative modulator of adipogenesis by repressing PPARγ function. Over expression in 3T3-L1 cells markedly attenuates adipogenesis while RNA interference enhances it. Sirt1 binds to PPARγ sites in the promoter regions of PPARγ target genes and represses PPARγ activity by docking with known corepressors, NcoR and SMRT. In fully differentiated 3T3-L1 cells, up regulation of Sirt1 reduces triglyceride content and stimulates free fatty acid release. These findings strongly suggest that Sirt1 stimulates fat mobilization. In Sirt $^{+/-}$ mice fasted overnight, serum free fatty acids were 40-45% lower than

wild type control mice suggesting that mobilization of fatty acids from white adipocytes in these mice is compromised (Picard F et al 2004). Sirt1 was recently found to be regulated during adipogenesis by C/EBPα (Jin et al 2010).

**SIRT2**

SIRT2 is a tubulin deacetylase that is required for normal mitotic progression and mitotic checkpoint function in early metaphase to prevent chromosomal instability (Haigis M and Sinclair D 2010).

Similar to SIRT1, SIRT2 is a negative regulator of adipogenesis. SIRT2 is the most abundant sirtuin expressed in adipocytes and its expression is down regulated during preadipocyte differentiation in 3T3-L1 cells (Jing E et al 2007). Forced expression of SIRT2 inhibits adipogenesis as well as promotes lipolysis in 3T3-L1 cells (Jing E et al 2007 and Wang F and Tong Q 2009). Mechanistically, SIRT2 suppresses adipogenesis by interacting with and deacetylating FOXO1, a known repressor of adipogenesis. Subsequently, FOXO1 binds to and represses PPARγ transcriptional activity (Jing E et al 2007 and Wang F and Tong Q 2009).

**FBI-1 (Factor that binds to inducer of short transcripts-1/Pokemon)**

FBI-1 contains four $C_2H_2$ zinc fingers at its C-terminus and a POZ domain at its N-terminus (Morrison D et al 1999). FBI-1 has been reported as a repressor of osteoclastogenesis, chondrogenesis and plays a role in oncogenic transformation (Cho W et al 2009).

FBI-1 acts as a dual regulator of adipogenesis by exerting repression activities via indirect and direct mechanisms. It is expressed in human and murine preadipocytes during early stages of differentiation. 3T3-L1 cells constitutively expressing FBI-1 show a reduction in DNA synthesis and reduced expression of cyclin A, cyclin-dependent kinase 2, and p107, proteins involved in

the regulation of mitotic clonal expression (Laudes et al 2004). FBI-1 indirectly reduces the transcriptional activity of cyclin A by binding to specificity protein (Sp1) (Laudes M et al 2004 and Laudes M et al 2008). Similar to other members of the POZ zinc finger transcription factors, FBI-1 recruits co-repressors to form a repressor complex. Co-immunoprecipitation assays show that FBI-1 binds directly to Sin3A and HDAC-1 to repress adipogenesis. FBI-1 promotes terminal differentiation of adipocytes by repressing promoter activity of E2F-4, a known PPARγ repressor (Laudes M et al 2008).

**Hic-5**

Hic-5 is a coactivator that contains four carboxyl LIM domains. While Hic 5 has been shown to bind to and stimulates PPARγ transcriptional activity to promote differentiation and maturation of epithelial cells (Drori S et al 2005), in adipogenesis Hic5 has been show to act as a repressor. Endogenous Hic-5 is expressed at detectable levels in undifferentiated 3T3-L1 cells and decreases during adipocyte differentiation. Forced expression of Hic-5 in 3T3-L1 cells induced to differentiate inhibits their differentiation and decreases mRNA expression of characteristic adipogenic genes, such as aP2, adipsin, and acrp30 while increasing the expression of genes characteristic of intestinal epithelial differentiation, keratin 20 L-FABP and KLF4 (Drori S et al 2005) in the present of rosiglitazone.

**CBP/p300**

Both CBP and its homologue p300 are transcriptional co-activators that have been implicated in various biological processes that include cell growth, transformation and apoptosis (Goodman R and Smolik S 2000). In addition to the role of CBP/p300 in the differentiation of various cell

lineages such as hematopoiesis and myogeneis, these co-activators have also been shown to be important in adipogenesis (Goodman R and Smolik S 2001).

CBP/p300 interacts with PPARγ in a ligand-dependent and independent manner and enhances its transcriptional activity (Gelman L et al 1999). Takahashi and colleagues later described that CBP/p300 are indispensable in adiopcyte differentiation (Takahashi N et al 2002). Experiments revealed that overexpression of CBP or p300 with PPARγ enhanced the expression of PPARγ target genes in NIH3T3 cells. Specific ribozyme mediated targeting of either CBP or p300 in 3T3-L1 cells suppressed the expression of adipogenic markers such as aP2, lipoprotein lipase and reduced the amount of lipid accumulation (Takahashi N et al 2002).

**Early B Cell Factor (O/E-1)**

The Early B cell factor family (O/E) of transcription factors (O/E-1, 2 and 3) share similar structure and are expressed in the nervous system and numerous structures that mediate sensory activities during development (Wang S et al 1997). O/E-1 is important in early B lymphocyte-specific gene expression, olfactory gene regulation and neuronal development (Hagman J et al 1993 and Wang S et al 1997).

All three O/E isoforms are expressed at various levels in mouse adipose tissue, and noninduced, preconfluent 3T3-L1 cells and are upregulated during adipocyte differentiation. Forced expression of O/E-1 in 3T3-L1 cells and mouse embryonic fibroblasts promotes adipogenesis and ectopic expression in uncommitted NIH 3T3 cells initiates adipocyte differentiation. A dominant negative form of O/E-1 impairs the differentiation of 3T3-L1 cells and reduces the expression of late-stage adipogenic genes such as, GPDH, adipsin, GLUT 4 and PPAR$\gamma_2$ (Akerblad P et al 2002). Dowell and Cooke found that O/E-1 negatively regulates

GLUT4 expression in 3T3-L1 cells upon insulin stimulation by binding a negative regulatory element region of the murine *glut4* gene promoter (Dowell and Cooke (2002).

**Conclusions**

Zinc finger transcription factors appear to have increasing importance in the regulation of adipocyte differentiation in vitro and in vivo. Given that ZF containing proteins are the largest family of transcriptional regulators it is likely that many more factors currently unknown will be discovered to be related to the adipogenic process.

**Table 1. Zinc Finger Transcription Factors in Adipogenesis**

| Protein Name | Zinc Finger Motif | # of Zinc Fingers | Associated Domains | Function in Adipogenesis | Function in osteogenesis and skeletal myogenesis |
|---|---|---|---|---|---|
| PPARγ | $Cys_2Cys_2$ | 2 | LBD, AF1, AF2 | ↑ Adipogenesis Tontonoz P et al, 1994 | ↓ Osteogenesis Marie P & Kaabeche K 2006 |
| KLF 15 | $C_2H_2$ | 3 | Unknown | ↑ Adipogenesis Mori T et al, 2005 | Myogenesis: unclear Haldar S et al, 2007 |
| KLF 5 | $C_2H_2$ | 3 | Unknown | ↑ Adipogenesis Oishi Y et al, 2005 | ↑Osteogenesis Shinoda et al, 2008 |
| KLF 6 | $C_2H_2$ | 3 | Unknown | ↑ Adipogenesis Li D et al, 2005 | Myogenesis: expressed role unknown Halder S et al, 2007 |
| KLF 9 | $C_2H_2$ | 3 | Unknown | ↑ Adipogenesis Pei H et al, 2010 | Unknown |
| KLF 4 | $C_2H_2$ | 3 | Unknown | ↑ Adipogenesis Birsoy K et al, 2004 | Unknown |
| KLF 2 | $C_2H_2$ | 3 | Unknown | ↓ Adipogenesis Banerjee S et al, 2003 Wu J et al, 2005 | Unknown |
| KLF 3 | $C_2H_2$ | 3 | Unknown | ↓ Adipogenesis Sue N et al, 2008 | Unknown |
| KLF 7 | $C_2H_2$ | 3 | Unknown | ↓ Adipogenesis Kanazawa A et al, 2005 | Unknown |
| Sp1 | $C_2H_2$ | 3 | Unknown | ↓ Adipogenesis Tang QQ et al, 1999 | ↓ Myogenesis |

**Table 1 (continued)**

| Protein Name | Zinc Finger Motif | # of Zinc Fingers | Associated Domains | Function in Adipogenesis | Function in osteogenesis and skeletal myogenesis |
|---|---|---|---|---|---|
| Krox 20 | $C_2H_2$ | 3 | Unknown | ↑ Adipogenesis Chen Z et al, 2004 | ↑ Osteogenesis Levi G et al, 1996 |
| Krox 24 | $C_2H_2$ | 3 | Unknown | ↓ Adipogenesis Boyle KB et al, 2009 | Osteogenesis: unclear Suva L et al, 1991 |
| Slug | $C_2H_2$ | 5 | Snag, Slug | ↑ Adipogenesis Nieto MA et al, 2002 | ↑ Osteogenesis Lambertini E et al, 2009 |
| Schunrri-2 | $C_2H_2$ | 7 (3 pairs, 1 unpaired) | Unknown | ↑ Adipogenesis Jin W et al, 2006 | Unknown |
| FBI-1 | $C_2H_2$ | 4 | 1 BTB/POZ | ↑ and ↓ Adipogenesis Laudes M et al, 2004 Laudes M et al, 2008 | ↓ Osteogenesis Kukita A et al, 1999 |
| Zfp 423 | | 30 | Unknown | ↑ Adipogenesis Gupta R et al, 2010 | Unknown |
| ZNF638 | $C_2H_2$ matrin type | 2 | RS, RRM | ↑ Adipogenesis Hayes and Meruvu et al, unpublished data | Unknown |
| HZF | $C_2H_2$ matrin type | 3 | Unknown | ↑ Adipogenesis Kawagishi H et al, 2008 | Unknown |
| GATA-2 | GATA-type | 2 | Unknown | ↓ Adipogenesis Tong Q et al, 2005 | Unknown |
| GATA-3 | GATA-type | 2 | Unknown | ↓ Adipogenesis Tong Q et al, 2005 | Unknown |

**Table 1 (continued)**

| Protein Name | Zinc Finger Motif | # of Zinc Fingers | Associated Domains | Function in Adipogenesis | Function in osteogenesis and skeletal myogenesis |
|---|---|---|---|---|---|
| CBP/P300 | TAZ<br>ZZ | 2 TAZ<br>1 ZZ | 1 Bromodomain<br>1 KIX | ↑ Adipogenesis<br>Gelman L et al, 1999<br>Takahashi N et al, 2002 | ↑ Myogenesis<br>Puri PL et al, 1997<br>↑ Osteogenesis<br>Iioka T et al, 2003 |
| ETO | MYND (NHR 4) | 1 | 3 Nervy Homology Region (NHR) | ↓ Adipogenesis<br>Rochford J et al, 2004 | Unknown |
| Hydrogen peroxide-inducible clone 5 (Hic-5) | LIM | 4 | 4 LD | ↓ Adipogenesis<br>Drori S et al, 2005 | Myogenesis: unclear<br>Hu Y et al, 1999;Shibanuma et al, 2002 |
| O/E-1 | Zinc Knuckle | 1 | 1 IPT/TIG | ↑ Adipogenesis<br>Akerbald P et al, 2002 | ↑ osteogenesis<br>Hesslein DG et al, 2009 |
| MCPIP | $C_3H$ | 1 | 1 PIN | ↑ Adipogenesis<br>Younce C et al, 2009 | Unknown |
| SIRT1 | Zinc Ribbon | | 1 Nicotinamide-adenine dinucleotide (NAD) binding and catalytic domain | ↓ Adipogenesis<br>Picard F et al, 2004<br>Jin et al 2010 | ↓ myogenesis<br>Fulco M et al, 2003 |
| SIRT2 | Zinc Ribbon | | 1 Nicotinamide-adenine dinucleotide (NAD) binding and catalytic domain | ↓ Adipogenesis<br>Jing E et al, 2007<br>Wang F and Tong Q, 2009 | Unknown |

**Figure 1. Zinc Finger Transcription Factors in Adipogenesis.** For interpretation of the references to color in this and all figures, the reader is referred to the electronic version of this thesis.

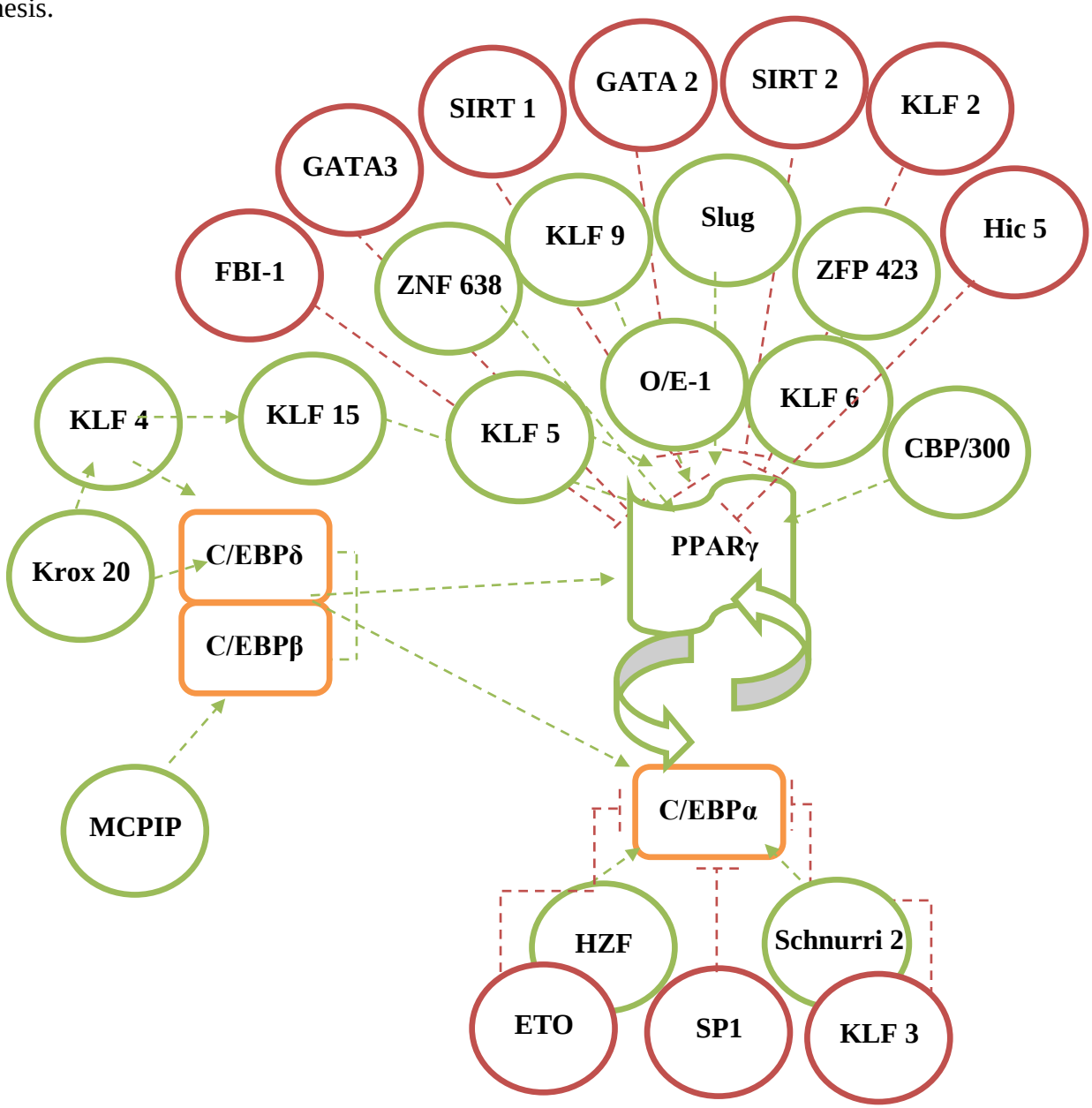

**III. Experimental Design to Identify and Characterize Novel Regulators of Adipogenesis**

To identify and characterize novel regulators of adipogenesis, we developed several specific aims: specific aim 1 was to determine the in vivo role of ZNF638 in adipose tissue. Specific aim 2 was to identify the mechanism of action of a novel isoform of ZNF638, nuclear matrix coactivator 1 (NMC1). Specific aim 3 was to determine the in vivo role of SGK1 in adipose tissue.

To address specific aim 1, we generated a fat specific (under the control of the aP2 promoter) conditional knockdown mouse of ZNF638 using cre-loxP induced RNA interferance (Fat-ZNF638-KD). We hypothesized that fat specific knockdown of ZNF638 in vivo would result in a lean phenotype characterized by less adipose tissue when placed on regular NIH mouse chow and when challenged on a high fat diet. To test this hypothesis, Fat-ZNF638-KD mice were evaluated at postnatal day one, at weaning (3 weeks) and after a high fat diet challenge. Histopathology and immunohistochemistry were used to evaluate adipocyte morphology and gene expression in one day old and three week old mice. 10 week old Fat-ZNF638-KD mice and wild type littermate controls where challenged on a high fat diet for eight weeks. Changes in weight, fat and lean mass were determined by measuring body weight and body composition using a table top MRI before and after challenge. Metabolic parameters were measured by using indirect calorimetry. Histopathology and morphometrics were used to evaluate adipocyte morphology. Evaluation of mRNA expression levels in the visceral white adipose tissue were used to determine if there was down regulation of adipocyte specific genes.

For specific aim 2, we hypothesized that nuclear coactivator 1 (NMC1), a novel isoform of ZNF638, interacts with other transcriptional regulators involved in adipocyte differentiation. To test this hypothesis, we utilized a novel high throughput cell based screening strategy to identify

novel protein-protein interactions with NMC1. Luciferase reporter assays were used to confirm positive interactors. 3T3-L1 cells were used to determined expression levels and cellular localization of candidate gene, Smad4-interacting factor (SMIF), during adipocyte differentiation. Furthermore luciferase reporter assays and GST-pulldown assays were used to determine if SMIF interacts with and affects the transcriptional activity of PPARγ, the master regulator of the terminal phase of adipocyte differentiation.

For specific aim 3, we hypothesized that adipocyte specific ablation of SGK1 would result in a lean phenotype and resistance to diet induced obesity. To address specific aim 3, we generated fat specific knockout of SGK1 by crossing SGK $^{flox/flox}$ mice with ap2-cre mice to achieve ablation specifically in the adipose tissue. Similar to specific aim 3, six week old SGK1-Fat-KO mice and wild type littermate controls were challenged on a high fat diet for 12 weeks. Changes in weight, fat and lean mass were measured before and after challenge. Indirect calorimetry and serum analysis were used to measure changes in metabolic parameters. Lastly, histopathology was used to evaluate adipocyte morphology.

# CHAPTER ONE

## *In vivo* Characterization of a Novel Regulator of Adipogenesis

**Abstract:** ZNF638 is a zinc finger transcription factor recently identified in our laboratory as a novel, critical regulator of adipogenesis *in vitro*. In order to establish the role of this factor in vivo, we generated a conditional knockdown mouse of ZNF638 using Cre-LoxP induced RNA interference. The excision of the neocassette in fat tissue was implemented by crossing the ZNF638 knockdown mouse with transgenic mice that express Cre under the control of the ap2 promoter. Analysis of fat ZNF638 knockdown mice showed a significant decrease in body size and diminished weight compared to wild type mice at weaning onward. Furthermore, fat specific ZNF638 knockdown mice showed a significant reduction in visceral, perigonadal and subcutaneous white adipose tissues and a decrease in the percentage of body fat when challenged on high fat diet. Histologic examination of the adipocytes present in visceral white adipose tissue depot of ZNF638 knockdown mice indicated that they contain smaller lipid droplets compared to those present in wild type mice. Analysis of mRNA expression levels of key adipocyte genes involved in differentiation, lipid storage and metabolism, showed a reduction in those markers in the visceral depot of ZNF638 knockdown mice when compared to age and sex matched controls. In conclusion, our *in vivo* data suggest that ZNF638 plays a critical role in white fat.

## Introduction

Over the last three decades, obesity has become a national as well as a global pandemic (Dixon J 2010). With the surge of obesity and associated co-morbidities, there have been great efforts in elucidating the molecular mechanisms that control adipose tissue development and function. Previous studies have identified numerous transcription factors involved in adipocyte

differentiation. PPARγ is considered to be the master regulator of the terminal differentiation phase of adipogenesis and functions in a transcriptional cascade that includes members of the CCAT/enhancer binding protein (C/EBP) family of basic helix loop helix transcription factors, and Kruppel like factor family (Rosen E 2006). Although much is known about the molecular mechanisms regulating the terminal differentiation phase, the transcriptional regulation of early adipogenesis (determination phase) is largely unknown. With this, it is important to study the transcriptional regulation of early adipogenesis and to research novel proteins that may regulate the transcription factors involved in terminal differentiation.

We previously identified ZNF638 as a novel regulator of adipogenesis in vitro (Meruvu et al. unpublished data). ZNF638 is expressed during early phases of adipocyte differentiation, prior to the expression of PPARγ and concomitantly with the expression of the early regulators C/EBPβ and C/EBPδ. Through physical interaction and functional cooperation with C/EBPβ and C/EBPδ, ZNF638 can induce PPARγ expression (Meruvu et al. unpublished data) and its overexpression promotes adipogenesis. Conversely, knockdown of ZNF638 by small interfering RNAs inhibits fat differentiation and decreases the expression of adipocyte specific genes (Meruvu et al. unpublished data), suggesting a role of ZNF638 in adipogenesis in vitro.

In this study, we generated mice with adipose specific knockdown of ZNF638 (Fat-ZNF638-KD) by cre-loxP RNA interference. Fat-ZNF638-KD mice are smaller and weigh less at weaning than the wild type littermates. Furthermore, when challenged on high fat diet, they show resistance to weight gain. Fat-ZNF638-KD mice show marked reduction in subcutaneous, visceral and perigonadal white adipose tissue. Fat-ZNF638-KD mice have a higher metabolic rate and consume more food than their littermate controls. Analysis of white adipose depots of Fat-ZNF638-KD mice on HFD indicates the presence of smaller adipocytes. Furthermore,

mRNA expression levels of several genes involved in adipocyte differentiation and lipid uptake and storage are reduced in Fat-ZNF638-KD. Overall our data suggest that ZNF638 plays a critical role in fat biology *in vivo*.

## Materials and methods

### Generation of transgenic mice

ZNF638 shRNA mice were generated as described previously (Coumoul X, 2005). Briefly, single stranded DNA oligonucleotides were chemically synthesized and annealed to form double-stranded DNA that consisted of shRNA-ZNF638 sense sequence, the loop sequences AGCT, shRNA-ZNF638 antisense sequence and a string of five thymidine as a termination site of the RNA polymerase III. The double-stranded DNA oligonucleotide was cloned into the pBS/U6loxP vector (a gift from Dr. Chu-Xia Deng). The pBS/U6-ploxPneo-ZNF638 vector was digested by KpnI and Af1III restriction enzymes and purified from agarose gel using a Gel Extraction kit (Qiagen). Gel particles and other contaminants were removed by using Elutips (Schleicher and Schuell). The eluate was ethanol precipitated and washed twice with 70% ethanol to remove ethidium bromide. DNA was resuspended in 10mM Tris with 0.1 mM EDTA to a final concentration of 2 ng/µl and injected into oocytes isolated from C57/BL6 mice through pronuclear injection. To identify the transgene, the offspring was genotyped with the following primers: Gen1-F: 5'-ATGTGGAACAGAGGCTGCT-3' and Gen2-R: 5'-CCGTGATA TTGCTGAAGAGC-3'. These primers amplify a 102 bp product spanning from the U6 promoter and the connecting *neo* gene. Positive mice were crossed with wild-type C57/BL6 mice to obtain germ line transmission of the transgene.

**Functional Analysis of *ZNF638-RNAi* transgene**

Mice carrying the U6-ploxPneo-ZNF638-RNAi transgene were crossed with Ap2-cre transgenic mice to assess ZNF638-KD efficiency. The Ap2-cre mice were genotyped using the following primers: Jcre-F: 5'-GCGGTCTGGCAGTAAAAACTATC-3' and Jcre-R 5'- GTGA AACAGCATTGCTGTCACTT-3'. Cre mediated recombination was verified in visceral white adipose tissue using the following pair of primers: Cre-F: 5'-GACGCCGCCATCTCTGG-3' and T3: 5'-AATTAACCCTCACTAAAGGG-3'.

**Animal Experiments**

All animal experiments were performed according to procedures approved by the National Institutes of Health Animal Care and Use Committee. Animals were housed under, and maintained on, a fixed 12-hour light/dark cycle at 22°C. Mice were fed a standard mouse chow diet until the age of 6 to 10 weeks. At 6-10 weeks of age, animals were fed and maintained on a high fat diet (HFD) (Research Diets D12451, New Brunswick, NJ) for 8 weeks. The high fat-diet contained 45% kcal fat.

Three-week-old and 14-to 18-week old mice were sacrificed for tissue collection by $CO_2$ narcosis using an approved chamber receiving $CO_2$ from a pressurized gas cylinder followed by cervical dislocation, according to NIH ACCUC animal study approved procedures. One-day old mice were decapitated. Portions of tissues were snap frozen in liquid nitrogen and stored at -20°C for subsequent analysis.

**Body Composition Analysis**

Mice were weighed weekly. To assess body composition (percentage of fat), whole-body measurements of conscious mice were performed using a tabletop Bruker Minispec NMR Analyzer mq10 on mice prior to and after the high fat diet challenge. Total fat, lean and water mass were evaluated.

**Glucose Measurements in one-day-old mice**

Glucose was measured on one-day-old mice. Intravenous blood was taken from the jugular vein and measured for glucose levels by using a glucometer (Ascensia ELITE XL, Bayer).

**Food intake**

During the 8 week HFD challenge, food intake was measured in individually caged mice during a 6-day period. A sufficient amount of food was weighed and provided to the mice *ad libitum*. Tunnel type feeders (Rodent CAFÉ, OYS International) were used to measure consumption.

**Indirect Calorimetry**

At the end of the HFD diet challenge, oxygen consumption and carbon dioxide production were measured with an 8-chamber Oxymax system (Columbus Instruments) with one mouse per chamber and by testing mutant mice simultaneously with littermate controls. Motor activity (total and ambulating) was determined by infrared beam interruption (Columbus Instruments). Mice had free access to food and water. Food intake was measured in individually caged mice by tunnel type feeders and energy expenditure was determined by measuring resting and total $O_2$

consumption at ambient and (23ºC) and at thermoneutrality (30ºC). All parameters were normalized to body weight to account for the large disparity in body size between the two groups. Total oxygen consumption was measured for 24 h at room temperature (23°C), and energy expenditure was calculated as the average of all points excluding the data from the 1st h of the experiment. Core body temperature was measured using a rectal probe Thermalert TH-5 (Physitemp) inserted 1.0 cm deep.

**Histopathology and Immunohistochemistry**

Portions of white adipose tissue, brown adipose tissue, skin and liver and reproductive tract from three-week-old and adult mice were fixed in 4% paraformaldehyde, embedded in paraffin, and sectioned at 5-7 μm thickness. One-day-old mice were sectioned longitudinally for 22 serial sections at 5-7 μm thickness. Sections were stained with hematoxylin and eosin and photographed at 400x magnification.

Immunohistochemistry was performed on unstained sections of reproductive tract from 3-week-old mice and longitudinally sectioned one day old mice. Briefly, tissues were deparafinized in xylenes and rehydrated. Sections were treated with 3% hydrogen peroxide in methanol to block endogenous peroxidases, followed by steam retrieval with Dako-Target retrieval buffer (DAKO). Sections were blocked with DAKO blocking reagent (DAKO) followed by Avidin D and Biotin (DAKO) to reduce nonspecific staining. Sections were incubated with primary antibodies for one hour at room temperature, followed by incubation with the biotinylated secondary antibody and avidin-biotin-complexes (ABC) (Vectastain ABC kit, Vector Laboratories). Signals were visualized with diaminobenzidine (DAB). Sections were lightly

counterstained with hematoxylin. Primary antibodies used were fatty acid binding protein (FABP4, ab13979, Abcam) and uncoupling protein 1 (UCP1, ab10983, Abcam).

**Determination of Adipocyte Size**

For adult mice, the Aperio ScanScope XT Slide Scanner (Aperio Technologies, Vista, CA) system was used to capture whole slide digital images of visceral, perigonadal and subcutaneous white adipose depots with a 20x objective. Mature white adipocytes were identified by their unilocular appearance. Total areas of adipocytes were traced manually and analyzed with Spectrum (Aperio Technologies, Vista, CA). White adipocyte areas were measured in 100 cells per mouse in wild type and ZNF638-KD mice. All areas were expressed as $\mu m^2$. Annotation results were exported into Microsoft excel and Prism (Graph Pad Software) to compare cell size and for statistical analysis.

**RNA Analysis**

RNA was extracted from animal tissues using Trizol™ reagent, according to the manufacturer's instructions (Invitrogen) followed by TURBO DNAase treatment (Applied Biosystems). cDNA was obtained from one microgram of total RNA using the High-Capacity cDNA Archive Kit (Applied Biosystems). Real-time PCR was performed using ABI Prism 9700HT Sequence Detection System Instrument (Applied Biosystems) connected to Sequence Detector Software (SDS version 2.0; Applied Biosystem) for collection and analysis of data. The PCRs were set up in a reaction volume of 25 μl in a MicroAmp Optical 96-well plate. Each reaction contained 7.5 μl distilled water, 12.5 μl FastStart SYBR Green PCR Master Mix (ROX) (Roche Diagnostics), 5 μM of forward and reverse primers (IDT) and 20 ng of cDNA.

Thermocyling was carried out for 45 cycles in triplicate. Each cycle consisted of 50°C for 2 minutes, 95°C for 15 minutes, 94°C for 15 seconds, 59°C for 30 seconds, and 72°C for 30 seconds. Primers to detect 18 S were used to normalize sample data. For analysis of ZNF638, PPARγ and aP2, the following primers were used: ZNF638-F 5'-ATTGAGAGCTG TCGGCAGTTA-3', ZNF638-R 5'-GCAATGAGAACGTCTTCTTGGAG-3', PPARγ-F 5'-CTTTCCTGTCAAGATCGCCC-3', PPARγ-R 5'-AGTCTGCT GATCTGCGAGCC-3', aP2-F 5'-TCGATGAAATCACCGCAGAC-3' aP2-R 5'-TGTGGTCGACTTTCCATCCC-3'. A complete list of primers used for real-time PCR is in table 2.

**Statistical analysis**

Statistical comparisons between groups were made using Student *t* test and ANOVA performed with Graph Pad Software (Prism version 5.0, Graph Pad, San Diego, CA, USA). Results are presented as means ± SEM. A p value less than 0.05 was considered statistically significant.

## Results

**Adipose-Specific ZNF638 Gene Targeting**

The effect of knocking down the expression of ZNF638 in vivo using RNAi was studied using transgenic mice generated through pronuclear injection of *U6-ploxPneo-ZNF638* (Figure 2A). After breeding with C57BL/6J mice, nine offspring passed the *U6-ploxPneo-ZNF638* transgene through the germline. All transgenic founder mice were normal. Transgenic founder mice (*U6-ploxPneo-ZNF638*) were crossed to aP2-cre mice to generate Fat-ZNF638-KD. One founder line was expanded and used in this study. RNA was isolated from brown and visceral

white adipose tissue to examine the knockdown efficiency of ZNF638 in transgenic mice. There was 60-70% reduction of ZNF638 mRNA in the visceral white adipose tissue of transgenic mice (Figure 2B) while no significant knockdown of ZNF638 was detected in the intrascapular brown adipose tissue (Figure 2B).

**ZNF638 knockdown (Fat-ZNF638-KD) mice died at the early neonatal stage**

ZNF638 knockdown mice were obtained at frequency lower than the expected Mendelian ratio at weaning. The expected Mendelian ratio of 3 week old mice was 6% for *U6-ZNF638*;aP2-cre (Fat-ZNF638-KD) mice and for mice containing only the *U6-ploxPneo-ZNF638*, aP2-cre transgene or neither respectively was 19%, 19% and 56% (Table 3). Since genotype analysis revealed a potential survival issue prior to weaning, we then analyzed mice at birth. One-day-old Fat-ZNF638-KD mice were obtained at the expected Mendelian ratio. The percentage of ZNF638 knockdown mice were 13%, while mice containing only the *U6-ploxPneo-ZNF638*, aP2-cre transgene or neither were 19%, 13% and 62% (Table 3).

Visual and necropsy examinations of Fat-ZNF638-KD neonates revealed no gross abnormalities (Figure 3A). These mice had the presence of milk in the stomach indicating live birth and ability to suckle (data not shown). Furthermore, histologic examination of their lung revealed extended alveolar spaces that contained low numbers of alveolar macrophages (data not shown). These findings demonstrate that Fat-ZNF638-KD mice were able to breathe at birth. Potential causes for neonatal mortality were explored further by examining blood glucose levels at postnatal day one. Glucose levels were similar to those obtained from littermate controls (Figure 3B).

**One day old Fat-ZNF638-KD mice develop white and brown adipose tissue**

White adipose tissue appears at the latest stages of embryonic development with maturation occurring postnatally when energy storage is most needed. White adipose tissue is composed of several types of cells at different stages of development. Pre-adipocytes are defined as cells with no cytoplasmic lipid accumulation and immature adipocytes are cells that contain cytoplasmic lipid droplets of a smaller size (Tanaka et al 1997), while mature adipocytes have centralized hyperchromatic nuclei with moderate amounts of brightly eosinophilic cytoplasm with or without intracytoplasmic lipid (Tanaka et al 1997). Longitudinal sections of one day old wild type and Fat-ZNF638-KD mice were examined to identify white adipocytes at various stages of differentiation. Small amounts of mature white adipose tissue was identified on the dorsum surrounding intrascapular brown adipose tissue as well as in some subcutaneous regions in both genotypes (Figure 3C). Clusters or lobules of small pre-adipocytes and immature lipid laden cells were also identified, scattered multifocally throughout the subcutaneous tissue of wild type and Fat-ZNF638-KD mice. These cells were characterized by centrally located nuclei and abundant eosinophilic cytoplasm that often contained small lipid vacuoles. Cells were later confirmed to be white adipocyte precursors by positive FABP4 (aP2) and negative UCP1 antibody staining (Figure 3C). As shown in figure 3C, no difference was detected in cellular morphology of pre-adipocytes and immature lipid laden adipocytes in the subcutaneous tissue of ZNF638-KD mice when compared to the wild type controls. Also, immunohistochemical staining for aP2 and UCP1 was similar between the two groups.

Intrascapular brown adipose tissue is identifiable at embryonic day 14.5 in fetal life as a mass with two small lobules. We examined the intrascapular brown adipose tissue microscopically in

one day old wild type and knockdown mice and found no histologic difference. All other organs were present and were histologically normal (data not shown).

**3-week-old mice show growth retardation and had no perigonadal white adipose tissue**

Due to increased pre-weaning lethality, Fat-ZNF638-KD mice and littermate controls were sacrificed just prior to or at weaning (3 weeks of age). Gross examination of Fat-ZNF638-KD mice showed marked growth retardation (Figure 4A). Dissection revealed no subcutaneous, visceral or perigonadal white adipose tissue in Fat-ZNF638-KD mice compared to wild type controls.

Sections of skin and reproductive tract were examined histologically. Compared to wild type littermate controls, Fat-ZNF638-KD mice had little to no subcutaneous white adipose tissue (Figure 4B). Examination of the reproductive tract of wild type, littermate controls revealed abundant unilocular adipocytes surrounding the gonads (ovaries and testis) as well as along the uterine body (females) and accessory sex organs in males. On the contrary, no white adipose tissue in the vicinity or surrounding the reproductive tract was detected in Fat-ZNF638-KD. Interestingly, the reproductive tract of 3 weeks old Fat-ZNF638-KD appeared to have instead clusters of cells containing a centralized nucleus and abundant eosinophilic cytoplasm and rare, small intracytoplasmic lipid droplets (Figure 4C), resembling brown adipocytes. To determine if these were indeed brown adipocytes, we performed immunohistochemistry of sections of reproductive tract using antibodies against FABP4 (aP2) and UCP1. As shown in Figure 4D, Fat-ZNF638-KD mice contained more cells with positive staining for both FABP4 (aP2) and UCP1 (Figure 4D) compared to wild type mice.

**ZNF638 knockdown mice weigh less than wild type mice on a high fat diet**

ZNF638 knockdown mice had increased mortality at weaning as well as throughout adulthood with seven mice becoming moribund and euthanized prior to eighteen weeks of life. Only four Fat-ZNF638-KD female mice survived to 10 weeks of age. These females were smaller and weighed significantly less than the wild type littermate controls on a normal diet. To determine if these mice were resistant to diet induced obesity and insulin resistance, surviving Fat-ZNF638-KD mice and wild type litter mate controls were fed a high fat diet for 8 weeks. Fat and lean mass were measured prior to and after the high fat diet challenge and mice were weighed weekly. Although Fat-ZNF638-KD mice weighed less than wild type controls prior to high fat diet challenge, body composition by table top Nuclear Magnetic Resonance (NMR) showed that these mice had similar fat and lean mass when compared to wild type controls (Figures 5C and 5D). Control mice continued to gain weight throughout the challenge while Fat-ZNF638-KD mice gained little to no weight throughout the eight week period (Figure 5B). At the end of the high fat diet challenge, Fat-ZNF638-KD mice had 60% less fat mass compared to wild type controls (Figure 5C). Wild type mice had a significant decrease in lean mass after the eight week challenge while Fat-ZNF638-KD mice maintained their percentage of lean mass (Figure 5D).

Gross examination revealed a marked reduction of subcutaneous, visceral and perigonadal white adipose depots in Fat-ZNF638-KD mice compared to wild type littermates (Figure 5A). To further characterize the phenotype of white adipose tissue in the Fat-ZNF638-KD mice, sections of visceral, perigonadal and subcutaneous white adipose tissue, brown adipose tissue, liver, heart, and skeletal muscle were examined histologically. Visceral and perigonadal depots from wild type control mice were composed of primarily of large, fairly uniform, adipocytes that

contained a peripheralized nucleus. Comparable depots from Fat-ZNF638-KD mice were composed primarily of variably sized small adipocytes and lower numbers of intermingled medium sized adipocytes. Regions of visceral adipose tissue examined from Fat-ZNF638-KD mice also had scattered multifocal regions of small multilocular adipocytes that had slightly eosinophilic cytoplasm (Figure 5E). Haired skin from Fat-ZNF638-KD mice contained significantly less subcutaneous white adipose tissue when compared to littermate controls (Figure 5E). Quantification of adipocyte size in the visceral and subcutaneous depots revealed that adipocytes from wild type mice were significantly larger than ZNF638-KD mice after the high fat diet challenge (Figure 5F).

Under conditions of a positive energy balance such as obesity, brown adipocytes gradually accumulate lipid and acquire a more unilocular appearance similar to white adipocytes opposed to the typical multilocular morphology (Cinti S 2009). Intrascapular brown adipose tissue examined from wild type controls had extensive regions composed of large unilocular adipocytes similar to those observed in obese rodents. In Fat-ZNF638-KD mice, intrascapular brown adipose was composed of densely packed cells with hyperchromatic nuclei and strong eosinophilic cytoplasm that had little to no intracytoplasmic lipid (Figure 5E). Sections of liver examined from the wild type littermate had few hepatocytes that contained intracytoplasmic lipid droplets. There was no intracytoplasmic hepatic lipid accumulation observed in the Fat-ZNF638-KD mice (Figure 5E). There were no histological abnormalities observed in sections of skeletal muscle and heart (data not shown).

The majority of the Fat-ZNF638-KD mice failed to thrive after birth and either died or had to be removed from the study prematurely making difficult to perform metabolic studies. Two of the four Fat-ZNF638-KD mice kept on HFD were euthanized due to weakness and significant

weight loss during the high fat diet challenge. Therefore, metabolic parameters are described for only two surviving mice that survived beyond the eight week high fat diet challenge. Since Fat-ZNF638-KD mice weigh significantly less than wild type littermates, are resistant to diet induced obesity and have markedly reduced visceral, perigonadal and subcutaneous adiposity, it was hypothesized that potential mechanisms for reduced adiposity in Fat-ZNF638-KD mice would include reduced food intake and/or increased metabolic expenditure. Food consumption of Fat-ZNF638-KD mice was significantly higher than that of wild type mice (Figure 5F). Furthermore, Fat-ZNF638-KD mice had a higher resting and total metabolic rate compared to wild type mice both at ambient temperature and at 30ºC (Figures 5F). To characterize the mechanism of increased energy expenditure, total locomotor activity was measured. Fat-ZNF638-KD mice had significantly lower activity levels compared to controls (Figure 5F). These results suggest the presence of energy imbalance in Fat-ZNF638-KD mice during a high fat diet.

**Visceral WAT of Fat-ZNF638-KD Mice had decreased expression of key adipogenic genes**

The development of adipose tissue is tightly controlled by a delicate balance of events driven by a series of transcription factors that leads to the activation of a variety of differentiation-dependent target genes important for triglyceride uptake and storage. To further explore the molecular basis through which the knockdown of ZNF638 impairs adipogenesis, mRNA expression levels of key adipogenic genes responsible of adipocyte differentiation and lipid uptake were examined in visceral adipose tissue of adult mice, after high fat diet challenge. As shown in Figure 6A, significantly lower PPARγ and C/EBPα mRNA levels were detected in Fat-ZNF638-KD mice. C/EBPβ mRNA expression appeared similar between wild type littermate controls and Fat-ZNF638-KD mice. Furthermore, the visceral depot of Fat-ZNF638-KD mice

expressed significantly less leptin and adiponectin mRNA levels compared to controls (Figure 6A). Moreover, perilipin and lipoprotein lipase mRNA expression levels were significantly less in the visceral adipose depot of Fat-ZNF638-KD mice (Figure 6A) while fatty acid binding protein 4 (FABP4, aP2) expression levels in Fat-ZNF638-KD mice were similar to controls (Figure 6A).

No knockdown of ZNF638 was observed in the intrascapular brown adipose tissue of Fat-ZNF638-KD mice and no significant differences in brown adipocyte specific genes, UCP1 or PGC1α were detected (Figure 6B).

## Discussion

In this study, we show in an *in vivo* mouse model that ZNF638 is required for adipogenesis, as mice generated by cre-loxp RNA mediated interference of ZNF638 in adipose tissue have reduced subcutaneous, visceral and perigonadal adipose tissues. This finding supports our *in vitro* studies showing that knockdown of ZNF638 in an adipocytic cell line causes a marked decrease in adipogenesis.

Unexpectantly, Fat-ZNF638-KD mice exhibited increased postnatal lethality with only 4% instead of 6% surviving at weaning. Increased neonatal or postnatal lethality has been described in mouse models generated by total knockout of other critical factors involved in adipogenesis. Interestingly, other models with fat specific deletion have also been shown to have increased postnatal lethality or early death similarly to our model. In particular A-ZIP mice show early death with only 30% surviving into adulthood (Moitra J 1998). In addition, mice with adipose specific deletion of $G_s\alpha$ die prematurely of unknown cause (Chen M 2010). Although we could

not determine the cause of death in Fat-ZNF638-KD mice it is possibly due to a metabolic defect. Further studies on viable mice are needed to study this hypothesis.

Although the fact that Fat-ZNF638-KD mice develop normal white adipose tissue at postnatal day one may suggest that there is no defect in adipocyte differentiation in these mice, the interpretation of the data is complicated by the fact that adipose specific deletion of ZNF638 is accomplished after activation of the aP2 promoter. While this promoter provides an adipose restricted expression, the temporal expression of the ap2 cre recombinase is a late even in fat development, occurring during the late stages of tissue development. Thus, ZNF638 is deleted after adipocytes develop. The role of ZNF638 in inducing differentiation *in vivo* could alternatively be studied in preadipocytes or in total ZNF638 knockout mice. To date however no cre recombinases have been generated that can be expressed specifically in preadipocytes. Furthermore, total ablation of ZNF638 in mice caused embryonic lethality of unknown cause at around 8.5 days post coitus (Meruvu et al, unpublished data).

The appearance of BAT-like, UCP1+, cells in the perigonadal region of 3-week-old Fat-ZNF638-KD mice suggests that these cells have replaced the white adipose tissue (WAT) present in the area. This phenomenon of replacement of white adipose with brown adipose-like tissue *in vivo* has been shown in obese humans and in mice indicating that that these tissues can interconvert (Cinti 2 2009). Similarly, this “transdifferentiation” has been observed after cold acclimatization and prolonged beta3 adrenergic stimulation as BAT-like cells appear in regions once occupied by white adipocytes (Cinti S 2009). One reason explaining the appearance of BAT-like cells in Fat-ZNF638-KD mice could be an increase in sympathetic tone. Another explanation for the appearance of BAT-like cells in perigonadal region of Fat-ZNF638-KD mice is that ZNF638 is required for the maintenance of WAT, at the transcriptional level. While we

found BAT-like cells with increased UCP1 immunoreactivity in the perigonadal depots in Fat-ZNF638 knockdown mice, further studies are required to determine whether Fat-ZNF638-KD mice have increased sympathetic tone and if the increase in UCP1 represents an increase in brown adipocytes within the white adipose tissue, a white to brown adipocyte conversion or expansion of authentic brown adipocytes.

Fat-ZNF638-KD mice show a leaner phenotype compared to wild type mice after 8 weeks of high fat diet indicating that ZNF638 knockdown mice are resistant to diet induced obesity. We investigated two possible mechanisms for obesity resistance caused by adipose specific ablation of ZNF638: increase metabolic rate and decrease food intake. Fat-ZNF638-KD mice show increased resting and total metabolic rate at ambient temperature and at thermoneutrality, when compared to wild type littermate controls. These findings were not due to increase in locomotor activity because Fat-ZNF638-KD mice showed decreased locomotor activity while on a high fat diet when compared to wild type littermate controls. The increase in energy expenditure may be due to an increase in lean mass as Fat-ZNF638-KD mice maintained lean mass while on a high fat diet. The increased lean mass when compared to the wild type littermate controls would be expected to result in an increase in metabolic rate (Tansey J et al 2001). Furthermore, the lean phenotype shown after high fat diet challenge was also not due to a decrease in food consumption in Fat-ZNF638-KD mice since these mice ate significantly more than wild type littermate controls while on a high fat diet, potentially as a compensatory mechanism due to increased energy expenditure.

Knockdown of ZNF638 in 10T ½ cells led to a significant reduction in lipid droplet accumulation during adipocyte differentiation as well as a reduction of key genes involved in adipocyte differentiation, lipid uptake and storage, such as PPARγ, C/EBPα and adiponectin

(Meruvu et al unpublished data). Likewise, Fat-ZNF638-KD mice also exhibited gene expression changes suggesting a defect in adipocyte differentiation and lipid uptake and metabolism. We found that PPARγ and C/EBPα, genes essential for adipocyte differentiation were altered *in vivo* in Fat-ZNF638-KD mice. Similarly, the expression of genes involved in lipid metabolism, perilipin and lipoprotein lipase, was also reduced in the visceral white adipose tissue of Fat-ZNF638-KD mice.

In summary, we have generated adipose specific knockdown mice of ZNF638 in the visceral adipose tissue depot using a novel cre-loxp RNA interference mediated technique. Fat-ZNF638-KD mice show a marked reduction in subcutaneous, visceral and perigonadal adipose tissue and are resistant to diet induced obesity. Similarly to in vitro studies, visceral adipocytes of Fat-ZNF638-KD mice have reduced mRNA levels of key adipogenic gene involved in adipocyte differentiation and lipid storage. In the adult animals analyzed, knock down of ZNF638 caused also increased oxygen consumption as well as increased food intake and led to a leaner phenotype. Our results show that ZNF638 is a potent regulator of adipocyte biology also *in vivo*.

**Table 2. Primers for Gene Expression**

| Primer | Forward (F) primers 5′-3′ | Reverse (R) primers 5′-3′ |
|---|---|---|
| **ZNF638** | ATTGAGAGCTGTCGGCAGTTA | GCAATGAGAACGTCTTCTTGGAG |
| **aP2** | TCGATGAAATCACCGCAGAC | TGTGGTCGACTTTCCATCCC |
| **PPARg** | CTTTCCTGTCAAGATCGCCC | AGTCTGCTGATCTGCGAGCC |
| **C/EBPa** | GAACAGCAACGAGTACCGGGT | GCCATGGCCTTGACCAAGGAG |
| **C/EBPb** | CAAGCTGAGCGACGAGTACA | CAGCTGCTCCACCTTCTTCT |
| **Adiponectin** | TGTTCCTCTTAATCCTGCCCA | CCAACCTGCACAAGTTCCCTT |
| **Leptin** | GAGACCCCTGTGTCGGTTC | CTGCGTGTGTGAAATGTCATTG |
| **Perilipin** | ACAGCAGAATATGCCGCCAA | GGCTGACTCCTTGTCTGGTG |
| **Lipoprotein Lipase** | GGGAGTTTGGCTCCAGAGTTT | TGTGTCTTCAGGGGTCCTTAG |
| **UCP1** | GGCCCTTGTAAACAACAAAATAC | GGCAACAAGAGCTGACAGTAAAT |
| **PGC1** | ACCATGACTACTGTCAGTCACTC | GTCACAGGAGGCATCTTTGAAG |
| **18S** | AGTCCCTGCCCTTTGTACACA | CGATCCGAGGGCCTCACTA |

**Figure 2. The generation of ZNF638 knockdown (Fat-ZNF638-KD) mice.** (A) Schematic of *U6-ploxPneo-ZNF638* vector before and after deletion of *ploxPneo* by cre recombinase. (B) Quantitative analysis of ZNF638 RNA in wild type control and Fat-ZN638-KD mice. RT-PCR is normalized by 18s. There is a 60% reduction of ZNF638 mRNA in the visceral WAT of Fat-ZNF638-KD mice and no significant knockdown of ZNF638 in the intrascapular BAT when compared to WT littermate controls. WT, wild type; KD, knockdown, WAT, white adipose tissue; BAT, brown adipose tissue. *p<0.05 versus controls; mean ±SEM; NS, no significance.

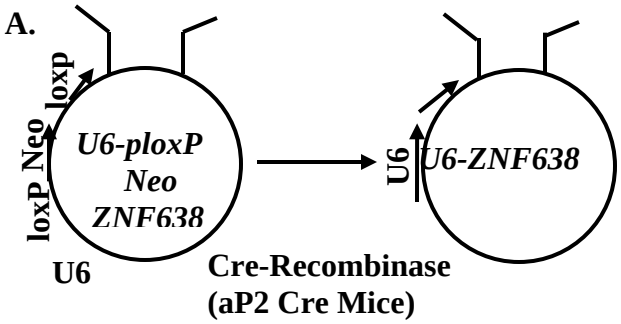


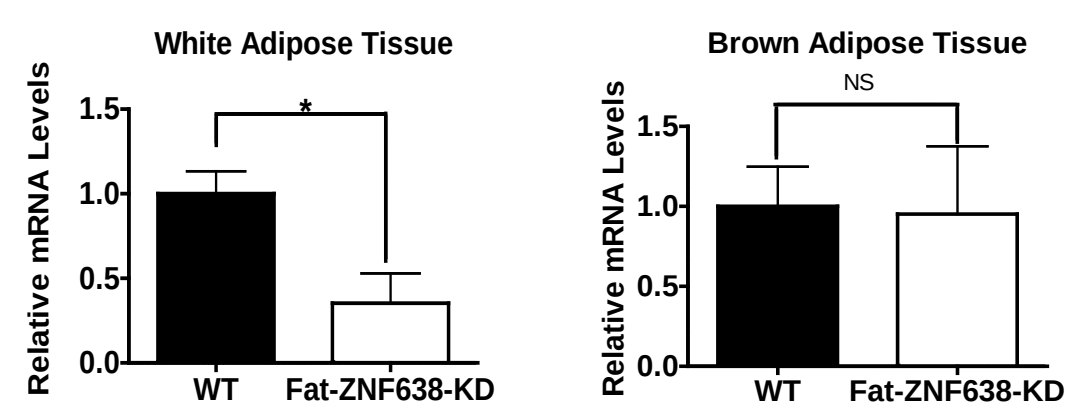

**Table 3. Fat-ZNF638-KD mice died at the early neonatal stage.**

| Ages | Total | WT | *U6-ploxPneo-ZNF638* | *U6-ZNF638;aP2-cre* | aP2-cre |
|---|---|---|---|---|---|
| **1-day-old** | 52 | 32 (62%) | 10 (19%) | 7 (13%) | 7 (13%) |
| **At weaning** | 257 | 148 (58%) | 43 (17%) | 11 (4%) | 56 (22%) |

**Figure 3. One-day-old Fat-ZNF638-KD mice have no gross abnormalities and are normoglycemic.** (A) One-day-old ZNF638 knockdown mice show no growth retardation and are able to suckle. (B) Glucose levels were measured from intravenous blood taken from the jugular vein in one-day-old Fat-ZNF638-KD and wild type control mice. Fat-ZNF638-KD mice are normoglycemic as compared to wild type controls. (WT, n=51; KD, n=7). (C) Longitudinal sections made from one-day-old WT and Fat-ZNF638-KD mice were analyzed at the level of the neck for the presence of white adipocytes. Top: Hemotoxylin and Eosin. Small clusters and lobules of pre-adipocytes and immature lipid-laden cells are present in the subcutaneous region of WT (left) and Fat-ZNF638-KD (right) mice. Middle and Bottom: Immunohistochemical expression of anti-FABP4 and anti-UCP1α polyclonal antibodies. Diffuse cytoplasmic FABP4 and negative UCP1α staining of primitive white adipocytes in the subcutaneous region of WT and Fat-ZNF638-KD mice indicates cells are of white adipocyte origin. (WT, n=4, ZNF638 KD, n=3). FABP4, fatty acid binding protein 4; UCP1, uncoupling protein 1.

**A.**

**B.**

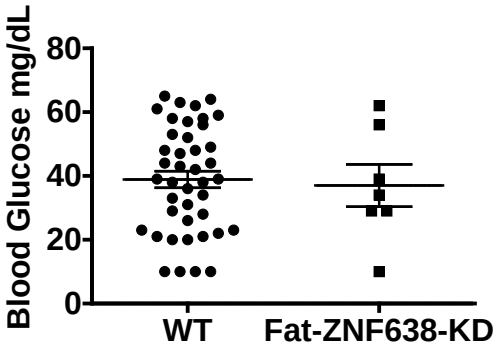

**Figure 3 (continued)**

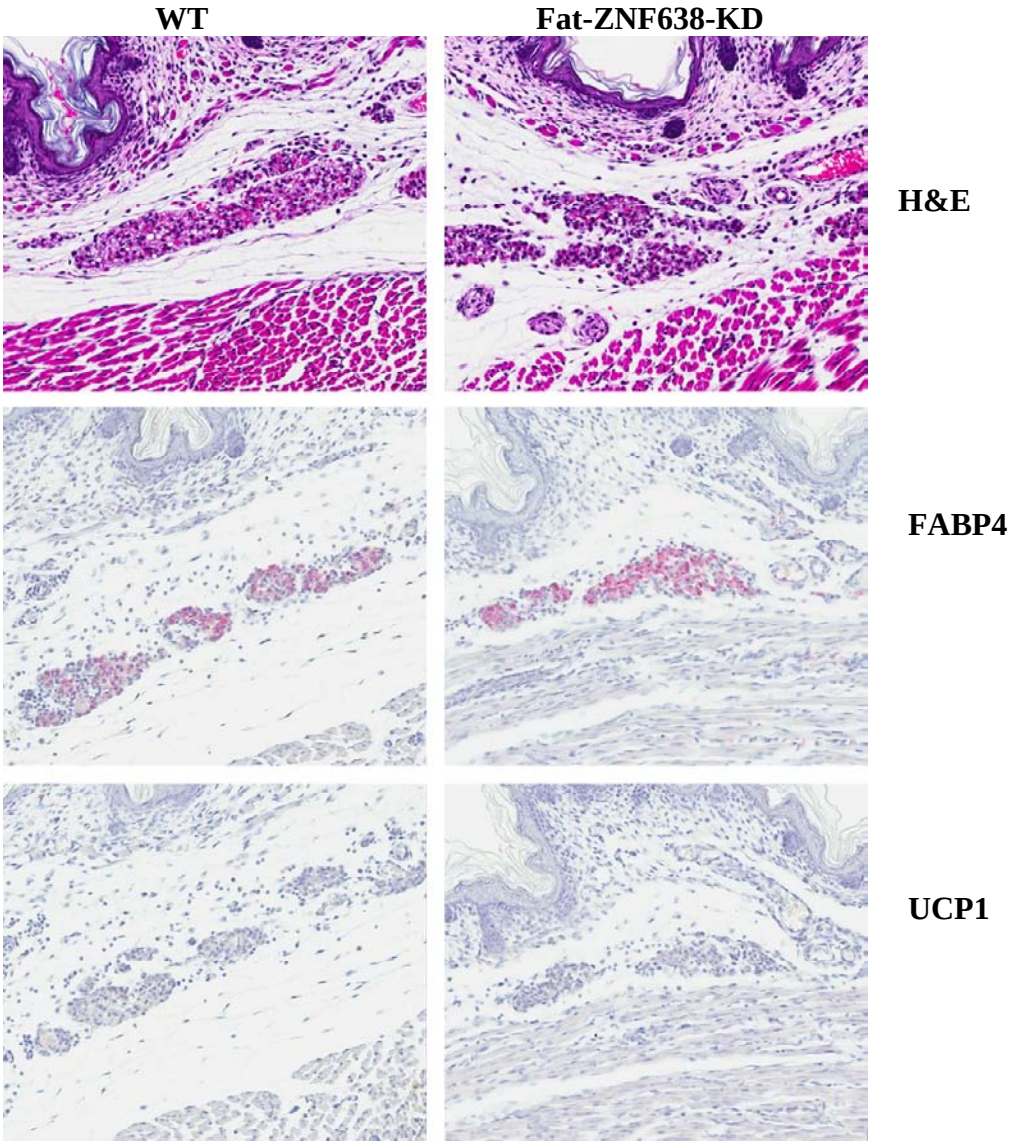

**Figure 4. Three-week-old show growth retardation and have no perigonadal white adipose tissue** (A) Three-week-old Fat-ZNF638-KD mice show growth retardation (right). (B) Top: Hemotoxylin and Eosin staining of subcutaneous and perigondal WAT. Three-week-old Fat-ZNF638-KD mice (right) have little to no subcutaneous WAT and no perigonadal WAT when compared to WT littermate controls (left). Bottom: Immunohistochemical expression of anti-FABP4 and anti-UCP1α in the perigonadal WAT. Perigonadal cells in three-week-old Fat-ZNF638-KD mice express FABP4 and UCP1α. (WT, n=3, KD, n=4). WAT, white adipose tissue; FABP4, fatty acid binding protein 4; UCP1, uncoupling protein 1.

**4A.**

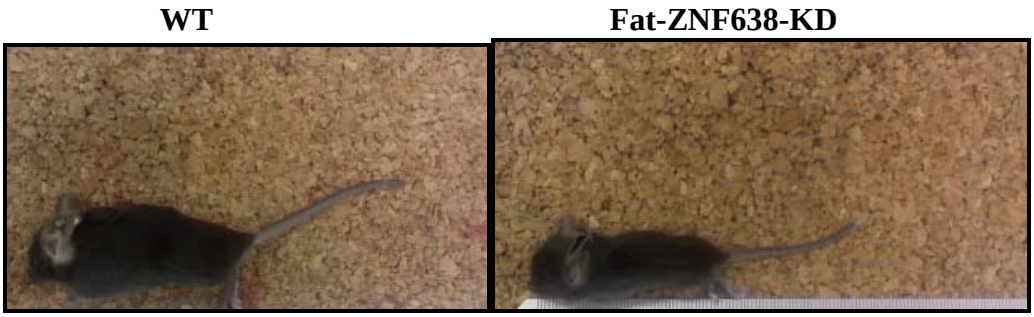

**Figure 4 (continued)**

**4B.**

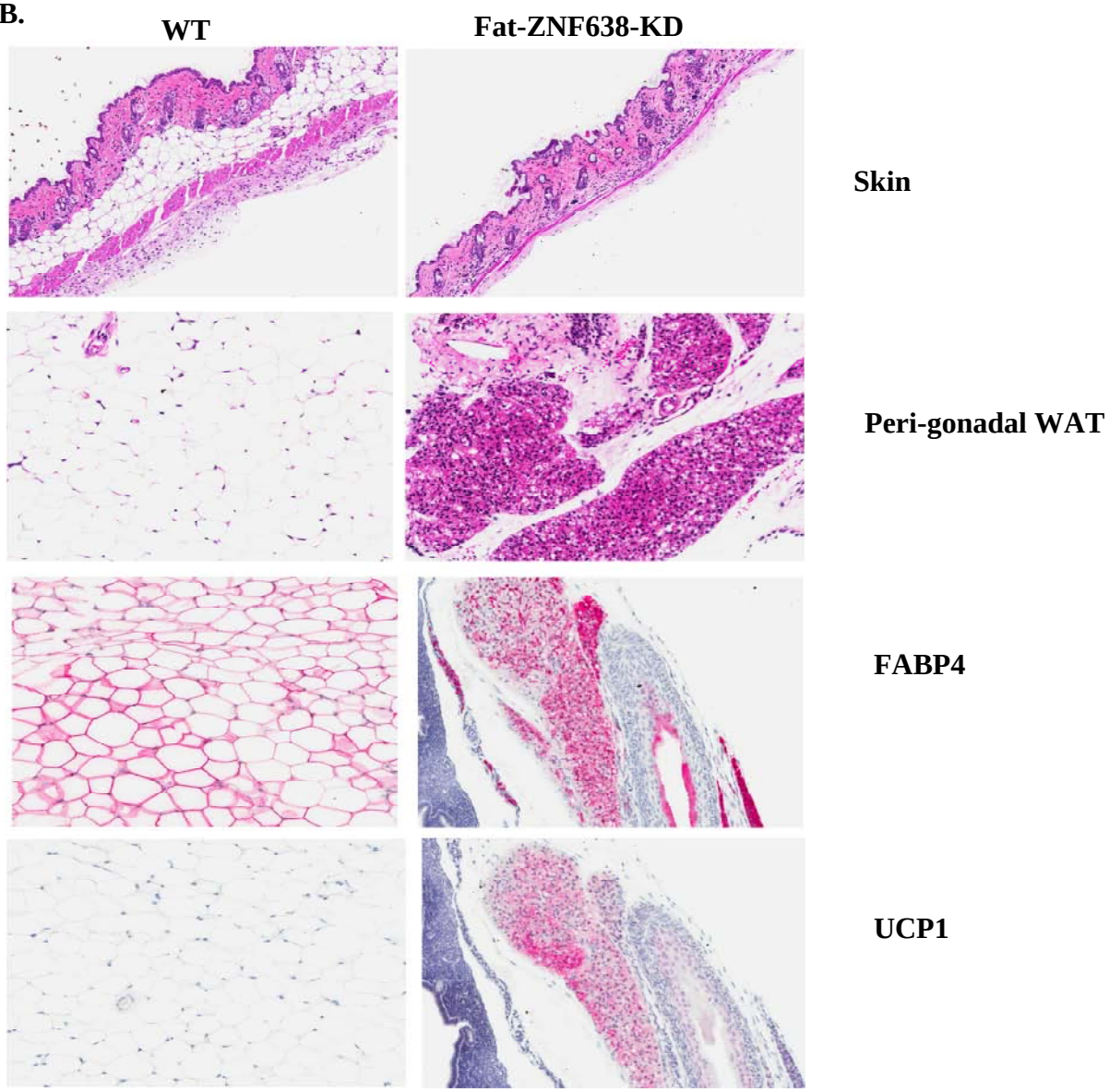

**Figure 5. ZNF638 knockdown mice have reduced white fat after a high fat diet** (A) Visceral, mesenteric, perirenal and perigondal depots are severely affected in ZNF638 knockdown mice (B) Control mice show a significant weight gain during the 8 week HFD challenge, while Fat-ZNF638-KD gained little to no weight during the challenge (WT, n=10, KD, n=6). (C) Fat and lean mass expressed as % body weight prior to and after 8 week high fat diet challenge. Control mice show a significant increase in fat mass and a significant decrease in lean mass while, Fat-ZNF638-KD mice show little change in fat mass and maintains lean mass after the 8 week HFD challenge (WT, n=6; KD, n=4). (D) Hematoxylin and Eosin staining of visceral, subcutaneous and perigonadal white adipose tissue, brown adipose tissue and liver from a wild type control (left) and a surviving adult Fat-ZNF638-KD mouse (right). Fat-ZNF638-KD mice have smaller visceral adipocytes when compared to WT littermate controls. HFD often leads to lipid accumulation in the BAT and liver (indicated in the controls), which is not present in the Fat-ZNF638-KD mice. (E) Graphic representation of visceral and subcutaneous WAT cells size after high fat diet, indicating a significant difference in Fat-ZNF638-KD WAT cells size compared to WT littermate controls. (F) The metabolic phenotype of surviving adult Fat-ZNF638-KD mice was determined at the end of the 8 week HFD challenge by measuring food intake, resting and total energy expenditure rate ($O_2$ consumption) and total activity. Food intake was measured in individually caged mice by tunnel type feeders and motor activity was determined by infrared beam interruption. Oxygen consumption and carbon dioxide production (energy expenditure) were measured over 24 hours at 30ºC and 23ºC with an 8-chamber Oxymax system with one mouse per chamber. (WT, n=5; ZNF638 KD, n=2). HFD, high fat diet. *p< 0.05, **p<0.01, ***p<0.001; mean ±SEM.

**5A.**

**WT** **Fat-ZNF638-KD**

**Figure 5 (continued)**

**5B.**

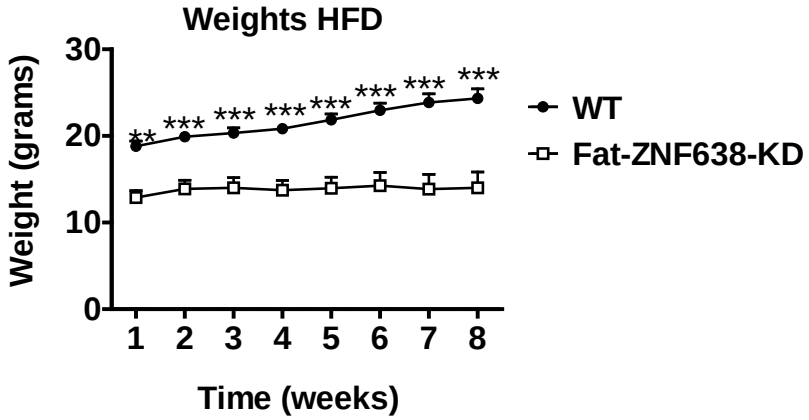


**5C.**

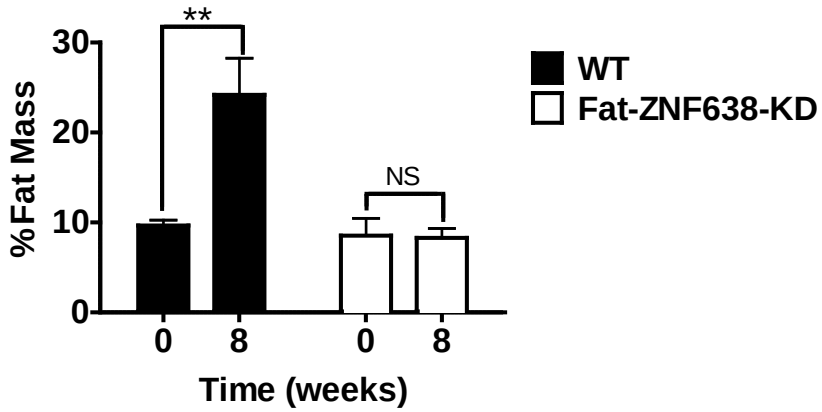


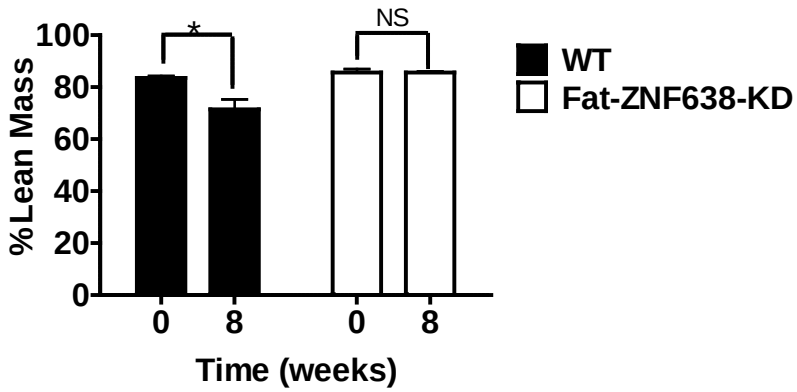

**Figure 5 (continued)**

**5D.**

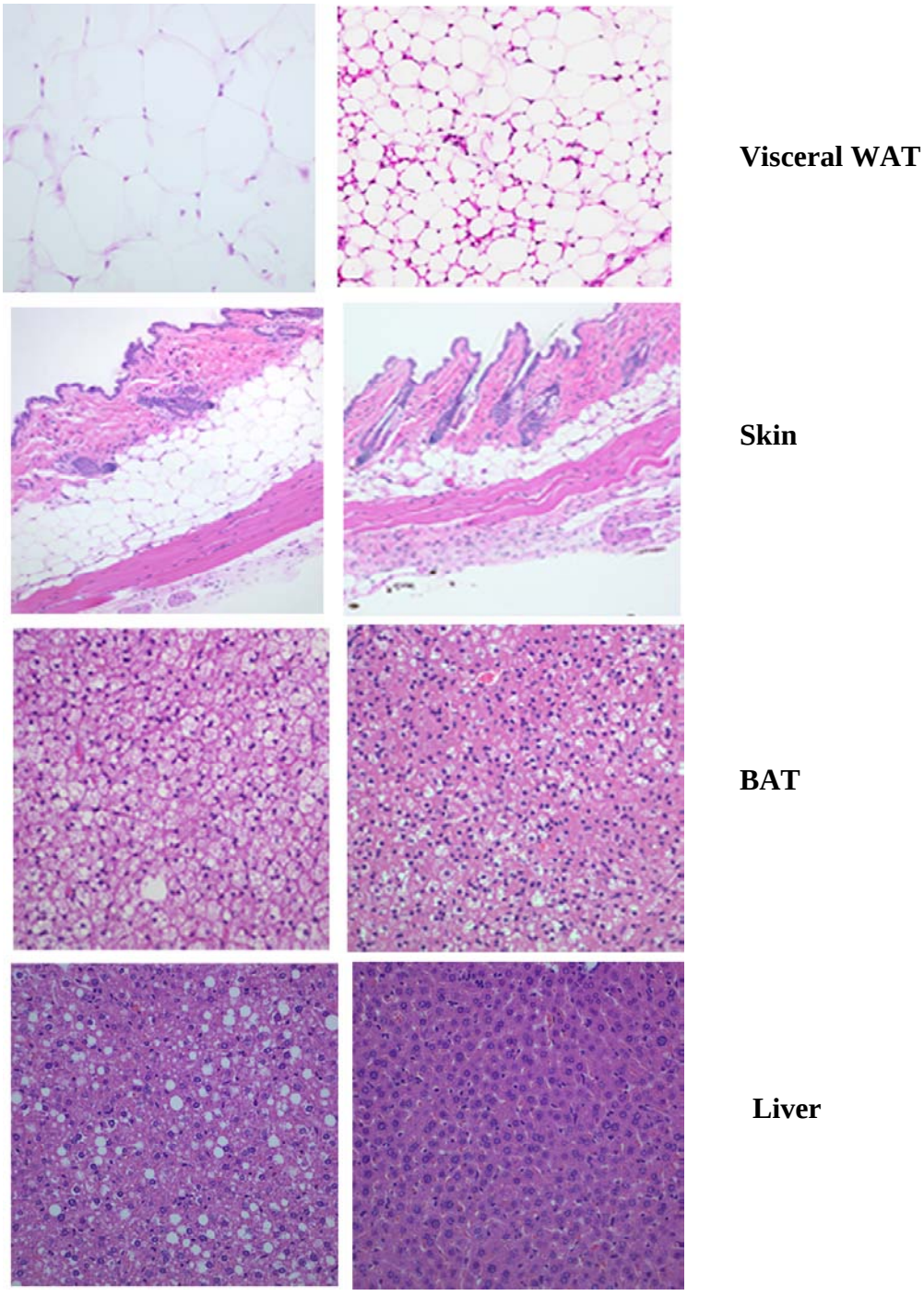

**Figure 5 (continued)**

**5E.**

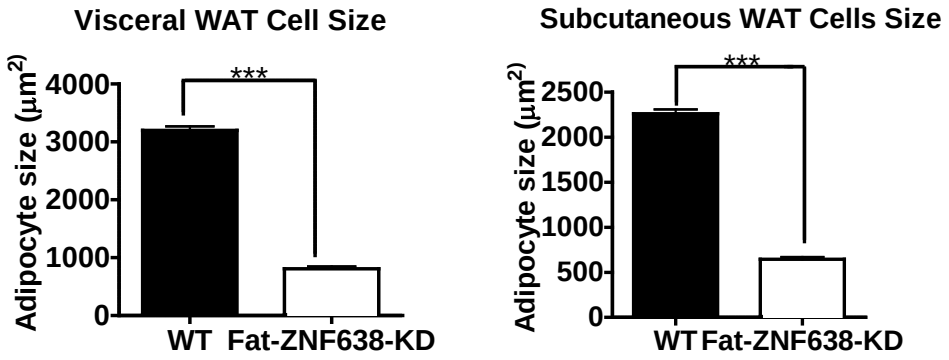


**5F.**

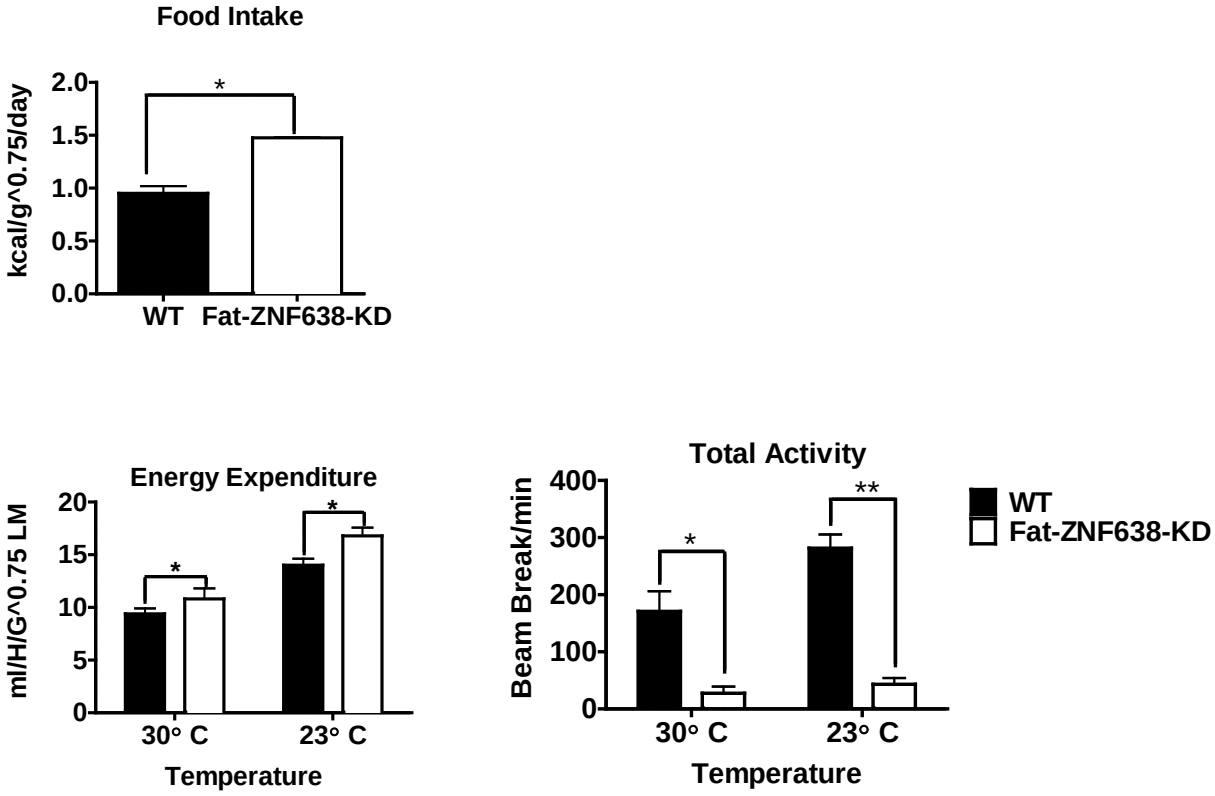

**Figure 6. Gene expression in visceral white and intrascapular brown adipose tissue from adult control and ZNF638 KD mice after high fat diet challenge.** (A) Quantitative expression of adipogenic genes in visceral white adipose tissue. (B) Quantitative expression of adipogenic genes in intrascapular brown adipose tissue (WT=6; KD, n=4,). Data is normalized to 18s and calculated as fold change. PPARγ, Peroxisome proliferator activated receptor γ; C/EBPα, CCAAT/enhancer-binding protein α; LPL, lipoprotein lipase; C/EBPβ, CCAAT/enhancer-binding protein β, FABP4, fatty acid binding protein 4; UCP1α, uncoupling protein 1α, PGC1α, PPARγ coactivator 1α. *p< 0.05, **p<0.01, ***p<0.001; mean ±SEM.

**6A. WAT**

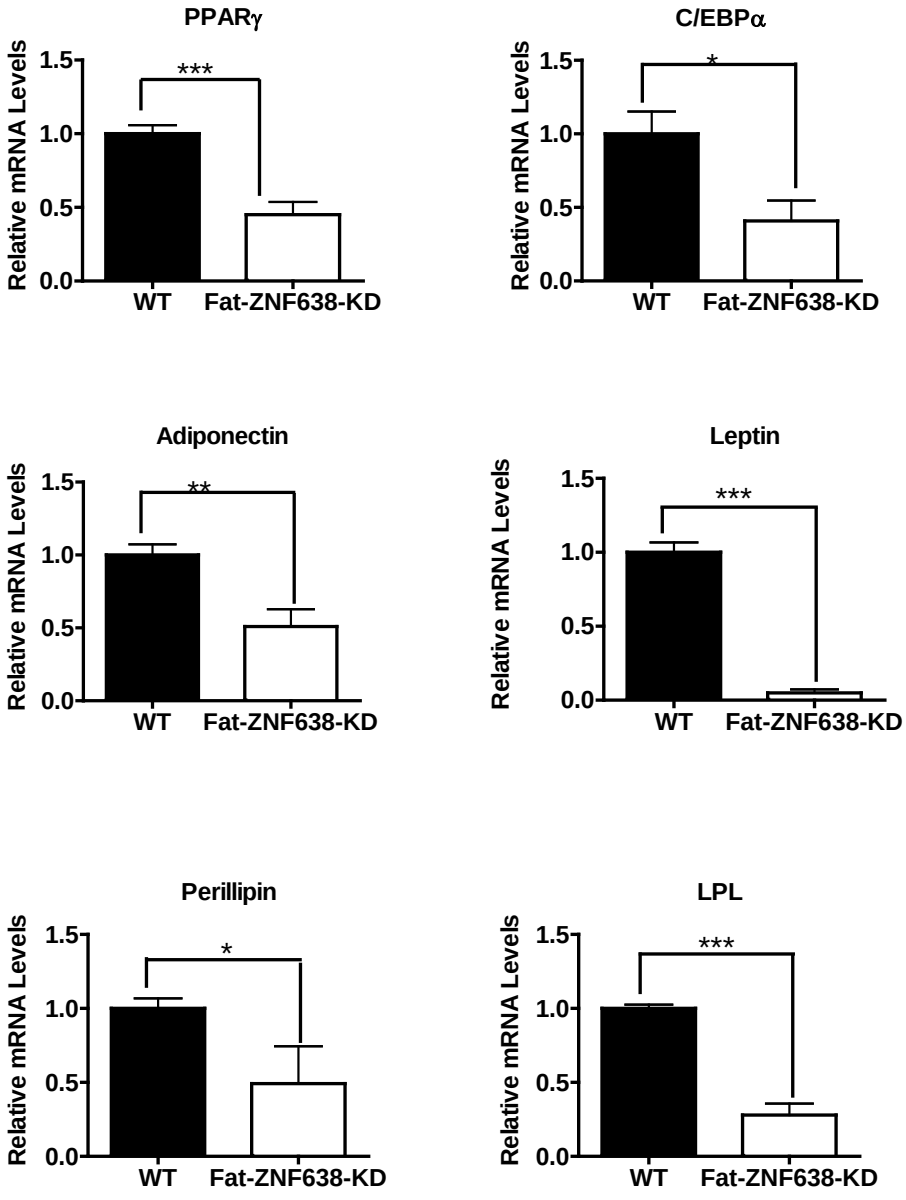

**Figure 6 (continued)**

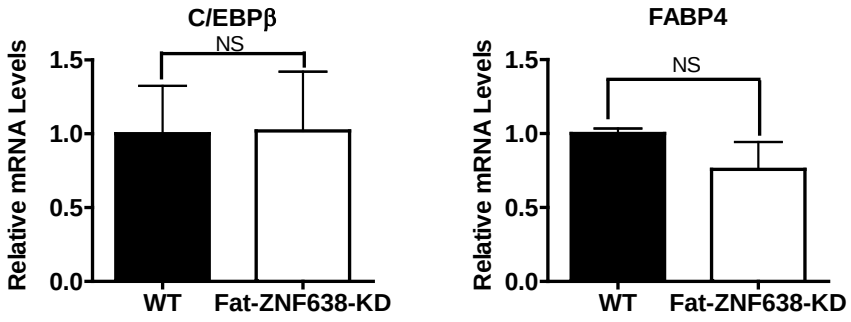


**6B.**

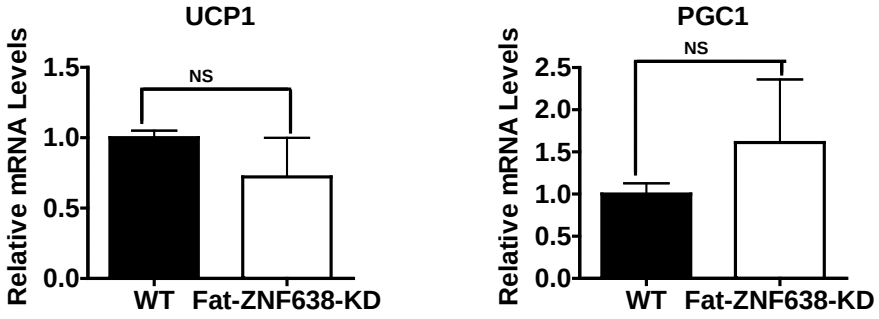

## CHAPTER TWO

### Identification of a novel molecule Smad4 Interacting Factor (SMIF) Involved in Adipogenesis

**Abstract:** ZNF638, a zinc finger protein, and its novel isoform, Nuclear Matrix Coactivator (NMC1) have recently been identified to be essential modulators of adipocyte development in vitro. We wanted to identify the mechanism of action of NMC1 by characterizing its functional interactions with transcription factors that are involved in adipogenesis/lipid metabolism. A novel high throughput cell based screening strategy termed the coactivator trap, an arrayed library of 837 plasmids coding for human transcription factors fused to a GAL4 domain, was used to screen for novel protein-protein interactions between NMC1 and other transcription factors. Eleven transcription factors, including CITED-2, ID3 and SMIF were identified to have a greater than two fold change in transcriptional activity upon cotransfection with NMC1. All ten candidates were sequenced and transcriptional activity was reconfirmed. Of the candidate genes identified, smad4-interacting protein (SMIF), or mRNA-decapping enzyme 1A, was further studied. Previous studies have shown that SMIF forms a BMP4 inducible complex with Smad4 and is a crucial activator of TGFβ signaling. In this study, we show that SMIF is highly regulated during adipogenesis with the highest expression in undifferentiated 3T3-L1 cells, with SMIF mRNA expression dramatically decreasing to nearly undetectable levels as differentiation progresses. We show that SMIF physically interacts with PPARγ and transcriptionally inhibits its activity. In conclusion, our *in vitro* data proposes that SMIF may be a novel regulator of adipogenesis through the control of PPARγ activity. Further studies are needed to determine SMIFs effects on adipocyte differentiation and its mechanism of action.

## Introduction

Transcription is regulated by large multi-subunit complexes that can be grouped into three general categories: transcription factors, coregulators (coactivators and corepressors) and components of the basal transcriptional machinery. DNA binding proteins recognize discrete sequences or response elements within promoters and in general function as scaffolds that direct the recruitment of coregulatory proteins (Amelio, Miraglia et al. 2007). Coregulators, that are capable of directly binding to transcription factors and positively regulate target gene transcription, are designated as coactivators, while negative regulatory proteins inhibit target gene transcription are referred to as corepressors (Yu and Reddy 2007).

PPARγ, the master regulator of adipogenesis, requires the interaction with coregulators for efficient transcriptional regulation. To date there have been no reports of a specific coregulator that interacts solely with PPARγ and generally it has been shown that many cofactors known to interact with other nuclear receptor family members are also able to regulate PPARγ activity. These cofactors include the coactivator CBP/300, TRAP220 and the SRC family of coactivators while corepressors include SMART, NcoR, and RIP140 (Tontonoz and Spiegelman 2008).

We recently identified ZNF638 as a novel regulator of adipogenesis (Meruvu et al unpublished data). ZNF638 was found to be highly regulated during adipogenesis and overexpression studies revealed that it promotes adipogenesis (Meruvu et al, unpublished data). Analysis of ZNF638 knockdown (Fat-ZNF638-KD) mice showed a marked deficiency in adipose tissue and resistance to diet induced obesity (Hayes et al, unpublished data). Four novel isoforms of ZNF638, produced by alternative splicing of a common pre-mRNA, have been previously cloned from mouse heart (ZNF638 α, β, γ and δ) (Matsushima Y et al 1996). Our laboratory has recently identified a novel isoform of ZNF638 cloned from brown adipocytes that

was called nuclear matrix coactivator 1 (NMC1) (Meruvu et al, unpublished). This isoform is 150 kd and contains a RS, RRM1, ZF1 and ZF2 domains, while lacking the RRM2, DNA binding domains and acidic repeats present in the full length ZNF638 isoform. Similarly to ZNF638, NMC1 expression is regulated during adipogenesis. Furthermore, its overexpression and knockdown modulates adipocyte differentiation (Meruvu et al, unpublished data).

To better understand the mechanisms by which NMC1 affects adipocyte differentiation, we sought to identify novel NMC1 interacting transcription factors. We used a high-throughput cell based screening strategy, termed the "coactivator trap" to study the functional interactions of NMC1 with all transcription factors. The coactivator trap has recently been used to identify novel interacting partners of TORCs (Amelio A et al 2007).

## Materials and Methods

### Antibodies and Reagents

Anti-SMIF antibody was purchased from Abcam. Anti-B-actin antibody was purchased from Sigma-Aldrich (St. Louis, MO, USA). Secondary antibody, Horseradish peroxidase-conjugated anti-mouse IgG was purchased from Amersham Biosciences (Piscataway, NJ, USA). Dexamethasone, insulin, and 3-isobutil-1-methylxantine (IBMX) were purchased from Sigma-Aldrich (St. Louis, MO, USA). Troglitazone (Rezulin) was purchased from Parke-Davis (Morris Plains, NJ, USA).

**Plasmids**

For overexpression studies, SMIF cDNA was cloned into TOPO pcDNA 3.3 (Invitrogen) after PCR amplication of 3T3-L1 cells using TripleMaster Taq Polymerase (Eppendorf) with the following primers SMIF F-5′-AATTC AAGCTTGCCACCATGGACTACAAAGACGATGA CGATA AA AGTCTGGCGGCCTTGAA-3′ and SMIF R-5′ CTTAAG TCATAGGTTGTGGT TGT-3′. SMIF cDNA was subsequently inserted into pMSCV (Clonetech) and Pgex-4T3 plasmids using EcorRI restriction enzyme.

**High Throughput Transfection and Reporter Assay (Coactivator Trap)**

The coactivator trap was performed as previously described (Amelio et al). Briefly, HEK293T cells were cultured in DMEM (Invitrogen) supplemented with 10% FBS and antibiotics (100 units/ml of penicillin and 100 μg/ml of streptomycin). Reverse transfection was carried out using the arrayed transcription factor library collection containing 10 ng of transcription factor CM-GAL4 fusion cDNA per well. Serum-free DMEM (20 μl), containing test cDNA (cDNA encoding NMC1), the reporter GAL4::lucifease, and Fugene 6 (Roche Diagnostics) was added into each well. After a 20-min incubation at room temperature, DMEM containing 20% FBS (20 μl) containing $10^5$ 293T cells in suspension was dispensed into each well. Cells were cultured for 24 h in a humidified incubator at 37°C in 5% $CO_2$. BrightGlo (Promega) reagent (35 μl) was added to each well and luciferase luminescence was measured with an Acquest plate reader (LJL Biosystems). The screening assay was performed in duplicate.

**Cell Culture**

HEK293, 3T3-L1, 10T1/2 cell lines (ATCC) were grown in Dulbecco's modified Eagle's medium (DMEM) (Mediatech) supplemented with 10% Fetal Bovine Serum (Hyclone) and 1% penicillin/streptomycin (Mediatech) in 5% $CO_2$.

**Small scale Transfection Assays**

$3x10^5$ cells were transfected with Nucleofector or Shuttle devices (Amaxa) according to the optimized protocols available for each cell line following the manufacturer's instructions. Cells were transfected with 1 µg of cDNA or 100nM of siRNA (ON-Target*plus SMART*pool) and induced to differentiate in by an induction medium containing troglitazone (10µM), insulin (5 µg/ml), IBMX (0.5 µM) and dexamethasone (1µM) 24 hours after transfection and harvested 48 hours later. All experiments were performed in triplicate.

**Luciferase Assay**

To validate the screen results, Gal4 luciferase reporter plasmid and NMC1 were cotransfected with the following gal4 fusion protein plasmids: PPARγ-gal4, SMIF-gal4, Btbd3-gal4, TBPL1-gal4, Znf643-gal4, Creb-gal4, SIRT-gal4, PITX-gal4, ID3-gal4, TCF19-gal4, CITED2-gal4, and NKYB-gal4. PPRE-luciferase reporter plasmid was transfected with PPARγ and SMIF pcDNA plasmid. Reporter plasmids along with effector plasmids were transfected into HEK293 cells at 80-90% confluence using FuGENE 6 (Roche). Cells were harvested after 48 hours and luciferase was analyzed using a Promega dual-luciferase assay kit as recommended by the manufacturer. All experiments were repeated at least 3 times.

**Adipocyte Differentiation**

For adipocyte differentiation, confluent 3T3-L1 were exposed to an induction medium containing dexamethasone (1 µM), insulin (5 µg/ml), IBMX (0.5 µM), and 10% FBS. After forty-eight hours of inductions, cells were maintained on insulin (5 µg/ml), penicillin/streptomycin and 10% FBS until collection. Cells were harvested at different time points for RNA and protein analysis. For 10T ½ differentiation, cells were cultured in DMEM, supplemented with 10% FBS, penicillin/streptomycin, troglitazone (10 µM) and insulin (5 µg/ml).

**Gene Expression Analysis**

Total RNA was extracted from cultured cells or tissues with Trizol (Invitrogen) and treated with DNase (Ambion). mRNA was reverse transcribed using the High Capacity cDNA archive kit (Applied Biosystems). Real time PCR (RT-PCR) was performed with ABI PRISM 7900HT Sequence Detection System (Applied Biosystems) using SYBR green (Roche). Primers to detect 18S were used to normalize sample data. For analysis of SMIF, PPARγ and aP2, the following primers were used: PPARγ-F5'-CTTTCCTGTCAAGATCGCCC-3', PPARγ-R5'-AGTCT GCTGATCTGCGAGC-3', aP2-F 5'-TCGATGAAATCACCGCAGAC-3', aP2-R 5'-TGTG GTCGACT TTCCATCCC-3'.

**Immunofluorescence**

3T3-L1 cells were plated on Lab-Tek Slides (Nalge Nunc International) and fixed in 4% paraformaldehyde (Invitrogen) for 15 minutes at 37ºC. Cells were stained for anti-SMIF with the

SelectFX Alexa Fluor 488 Perioxisome Labeling Kit (Invitrogen), according to the manufacturer's protocol. Briefly, cells were permeabilized with permeabilization solution (100X, 20% Triton X-100) for 5 minutes, then washed with PBS and treated with blocking solution containing 3% BSA and PBS for 1 hour at room temperature. Cells were subsequently incubated overnight in anti-SMIF at a dilution of 1:100. Cells were washed 3 times with blocking solution and incubated in Alexa Fluor 488 anti-mouse antibody at 1:1000 dilution for 30 minutes. Slides were mounted with DAPI-containing solution (Invitrogen).

**Retrovirus**

SMIF cDNA was inserted in pMSCV plasmid (Clonetech) at the EcorRI restriction site. Recombinant pMSCV viral packaging was achieved by transfection of the following plasmids using Fugene 6 into 293 FT cells: pMSCV with and without SMIF (10 µg), GAG-POL (7µg) and VSVG (2.5µg). Cells were maintained in DMEM containing 10% FBS, 1% penicillin/ streptomycin and 10 mM HEPES for 48 hours. Viral supernatants were supplemented with 8 µg polybrene, filtered through a 0.45 µm filter and added to 10T ½ cells for infections for 24 hours. Cells were selected with 2 µg/ml of puromycin, expanded and seeded for differentiation experiments.

**GST Pulldown Assay**

SMIF cDNA was inserted into Pgex-4T3 plasmid (Clonetech) using the EcorRI restriction enzyme to express GST-SMIF. GST-SMIF fusion protein was generated in Escherichia coli (BL21 strain, Stratagene, La Jolla, CA). Cells were cultured in LB medium (Life Technologies, Inc.) and ampicillin to a density of A 600 = 0.75 and induced by addition of isopropyl-1-thio-β-

d-galactopyranoside (IPTG) to a final concentration of 1 mm. The isopropyl-1-thio-β-d-galactopyranoside-induced cultures were grown at room temperature for an additional 2 hours, before cells were harvested by centrifugation for 10 min at 7700 ×g at 4° C. The cell pellet was resuspended in 16 ml of PBS and sonicated on ice for 2 minutes. 800 µl of 20% Triton X-100 was added to the lysate, rocked at room temperature for 30 minutes and centrifuged at 12,000 x g for 10 minutes at 4°C. The GST-PPARγ fusion proteins were purified from the cell pellet lysate using 200 µl of glutathione-Sepharose 4B beads (Amersham Pharmacia Biotech) rocked at room temperature for 30 minutes. Beads/cell lysate were washed three times with PBS to remove unbound material, resuspended in 150 µl of PBS to make a 50% slurry and stored at 4º C. 30 µl of GST-SMIF was run on a 15% sodium dodecyl sulfate-polyacrylamide gel (SDS-PAGE) and stained with Coomassie blue to visualize and quantify the GST labeled protein. The following were used as standards: 1 µg, 2 µg, 4 µg and 8 µg of Bovine Serum Albumin (BSA). Binding assays were carried out as follows: 5 µl of $^{35}$S-methionine-labelled full-length PPARγ, prepared using TNT transcription-translation system (Promega), was incubated with GST-SMIF for 1 hour at room temperature in GST binding buffer (1 M HEPES containing 2 M KCl, 50% glycerol, 0.5 EDTA, 1 M DTT, 1 M MgCl and 20 % NP-40). The beads were washed three times with binding buffer and bound proteins were eluted in 30 µl of 2x sample loading buffer and run on a 12.5% SDS polyacrylamide gel electrophoresis for analysis by autoradiography.

## Results

### Identification of novel NMC1 interacting proteins through the transcription factor trap

The coactivator trap was developed and used previously to screen for interacting partners of TORCs (Amelio A et al 2007). In an effort to understand the mechanisms by which NMC1 influences adipocyte differentiation, we sought to identify NMC1 interacting factors.

To determine positive interactors (hits) from the coactivator trap assay for later experimental validation, we included PPARγ as a positive control. We considered positive interactors gal4 fusion proteins that when coexpressed with NMC1 exceeded a 2 fold change in transcriptional activation of a Gal4 reporter. To validate the proteins activating the Gal4 reporter identified in the screen, we performed luciferase assays at a smaller scale (Figure 7). Of the eleven reconfirmed interacting proteins, DCP1a, or SMIF, was of particular interest because a previous study implicated SMIF as a Smad4 coactivator that functions in TGFβ signaling (Bai et al 2003). TGFβ signaling pathways have a central role in adipogenesis (Choy L et al 2000).

### SMIF is highly regulated during adipocyte differentiation

To determine whether SMIF is expressed in murine adipose tissues and to quantify its levels in this tissue relative to other organs, we analyzed the SMIF mRNA levels by real-time PCR, in metabolic tissues. As shown in Figure 8A, the highest level of SMIF expression was identified in the kidney followed by the spleen, heart and muscle. Interestingly, SMIF RNA levels were detected also in white and brown adipose tissue. To investigate whether SMIF mRNA is regulated during adipogenesis *in vitro*, we analyzed SMIF gene expression during different stages of differentiation in 3T3-L1. We observed that SMIF mRNA was expressed in confluent 3T3-L1 preadipocytes and markedly diminished upon adipocyte differentiation (Figure 8B). As

expected, other factors such as PPARγ and adipocyte fatty acid binding protein (aP2) were induced during 3T3-L1 differentiation. The SMIF expression pattern was similar to that of other transcription factors that have been shown to inhibit adipogenesis such as KLF2, KLF3 and GATA2 and GATA3 (Tong Q, 2000, Banerjee S, 2003, Sue N, 2008).

**Endogenous SMIF translocates to the nucleus during adipocyte differentiation**

Previous studies demonstrated that SMIF translocates to the nucleus only in response to TGFβ treatment (Bai R et al 2003). Immunoflourescence experiments in 3T3-L1 preadipocytes demonstrated that SMIF was able to shuttle back and forth from the nucleus to the cytoplasm throughout adipocyte differentiation only in the presence of adipogenic inducers (10% FBS, IBMX, dexamethasone and insulin). SMIF was found to be predominantly located in the nucleus at day 0 when 3T3-L1 cells are confluent and prior to the addition of the inducing cocktail. SMIF was again primarily nuclear at day 4. At later time points in 3T3-L1 differentiation, when cells have accumulated intracytoplasmic lipid droplets, SMIF was predominantly located within the cytoplasm (Figure 9). No nuclear localization signal could be found in SMIF. Thus, we suggest that cellular localization of SMIF is dependent on its interaction with proteins, possibly Smad4 as suggested by Bai and colleagues (Bai et al 2003).

**Stable transfection of SMIF causes slow cell growth and loss of cellular adherence**

The reduced expression of SMIF mRNA expression during 3T3-L1 differentiation suggested a potentially inhibitory role in adipogenesis. To investigate this possibility, we retrovirally overexpressed SMIF and empty vector (EV) as a control in 10T ½ cells. For adipocyte differentiation, cells were plated in 24 well plates. After 24 hours, the majority of the cells

underwent several morphologic changes. Compared to the EV-infected cells, SMIF overexpressing cells grew significantly slower. Under phase-contrast microscopy cells overexpressing SMIF became rounded rather than becoming the normal elongated shape of fibroblasts and detached from the culture dish. Cell suspensions were collected and trypan blue dye was used as a marker of cell viability. Results showed that almost 100% of SMIF overexpressing cells were viable. To verify SMIF overexpression in SMIF-infected cells, we assessed SMIF mRNA expression by RT-PCR. SMIF-infected cells had three folds higher levels of SMIF mRNA expression when compared to the empty vector expressing cells. SMIF-infected cells treated with adipogenic inducers often formed clumps and did not accumulate intracellular lipid (data not shown).

**SMIF inhibits PPARγ transcriptional activity**

PPARγ is considered to be the master regulator of adipogenesis. To determine if SMIF mediates the transcriptional activity of PPARγ, we cotransfected SMIF and the DR1-luc reporter. Cotransfection of SMIF and the DR1-luc, resulted in an ~50% inhibition of PPARγ activity (Figure 10). These data suggest that SMIF inhibition may be mediated by direct interaction with PPARγ or inhibition of regulatory factors that can induce PPARγ expression. With respect to the first possibility, GST pulldown studies were performed. Using in vitro translated $^{35}$S-radiolabeled PPARγ and GST fusion proteins containing SMIF, we demonstrated that PPARγ interacts with GST-SMIF fusion protein (Figure 11).

## Discussion

Smad4 interacting protein (SMIF) or mRNA decapping enzyme alpha (DCP1a) was initially identified as a key component of mRNA decay process in *S.* cerevisiae and later identified to interact with Smad4 and act as a crucial activator of TGFβ signaling (Andersen J 2002 and Bai R et al 2003). TGFβ signaling regulates the differentiation program of a variety of cell types including adipocytes. TGFβ inhibits adipocyte differentiation by Smad3 interacting with C/EBP and repressing C/EBP transactivation function (Choy L and Derynck R 2003). Furthermore, transgenic overexpression of TGFβ1 in adipose tissue severely reduces both white and brown adipose tissue depots and results in the failure of adipocytes to differentiation (Clouthier et al 1997). It has also been demonstrated that Smad 2, Smad 6 and Smad 7 act as negative regulators of adipogenesis (Choy L et al 2000).

In this study, we show that SMIF, a Smad 4 interacting protein, may play an important role in adipocyte differentiation. Here we provide evidence that SMIF is highly regulated during adipocyte differentiation in 3T3-L1 cells. Similarly to negative modulators of adipogenesis, SMIF is expressed in preadipocytes and its expression is markedly reduced in mature adipocytes. To determine if the absence of SMIF would potentiate adipocyte differentiation, we knocked down SMIF expression with gene targeted small interfering RNAs (siRNA). Several attempts at si-mediated knockdown of SMIF were unsuccessful. This may be due to the already low levels of SMIF during 3T3-L1 cells. In addition, gain of function experiments via transient overexpression of SMIF were unsuccessful in 10T ½ cells, a mesenchymal stem cell line also used for in vitro studies of adipogenesis. To overcome these inconsistencies, we retrovirally overexpressed SMIF and an empty vector control in 10T ½ cells. Overexpression of SMIF

caused slow cell growth and loss of cellular adherence when cells were plated on 24 well plates. Infected cells were confirmed to overexpress SMIF, with three folds higher levels of SMIF mRNA expression when compared to the empty vector expressing cells. Upon stimulation with adipogenic inducers, cells often formed clumps and did not accumulate lipid. This cellular phenotype, resulting from SMIF overexpression, has not been described in previous SMIF overexpression studies however 10T ½ cells were not used in previous reports. Our findings may suggest a role for SMIF in normal cell growth of 10T ½ cells.

Previous studies have shown that SMIF does not have a nuclear localization signal and shuttles in and out of the nucleus dependent on Smad4 after stimulation with Transforming growth factor β (TGFβ) and Bone morphogenic protein 4 (BMP4) (Bai R et al 2002). In our study, we show that SMIF translocation from the cytoplasm in 3T3-L1 cells is independent of TGFβ and BMP stimulation in pre-adipocytes. Differently from previous studies where cells were only transiently stimulated with either BMP4 or TGFβ, in this study 3T3-L1 cells were exposed to a cocktail of inducers containing fetal bovine serum (FBS), dexamethasone, isobutlmethylxanthine, and insulin, to promote adipocyte differentiation. These results may suggest that there may be other stimulants that can induce the nuclear localization of SMIF. There is significant evidence that shows cross talk between insulin and the TGFβ pathways (Remy I et al 2004). Exploration of the individual components of the differentiation cocktail would be beneficial to determine if one or all are necessary for the nuclear shuttling of SMIF.

Previous reports show that together with Smad4, SMIF shows TGFβ dependent transcriptional activity. SMIF also shows TGFβ- and SMAD4-independent transcriptional activity in yeast (Bai R et al 2003). These data may suggest an active function for SMIF in a broader range of signaling events under certain cellular contexts. Our results show that SMIF can

inhibit PPARγ transcriptional activity. The mechanism for suppression could be via the inhibition of transcription factors that positively regulate PPARγ. Alternatively, SMIF could act as a coactivator of a transcription factor that inhibits PPARγ activation. Our data suggest that SMIF can bind directly to PPARγ; however, additional experiments are necessary to determine if SMIF binds to the promoter regions of PPARγ target genes.

In conclusion, we have identified a potential modulator of adipogenesis as SMIF is highly regulated during adipocyte differentiation and can directly bind to and inhibit the transcriptional activity of PPARγ. Additional experiments are necessary to further dissect the mechanism of action of SMIF in adipocyte biology such as its role with Smad4 and TGFβ. Although our results show that SMIF can bind directly to PPARγ, future experiments would also involve a detailed examination of the PPARγ promoter for SMIF binding sites.

**Figure 7. The functional transcription factor trap identifies proteins that interact with NMC1.** Shown is a transient transfection assay with GAL4 UAS::luciferase reporter in HEK293 cotransfected with NMC1. Results are expressed as fold change compared with vector (pCDNA 3.1). NMC1, Nuclear Matrix Coactivator 1; PPARγ, peroxisome proliferator-activated receptor γ; SMIF, smad4 interacting factor; Btbd3, BTB/POZ domain-containing protein; TBPL1, TATA box binding protein related factor 1; ZNF643, zinc finger 643; SIRT, sirtuin 1; Creb 5, cAMP responsive element binding protein 5; PITX, paired-like homeodomain 2; ID3, inhibitor of DNA binding 3; TCF19, transcription factor 19; CITED2, Cbp/300-interacting transdomain with Glu/Asp rich carboxy-terminal domain. *p<0.05; mean ±SEM.

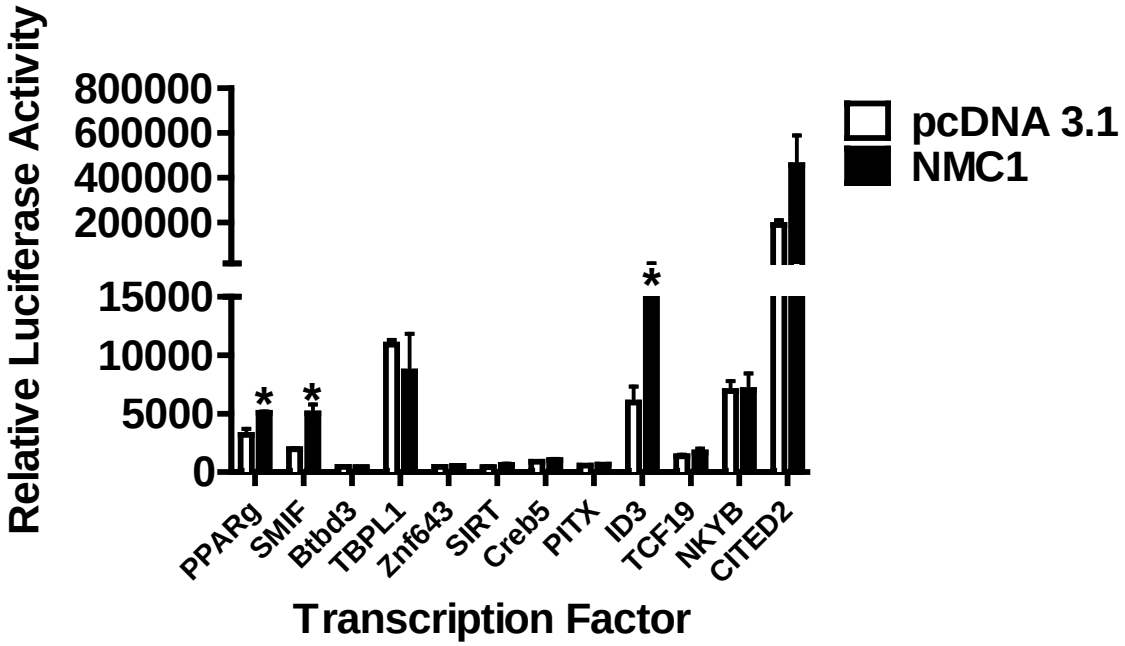

**Figure 8. SMIF is expressed in fat tissue and expression levels are drastically reduced during adipogenesis.** (A) SMIF mRNA levels in selected tissues obtained from C57BL/6J 8-wk-old male mice. Relative mRNA levels were determined by RT-PCR and normalized using 18S. (B) SMIF expression during 3T3-L1 differentiation. 3T3-L1 cells were induced to differentiate using hormonal agents as described in the materials and methods. Cells were harvested at the indicated number of days of post induction and total RNA was isolated and subjected to RT-PCR analysis. BAT, Brown adipose tissue; WAT, white adipose tissue.

**8A.**

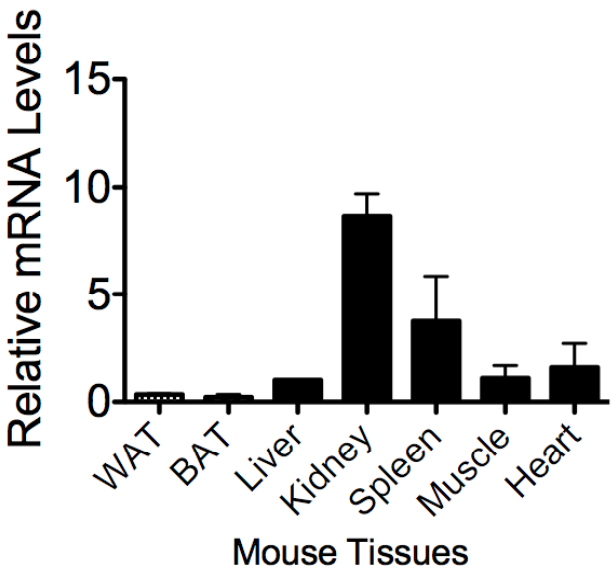


**8B.**

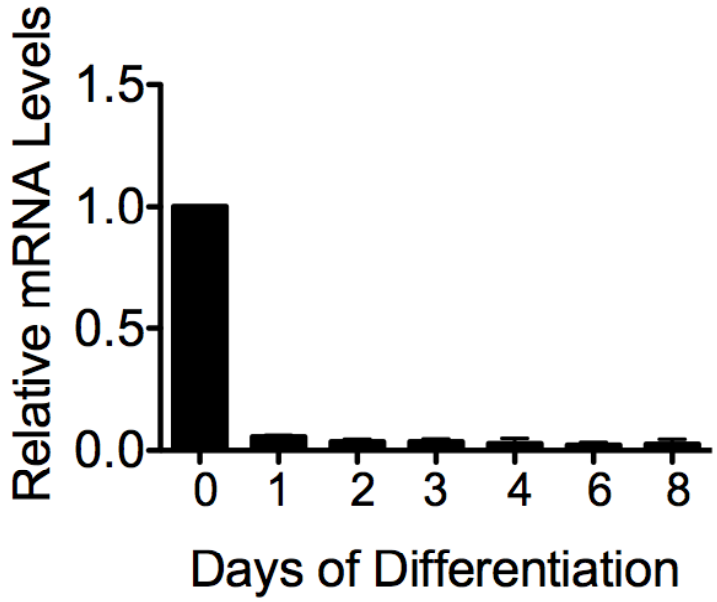

**Figure 9. SMIF translocates in and out of the nucleus independently of TGFβ and BMP stimulation in 3T3-L1 cells.** The subcellular localization of endogenous SMIF during hormonally induced adipocyte differentiation of 3T3T-L1 cells was analyzed by immunostaining using an antibody specific for SMIF at days 0, 2, 3 4 and 8. To visualize the nuclei 3T3-L1 cells were stained with 4′ 6-diamidino-2-phenylindole (DAPI) and immunostained cells were visualized and photographed by Axioplan 2 imaging microscope (Carl Zeiss).

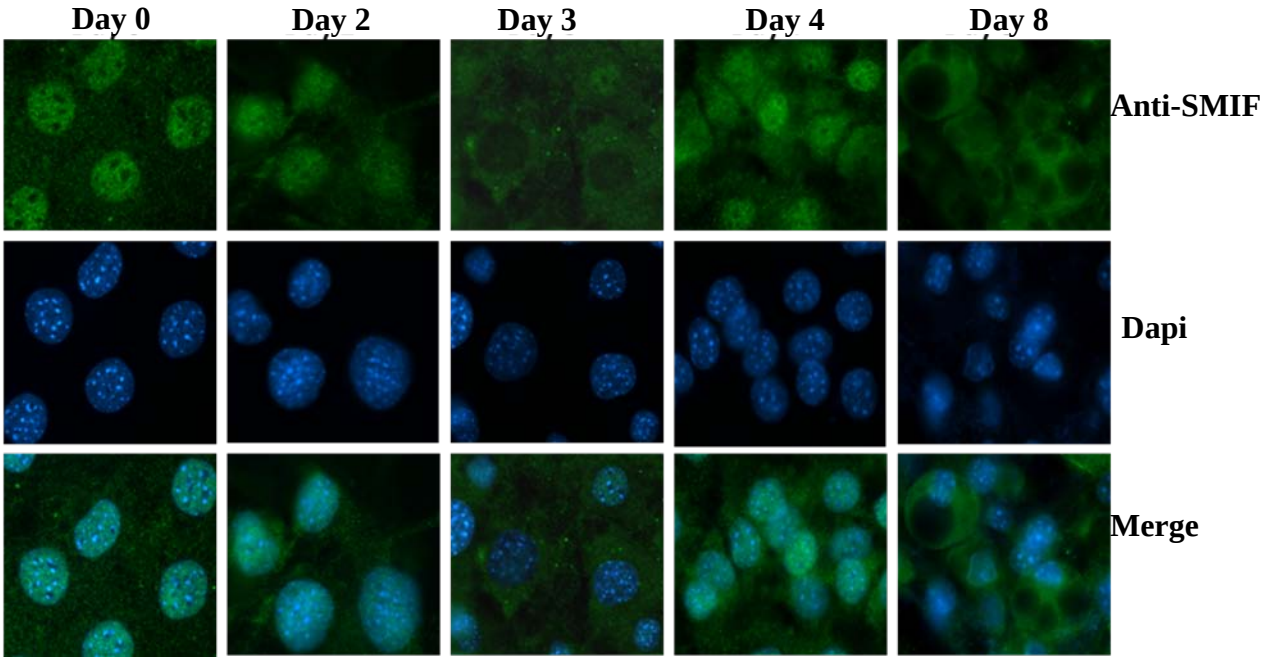

**Figure 10. SMIF represses PPARγ transcriptional activity.** HEK293 cells transiently transfected with the Peroxisome Proliferator Response Element (PPRE) of PPARγ (DR1-luc) and SMIF expression construct. Luciferase assays were performed as described under materials and methods. Results are expressed as fold repression compared with vector (pCDNA 3.1).*$p<0.05$; mean ±SEM.

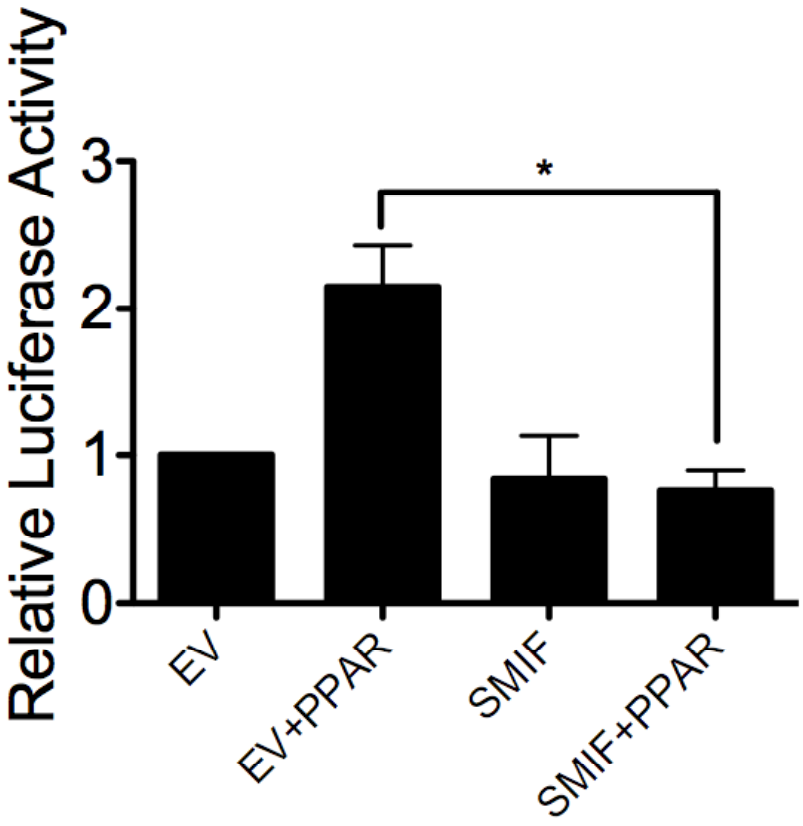

**Figure 11. SMIF binds to PPARγ.** Glutathione beads bound with *E. coli*-cell expressed GST SMIF or GST were incubated with a $^{35}$S-methionine-labelled full-length PPARγ. After washing extensively, the protein bound on the beads were analyzed by SDS-PAGE and visualized by auto radiography. Results show that SMIF binds to full length PPARγ.

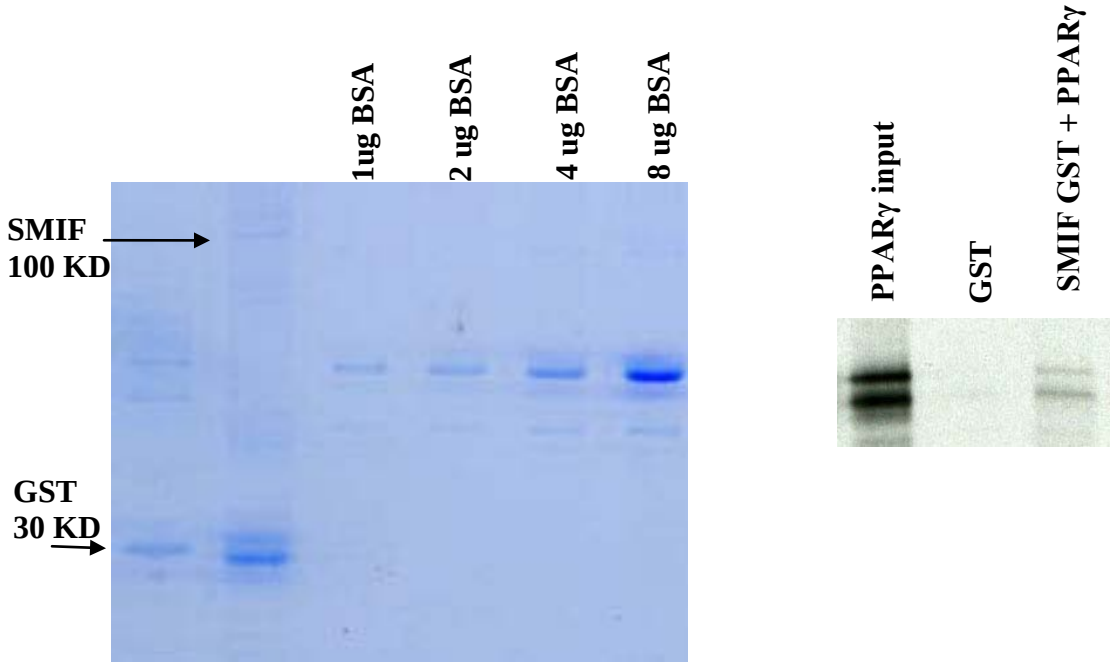

## CHAPTER THREE

### Effects of Fat specific ablation of the Serum Glucocorticoid Kinase 1

**Abstract**: The serum and glucocorticoid inducible kinase 1 (SGK1) is an inducible kinase known to control sodium reabsorption in response to mineralcorticoids in the kidney. We have recently shown that SGK1 is also highly and acutely induced in preadipocytes after glucocorticoids treatment and that it plays a role in the initial stages of fat differentiation *in vitro*. Here we assessed the potential role of SGK1 in adipose tissue biology and studied the effects of fat specific deletion of SGK1 in mice by generating a fat specific SGK1-KO mouse. Our results show that SGK1-Fat-KO female mice have an overall increase in visceral and inguinal fat mass under high fat diet conditions and increased serum insulin levels. In addition, SGK1-Fat-KO female mice showed a higher tendency to develop insulin resistance when compared to their littermate controls. Overall, our analysis of SGK1 effects on adult fat tissue biology suggests that adipose specific ablation of SGK1 *in vivo* increases fat mass with a trend in induction of insulin resistance selectively in female mice.

### Introduction

Adipocyte differentiation has been studied extensively using multipotent stem cell line, such as 10T ½ cells and NIH-3T3, and in 3T3-L1 and 3T3-F442A committed preadipocytes,. To undergo differentiation, these cells are grown to confluence and exposed to a proadipogenic cocktail that includes fetal bovine serum (FBS), dexamethasone, 3-isobutyl-1-methylxanthine (IBMX), and insulin. These inducers are known to activate a transcriptional cascade involving the expression of KLF4, C/EBPβ and CEBPδ leading to the induction of PPARγ and C/EBPα,

the master regulators of late differentiation (Birsoy K) (Yeh W). Although much has been learned about the transcriptional regulation of adipocyte differentiation, less is known about the signaling pathways linking the receptors for the early adipogenic stimuli to the transcriptional regulators of this process.

The AGC kinases have recently emerged as an integral component of intracellular signaling pathways activated under endocrine cues, such as insulin and glucocorticoids, which are important for adipocyte differentiation. Protein kinase C isoforms -βI and -ε have both been shown to promote adipocyte differentiation while the δ isoform inhibits adipogenesis (Webb P) (Zhou Y). Furthermore, activation of protein kinase A (PKA) and Akt by cAMP has recently been shown to be essential for the transcriptional activation of PPARγ (Kim S). Likewise, mice with ablation of the ribosomal protein S6 kinase (S6K) have reduced adipose tissue, increased energy expenditure and are protected from diet induced obesity and from insulin resistance (Um H).

Serum glucocorticoid kinase 1 (SGK1), the newest AGC kinase, was originally cloned as glucocorticoid-sensitive or a volume-regulated gene and was subsequently shown to be strongly upregulated by mineralcorticoids, serum, cyclic AMP and insulin (Wulff P) (Perrotti N). Although SGK1 is expressed in a variety of tissues, its functional role has been studied in the kidney, specifically in the aldosterone sensitive distal nephron, where SGK1 stimulates ENaC to control renal $Na^+$ excretion in response to aldosterone, insulin and IGF-1 (Huang D). The analysis *in vivo* of the function of SGK1 has been limited to mice with global deletion of SGK1. SGK1 -/- mice have impaired mineralcorticoid regulation of sodium reabsorption in the distal tubules of the kidney on a salt deficient diet, causing urinary salt wasting, decreased blood pressure and glomerular filtration rate (Wulff P) (Fejes-Toth G).

We have previously shown that SGK1 is highly induced *in vitro* in preadipocytes during their initial phases of differentiation, in response to dexamethasone treatment. Furthermore, through gain and loss of function experiments we have demonstrated that SGK1 mediates the early events of adipocyte differentiation controlled by glucocorticoids via regulation of Foxo1 phosphorylation (Pietro N). Although these data indicate a critical role of SGK1 in controlling the early stages of adipocyte formation, the specific importance of SGK1 in mature adipocytes has not yet been fully clarified. Here we investigated the role of SGK1 selectively in fat biology, in mice with specific ablation of SGK1 in adult adipose tissue. Our data show that after high fat diet (HFD), female SGK1-Fat-KO mice have increased adiposity in both visceral and inguinal depot when compared to wild type controls and increased propensity to develop insulin resistance, while male SGK1-Fat-KO mice showed no alterations in adipose tissue mass and function.

## Material and Methods

### Generation of fat specific SGK1 knockout mice

Mice with loxP sites surrounding SGK1 exons 2-6 (SGK $^{fl/fl}$) (Fejes-Toth G) were mated with aP2-cre mice (Jackson Laboratories, Bar Harbor, Maine) to generate SGK1 $^{fl/fl}$/ ap2-cre mice. SGK $^{fl/fl}$ littermates were used as controls. Mice were genotyped by PCR using mouse tail DNA. SGK1$^{fl/fl}$ mice were identified by using primers that recognize the floxed SGK1 allele (SGK1-F: 5'-CTCATTCCAGACCGCTGACAA-3' and SGK1-R: 5'-AAAGCTTATCTCAAA CCCAAACCAA-3'). Presence of the aP2-cre transgene was determined by PCR using cre-

specific primers (Jcre-F: 5’-GCGGTCTGGCAGTAAAAACTATC-3’ and Jcre-R: 5’-GTGAA ACAGCATTGCTGTCACT T-3’). SGK1 mRNA levels were determined by quantitative PCR using the forward primer SGK1-/- 5’-AGGGCAGTTTTGGAAAGGTT-3’ and the reverse SGK1-/- 5’-CAGAACATTCCGCTCTGAC A-3’. These primers span nucleotides 1051-1165 in the mouse SGK1 gene, a region that is missing after Cre-mediated excision of the floxed SGK1 gene.

**Animal Experiments**

All animal experiments were performed according to procedures approved by the National Institutes of Health Animal Care and Use Committee. Animals were housed and maintained on a fixed 12-hour light/dark cycle at 22°C. Male and female mice were fed a standard mouse chow diet until 6 weeks of age and subsequently fed a high fat diet containing 45% kcal fat (Research Diets D12451, New Brunswick, NJ) for 12 weeks. After HFD, mice were sacrificed for tissue collection by $CO_2$ narcosis using an approved chamber receiving $CO_2$ from a pressurized gas cylinder followed by cervical dislocation, according to NIH ACCUC animal study approved procedures. Immediately following euthanasia, visceral and inguinal white adipose depots, and liver and brown adipose tissues were weighed. Portions of tissues were collected for histologic examination or snap frozen in liquid nitrogen and stored at -20°C for subsequent RNA analysis.

**Analysis of Body Composition, Food Intake, Metabolic Rate and Locomotor Activity**

Body composition was measured in non anesthetized mice using the Minispec mq10 NMR analyzer (Bruker Optics Inc., Woodlands, TX) prior to and after high fat diet. Total fat, lean and

water mass were evaluated. While on HFD, food intake was measured in 18-week-old mice during a 6-day period. Food was weighed and provided to the mice *ad libitum* using tunnel type feeders (Rodent CAFÉ, OYS International). Oxygen consumption and carbon dioxide production were measured with an 8-chamber Oxymax system (Columbus Instruments) with one mouse per chamber and by testing SGK1-Fat-KO mice simultaneously with WT littermate controls. Total oxygen consumption was measured for 24 h at room temperature (23°C), and energy expenditure was calculated as the average of all points excluding the data from the 1st h of the experiment. Motor activity (total and ambulating) was determined by infra-red beam interruption (Opto-Varimex mini; Columbus Instruments). Food and water were available at all times.

**Biochemical Assays**

Blood was obtained from the tail vein in non-fasted mice that were kept for 12-weeks on a high fat diet. Serum insulin, leptin and adiponectin were measured by radioimmunoassay (RIA) (Linco). Serum triglycerides (Thermo DMA, Louisville, CO) and free fatty acid (FFA) (Roche Applied Science, Indianapolis, IN) were measured according to the manufacturer's procedures.

**Insulin and Glucose tolerance tests**

Insulin tolerance tests were performed on non-fasted mice at 8 am. Human insulin (Humulin R, Eli Lilly) was injected intraperitoneally (0.75 IU/kg body weight). Blood glucose levels were measured before and at 15, 30, 45 and 60 minutes after the injection (Glucometer Elite, Bayer). For glucose tolerance tests, mice were fasted overnight. Glucose (2 g/kg body weight) was injected intraperitoneally. Blood glucose levels were measured before and at 15, 30, 60 and 120 minutes after the injection (Glucometer Elite, Bayer).

**Histological Analysis**

For standard histology, sections of visceral and inguinal white adipose tissue, brown adipose tissue and liver were fixed overnight in 4% paraformaldehyde. Hematoxylin and eosin (H&E) staining was performed at Histoserv Inc (Germantown, MD).

**RNA Analysis**

RNA was extracted from animal tissues using Trizol$^{TM}$ reagent, according to the manufacturer's instructions (Invitrogen) followed by TURBO DNAase treatment (Applied Biosystems). cDNA was obtained from one microgram of total RNA using the High-Capacity cDNA Archive Kit (Applied Biosystems). Real-time PCR was performed using ABI Prism 9700HT Sequence Detection System Instrument (Applied Biosystems) connected to Sequence Detector Software (SDS version 2.0; Applied Biosystem) for collection and analysis of data. Primers to detect 18S were used to normalize sample data (18S-F: 5′-AGTCCCTGCCC TTTGTACACA-3′ and 18S-R: 5′-CGATCCGAGGGCCTCACTA-3′).

**Statistical Analysis**

Data are expressed as mean ± SEM. Statistical significance was determined using paired or unpaired Student's test or one-way ANOVA using Graph Pad Software (Prism version 5.0, Graph Pad, San Diego, CA, USA). A p value less than 0.05 was considered statistically significant.

## Results

### Generation of SGK1 adipose specific knockout mice

In order to determine the effects of SGK1 specific deletion in adipose tissue, we generated SGK1 adipose specific knockout mice by mating SGK1 $^{fl/fl}$ (Fejes-Toth G) to aP2-cre mice (Jackson Laboratories, Bar Harbor, Maine). To assess the extent of SGK1 ablation in fat tissues in SGK-/- mice, we measured the SGK1 mRNA levels in visceral and brown fat. As shown in Fig. 12, female SGK1-Fat-KO mice showed a 50% reduction in SGK1 levels in visceral adipose tissue and 70% reduction in BAT. Males SGK1-Fat-KO mice showed a similar pattern of SGK1 ablation: a 50% decrease in SGK1 mRNA was detected in visceral fat and a 60% reduction in BAT when compared to wild type mice (Figure 12). As a control of the specificity of aP2-cre deletion effects, we measured the levels of SGK1 in the kidney. As shown in Fig. 12C, no reduction in SGK1 mRNA expression levels was detected in the kidney of SGK1-Fat-KO mice. Gross examination of tissues revealed no anatomical abnormalities in SGK1-Fat-KO.

### SGK1-Fat-KO female mice have increased fat mass

To determine whether the ablation of SGK1 in WAT would affect adipose tissue expansion on high fat diet and the development of insulin resistance, six week old male and female WT and SGK1-Fat-KO mice were fed a high fat diet for 12 weeks. As shown in Fig 13A, this diet caused a similar increase in total body weight in SGK1-Fat-KO mice and in their littermate wild-type controls. However, when specifically fat mass was analyzed, although female wild type and SGK1-Fat-KO mice had similar weight gain during on high fat diet, the total fat mass accumulated in the SGK1-Fat-KO mice after the challenge was significantly higher than that of the control (Figure 13B). In concordance with a higher fat mass in female SGK1-Fat-KO mice,

the visceral and inguinal depots weighed significantly more when compared to the wild type mice (Figure 13D). In both sexes, there was no difference in relative weights of the brown adipose tissue (Figure 13D). Male SGK1-Fat-KO mice visceral and inguinal white adipose depot weights were comparable to wild type (Figure 13D). Histologic examination of brown adipose tissue showed that WT brown adipocytes were more uniformly polygonal, composed primarily of multilocular cytoplasmic vacuoles and centralized nuclei, while cells from female SGK1-Fat-KO mice were much larger and vastly variable in size, often displaying large multilocular vacuoles. Histological examination of visceral and inguinal depots confirmed that SGK1-Fat-KO mice of both sexes had normal white adipocyte morphology and no difference in liver morphology when compared to wild type controls

Although few animals were available to measure metabolic parameters, no significant differences in food intake and in physical activity (Figure 14C and D) were detected between the two genotypes. Resting and total energy expenditure was unaltered in female WT and SGK1-Fat-KO mice indicating no difference in metabolic rate (Figures 14A and 14B). Serum leptin, free fatty acids, triglycerides, adiponectin and levels were unaltered in SGK-Fat-KO mice indicating that lack of SGK1 does not affect lipid metabolism (Table 4).

**SGK1-Fat-KO female mice show a tendency to develop insulin resistance**

In order to assess the effects of lack of SGK1 on insulin sensitivity, we measured glucose and insulin levels in wt and KO mice. Female SGK1-Fat-KO mice showed a significant increase in circulating insulin levels (Table 1) and similarly showed a trend for insulin resistance as the peak plasma glucose concentration after glucose load was higher than that measured in wild type

controls (Figure 15A). Insulin tolerance in SGK1-Fat-KO mice was comparable to wild type mice in both sexes (Figure 15B).

## Discussion

In this report, we describe the generation of mice with adipose specific deletion of SGK1 to investigate the role of SGK1 in vivo in adipose tissue. We show here that in conditions of HFD, deletion of SGK1 causes increased fat mass, increased visceral and inguinal fat depot weights, hyperinsulinemia and a trend for insulin resistance.

Our results show that fat specific SGK1 ablation affects the fat mass and depot weight is novel since SGK1 global knockout (SGK1 KO) mice have previously been analyzed in the context of cardiovascular studies to determine the effects of high salt content diet in obese models and showed no obvious adipose tissue defects in high fat diet (Huang 2006). The total SGK1 KO mice showed a similar total body weight compared to wild type controls (Fejes-Toth G) (Huang D). Although our data recapitulates the overall total body weight phenotype observed previously in global SGK1 KO mice, our detailed analysis by NMR and fat pads weights revealed that mice carrying a specific deletion of the SGK1 gene in fat tissue have a significant increase in their fat mass and visceral and inguinal weight. This increase in weight is of 4 grams. These data suggest that SGK1 plays a critical novel role specifically in regulation of adipose tissue. It is possible that total SGK1 KO mice did not have any difference in depots or that a difference was present but it was not revealed in previous studies because NMR and weight analysis of fat mass and individual fat pads in total SGK1 KO mice was not performed.

Our data surprisingly shows that the fat depot differences between wild type and SGK1-Fat-KO mice are restricted to females. This sexual dimorphism in SGK1-Fat-KO mice could be due to several reasons, including the fact that the overall extent of SGK1 ablation mediated by aP2-

cre is different in the two genders however, mRNA analyses of SGK1 levels in abdominal and brown adipose tissues showed that the efficiency of deletion of SGK1 in the visceral depot was 50% in both female and male SGK1-Fat-KO mice. There was 70% and 60% reduction of SGK1 in female and male SGK1-Fat-KO respectively in the brown adipose tissue. The residual SGK1 mRNA expression in the adipose tissue of SGK1-Fat-KO mice may be due to incomplete and inefficient Cre-mediated excision of the SGK1 gene. Incomplete deletion through the aP2 promoter has already been described in the literature (Mao J) (Weis B). In alternative to this hypothesis, residual SGK1 mRNA expression could be due to the presence of a population of preadipocytes in which aP2 cre is not expressed yet since it may not be early enough to affect a small population of adipocytes as SGK1 expression precedes that of aP2. In alternative to these possibilities, it is possible to speculate that SGK1 plays a different role in different genders. There are several studies that show sexual dimorphism in obesity with female mice often protected from obesity by estrogen (Geer S) (Geisler JG). Although we have not investigated the causes of this dimorphisms, our results may suggest a link between estrogen and SGK1 signaling pathways. To date, the molecular mechanism regulating the cross-talk between estrogens and glucocorticoids are poorly understood. However, it has been previously reported in breast cancer cells that estrogen can inhibit glucocorticoid induction of SGK1 by reducing the recruitment of the glucocorticoid receptor to the SGK1 promoter (Zhang Y). It is possible that activation of residual SGK1 in SGK1-Fat-KO female mice could be impaired by the presence of estrogen, thereby accentuating the SGK1-Fat-KO phenotype.

In addition to the fat phenotype described, we observed that SGK1-Fat-KO mice are hyperinsulinemic and show a trend for insulin resistance as reflected by the decreased glucose tolerance. Interestingly, it was previously reported that total SGK1 KO mice are

hyperinsulinemic, glucose intolerant and insulin resistant after high fat diet challenge (Huang D) and that glucose uptake into several tissues, such as skeletal muscle and fat, was blunted (Bioni K). Our data point to a critical role of SGK1 in regulation of glucose uptake specifically in fat tissue since a trend for insulin resistance can be already observed in these mice and suggest that SGK1 ablation in the adipose tissue alone can cause a prediabetic state. The trend for insulin resistance observed in our females SGK1-Fat- KO mice could be due to the fact that SGK1 recombination in fat was inefficient or due to a residual population of adipocytes, with varying levels of functional SGK1. It is possible that if a more efficient deletion of SGK1 was achieved in fat, more significant effects on insulin signaling could be achieved. Alternatively, although lack of SGK1 in fat can contribute to whole body insulin resistance, SGK1 absence in fat alone may not be sufficient to cause it.

Our in vivo mammalian data showing that absence in SGK1 in adipose tissue causes an increase in fat mass and visceral adiposity is in line with those previously reported in studies in *C. elegans* model, showing that SGK1 inactivating mutations can cause an increase in lipid accumulation in the intestine, suggesting that the invertebrate model could accurately predict the mouse phenotype (Soukas A) (Jones K). Interestingly this is in contrast with the mutations described in humans, indicating that SGK1 gene polymorphisms cause an increase in SGK1 activity resulting in an increase in body mass index (BMI) (Dieter M).

In our study, female SGK1-Fat-KO mice showed an increase in fat mass when compared to wild type littermate controls. The increase in fat mass was due to increased visceral and inguinal weights of female SGK1-Fat-KO mice compared to controls. Interestingly, our analyses to identify the causes of their increased adiposity did not reveal any increase in food intake nor decreased activity or impaired energy expenditure. However, we observed increased lipid

accumulation in female SGK1-Fat-KO mice in brown adipose tissue which may suggest that brown tissue function is impaired. More studies in a larger cohort of WT and SGK1-KO mice are needed to further determine whether decreased oxygen consumption below detectable levels due to an inefficient function of brown fat would be responsible for the effects observed.

Our fat specific KO mouse, recapitulates in part the features observed in the total SGK1 KO mouse: overall no difference in weight. However, unlike results reported in SGK1 KO mice, SGK1-Fat-KO mice showed increased adipose tissue weight. In contrast to the total SGK1 KO, SGK1-Fat-KO mice did not show hypertriglyceridemia. It is possible to postulate that this difference may be due to global ablation of SGK1 specifically causing a defect in intestinal lipid absorption (Huang D).

Adipose tissue accretion is caused by either an increase in volume of adipocytes by increased triglyceride storage or by an increase in adipocyte number or both. Histologic examination of visceral and inguinal white adipose depots revealed similar size of adipocytes in both genotypes. Additional studies are necessary to determine if SGK1-Fat-KO mice have an increase in adipocyte number.

In conclusion, our study shows that ablation of SGK1 in the white adipose tissue results in sexual dimorphism in which female mice show increased fat mass, increased visceral and inguinal adiposity, hyperinsulinemia and a trend for insulin resistance.

**Figure 12. mRNA expression levels show decreased SGK1 expression in the fat adipose tissue of SGK1-Fat-KO mice.** SGK1 deletion was assessed in white and brown adipose tissue and kidney by RT-PCR using primers designed to amplify the cre-deleted region. Results show that in the visceral depot (A) there is a 50% reduction of SGK1 in SGK-Fat-KO females and males. (B) 70% and 60% reduction of SGK1levels was detected in female and male SGK1-Fat-KO, respectively, in the brown adipose tissue. (C) No reduction was observed in SGK1 mRNA expression levels in SGK1-Fat-KO mice when compared to wild type controls. RT-PCR is normalized by 18S. Female WT mice, n=8, Male WT mice, n=6; Female SGK1-fat-KO mice, n=7, Male SGK1-Fat-KO, n=3. **p<0.01, ***p<0.001; mean ±SEM, NS, no significance.

**A. WAT**

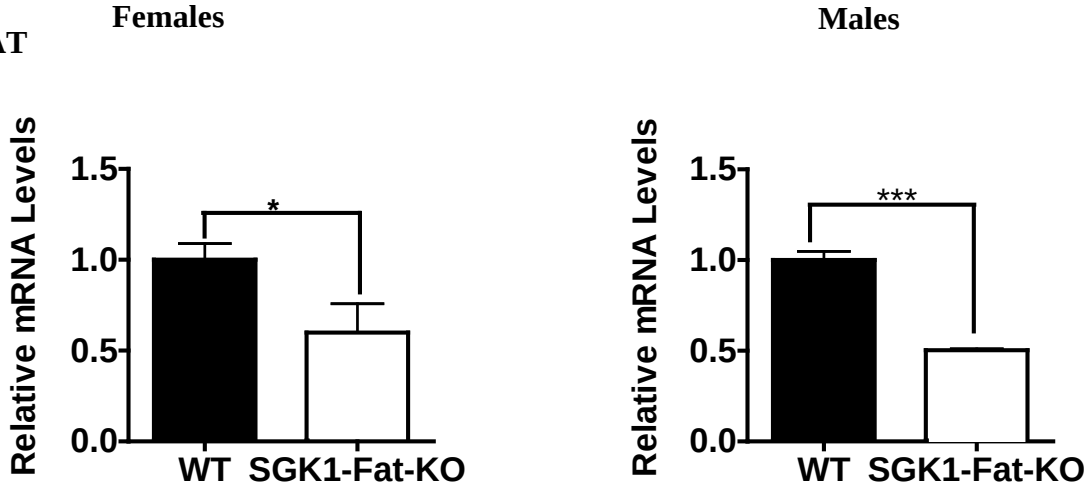


**B. BAT**

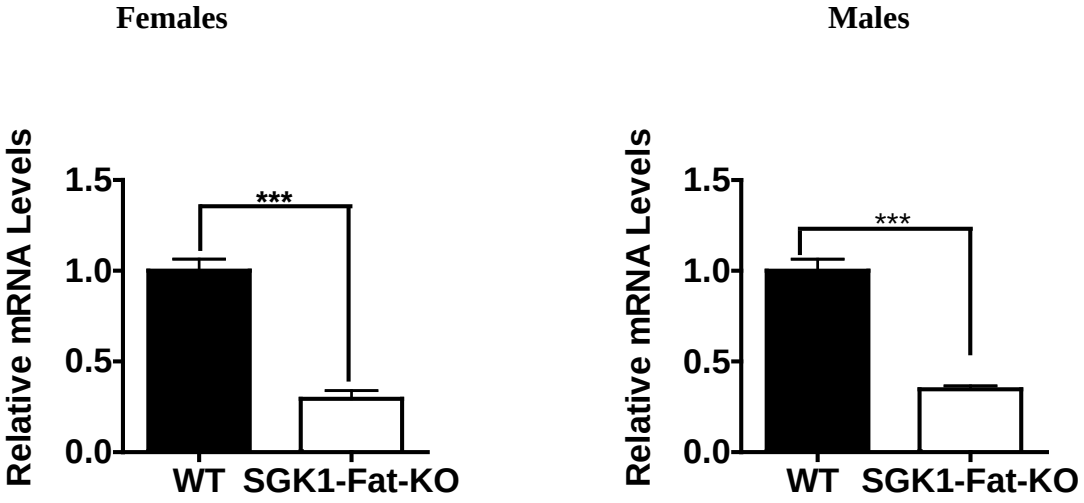

**Figure 12 (continued)**

**Females** **Males**

**C. Kidney**

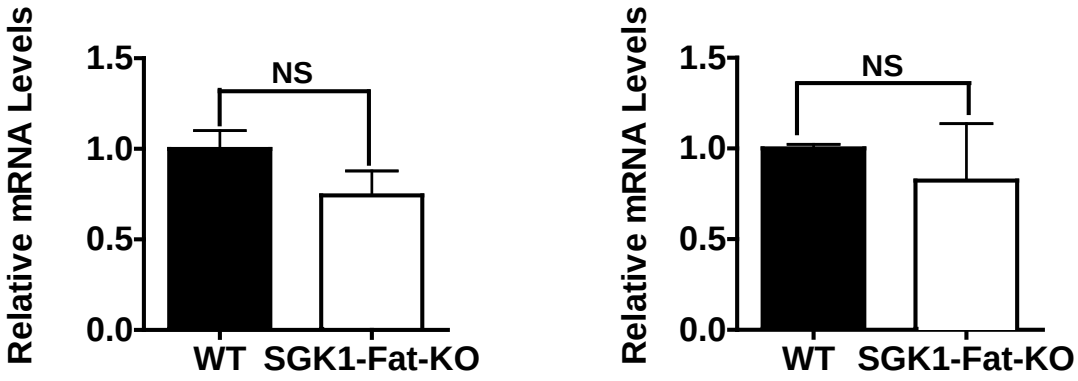

**Figure 13. SGK1-Fat-KO mice show an increase in fat mass and increased visceral and inguinal adiposity.** The *in vivo* phenotypic effects of fat specific ablation of SGK1 were determined by measuring (A) Body weight, (B) fat and (C) lean mass as % of body weight before and after a 12 week of HFD challenge, in female and male wild type (WT) and SGK1-Fat-KO mice. Body composition analysis shows that fat specific deficiency of SGK1 results in a significant increase in fat mass in female SGK1-Fat-KO mice. (D) Visceral, Inguinal and BAT weights expressed as % of body weight after HFD challenge show that female SGK1-Fat-KO mice have increased visceral and inguinal adiposity (E) Hemotoxylin and Eosin staining shows that female SGK1-Fat-KO mice have increased lipid accumulation in the BAT after HFD challenge. There is no morphological difference in WAT and liver when comparing female and male WT and SGK1-Fat-KO mice. Female WT mice, n=8, Female SGK1-Fat-KO mice, n=7; Male WT mice, n=6;, Male SGK1-Fat-KO, n=3. HFD, high fat diet; BAT, brown adipose tissue; WAT, white adipose tissue. *p<0.05; mean ±SEM, NS, no significance.

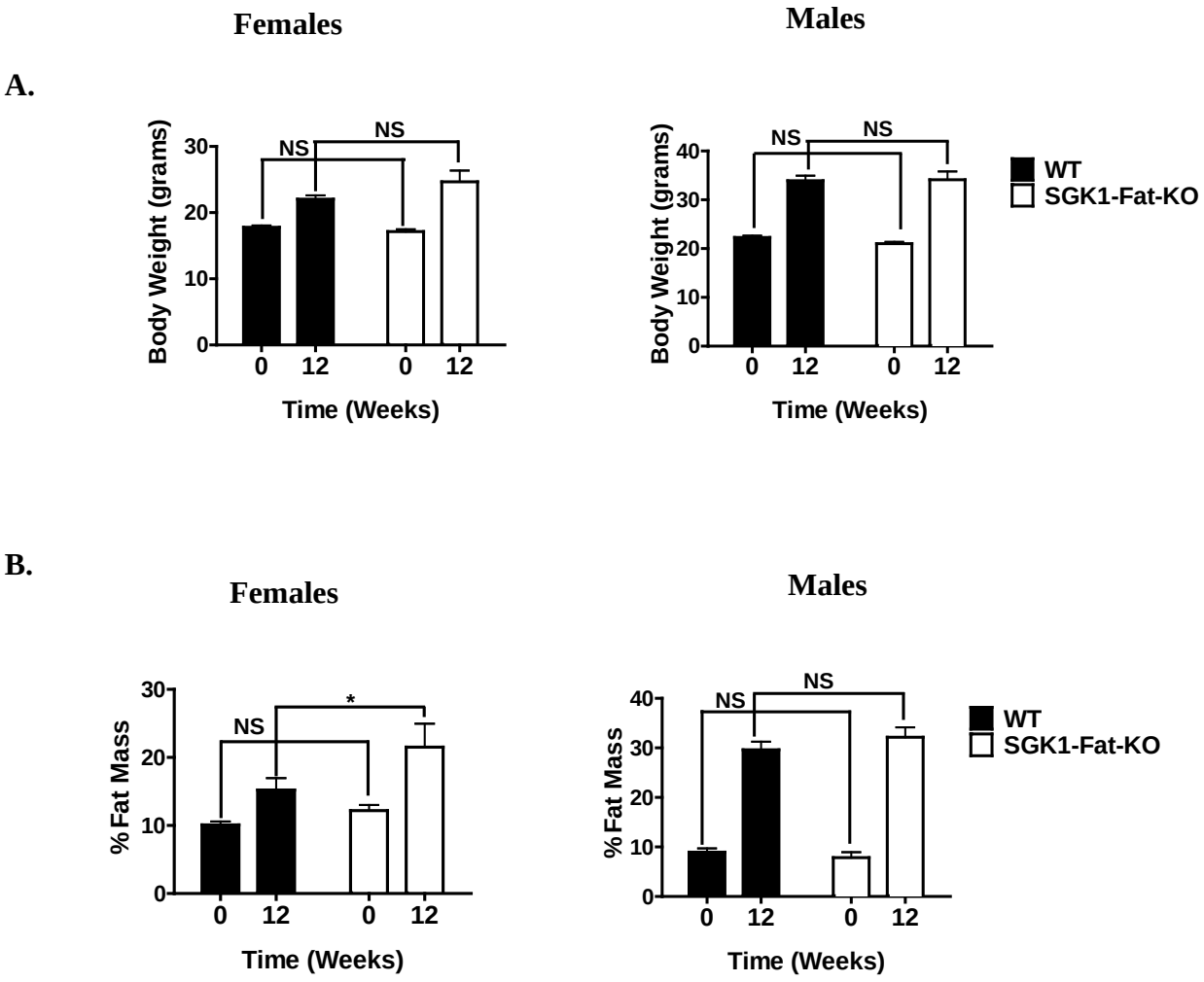

**Figure 13 (continued)**

**Females** **Males**

**C.**

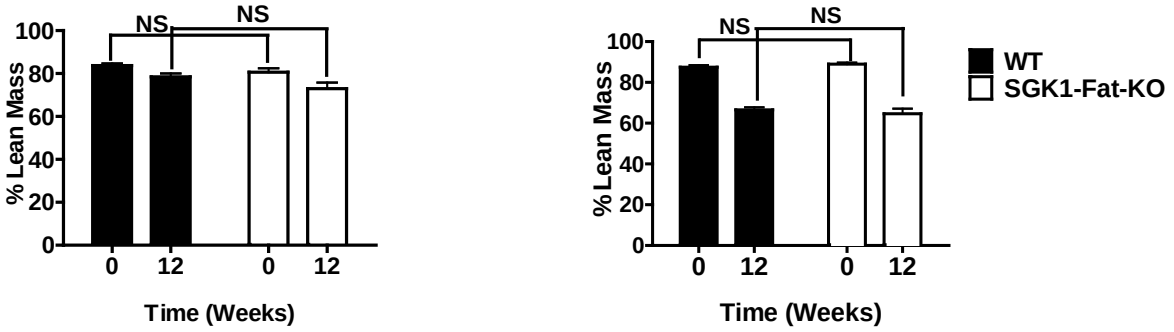


**D.**

**Females** **Males**

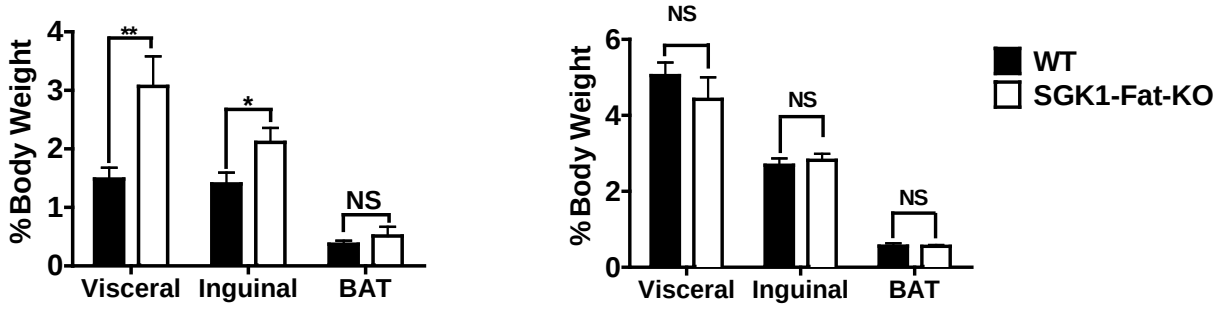

**Figure 13 (continued)**

**E. Females**

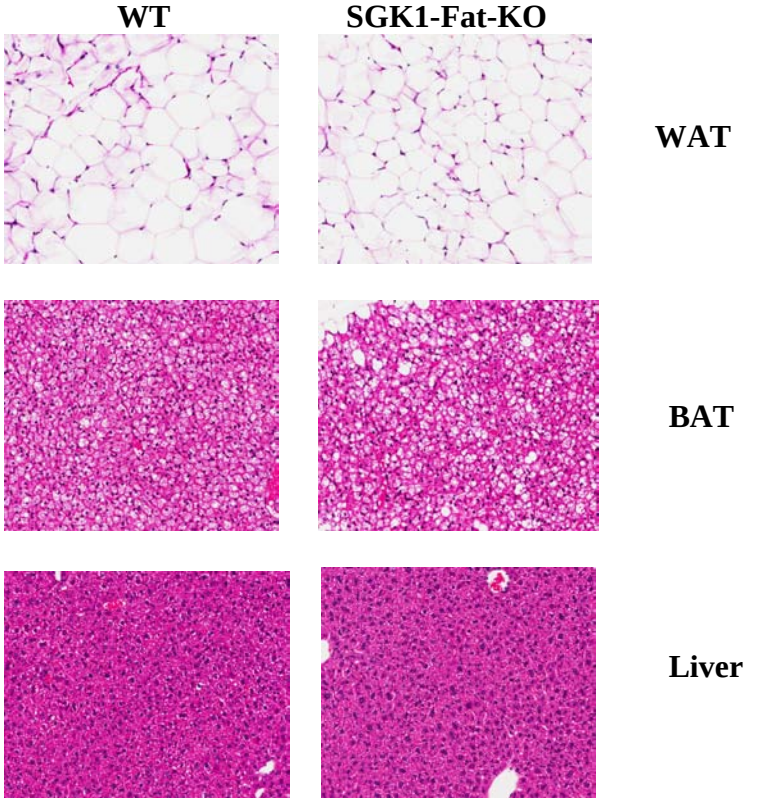


**E. Males**

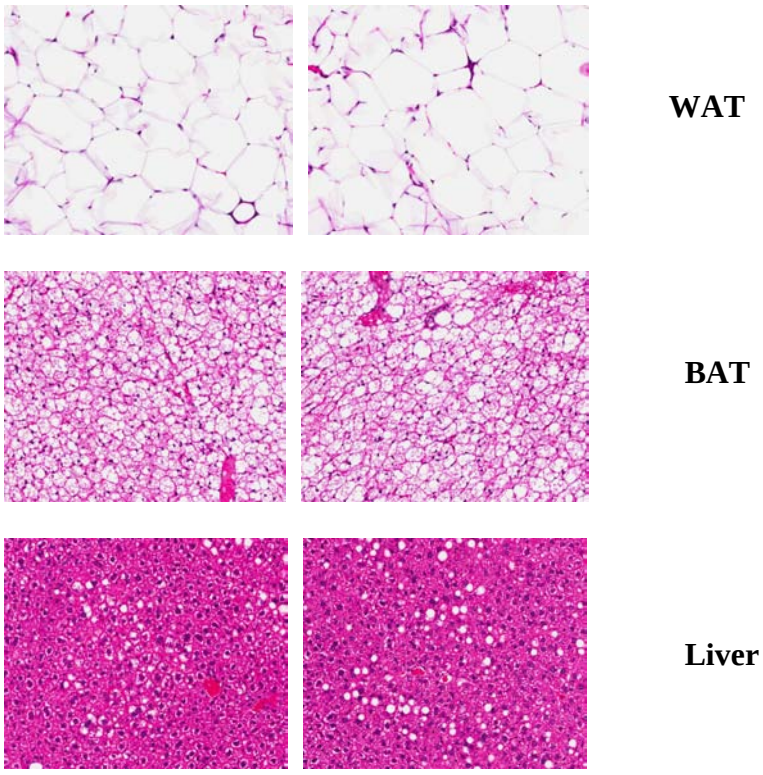

**Figure 14. Energy balance in adult female mice.** To determine the metabolic phenotype of female SGK1-Fat-KO mice (A) resting and total respiratory exchange ratio (RER; $Vco_2/vO_2$) (B) resting and total energy expenditure rate ($O_2$ consumption), (C) food intake, and (D) total activity were measured over 24 hr at 23ºC in female mice after a 12 HFD challenge. WT, n=3; SGK1-Fat-KO, n=2. NS, no significance.

**A.**

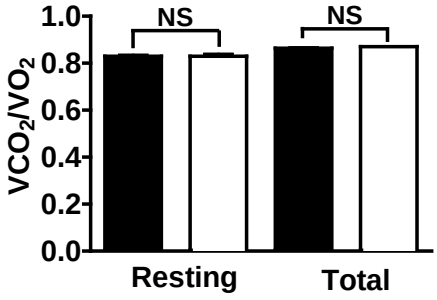


**B.**

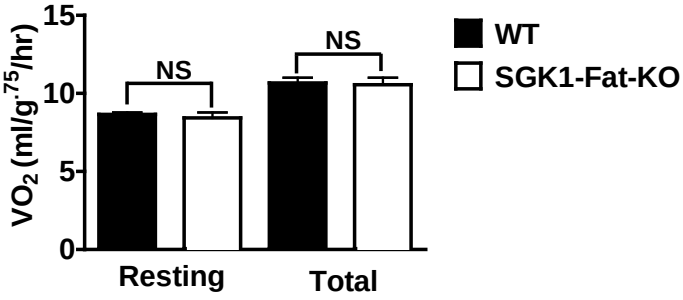


**C.**

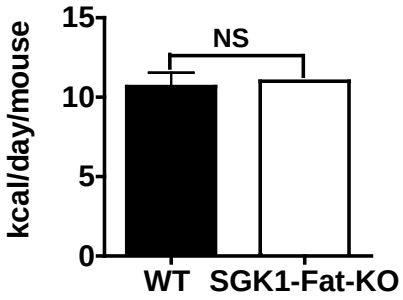


**D.**

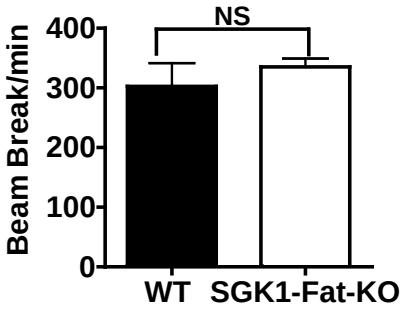

**Table 4. Serum Chemistries**

| | Females | | Males | |
|---|---|---|---|---|
| | Controls | SGK1-Fat-KO | Controls | SGK1-Fat-KO |
| Leptin (ng/ml) | 13.18 ± 2.284 | 20.4 ± 4.615 | 31.93 ± 3.695 | 30.32 ± 3.772 |
| Glucose (mg/dl) | 154.3 ± 14.05 | 150.7 ± 20.8 | 154.2 ± 9.551 | 162.7 ± 7.753 |
| Insulin (ng/ml) | 0.3425 ± 0.03437 | 0.6457 ± 0.1446* | 1.620 ± 0.3553 | 2.553 ± 0.2379 |
| Triglycerides (mg/dl) | 45.43 ± 3.482 | 51.00 ± 4.895 | 78.60 ± 5.474 | 82.72 ± 23.63 |
| Free Fatty Acids (mM) | 0.3953 ± 0.05442 | 0.4343 ± 0.07072 | 0.5000 ± 0.05471 | 0.4367 ± 0.08413 |
| Adiponectin (µg/ml) | 18.37 ± 1.054 | 22.21 ± 2.603 | 13.03 ± 1.901 | 9.327 ± 1.499 |

Serum chemistries were measured in nonfasted animals after a 12 week HFD challenge. Female WT mice, n=8, Male WT mice, n=6; Female SGK1-Fat-KO mice, n=7, Male SGK1-Fat-KO, n=3. *$p<0.05$ versus controls. Data are expressed as mean ±SEM. Female SGK1-Fat-KO mice show increased serum insulin levels after a 12 week HFD challenge.

**Figure 15. SGK1-Fat-KO mice show a trend for insulin resistance.** (A) Glucose tolerance and insulin tolerance tests (B) were performed on wild type and SGK1-fat-KO male and female mice after a HFD challenge. After overnight fasting, glucose (0.75 IU/kg body weight) or insulin (2 g/kg body weight) was injected into the peritoneal cavity adult wild type and SGK1-Fat-KO mice. Blood samples were collected from the tail at the indicated time points and glucose concentrations were measured. Female WT mice, n=8, Female SGK1-Fat-KO mice, n=7, Male WT mice, n=6; Male SGK1-Fat-KO, n=3. *p<0.05;mean ±SEM.

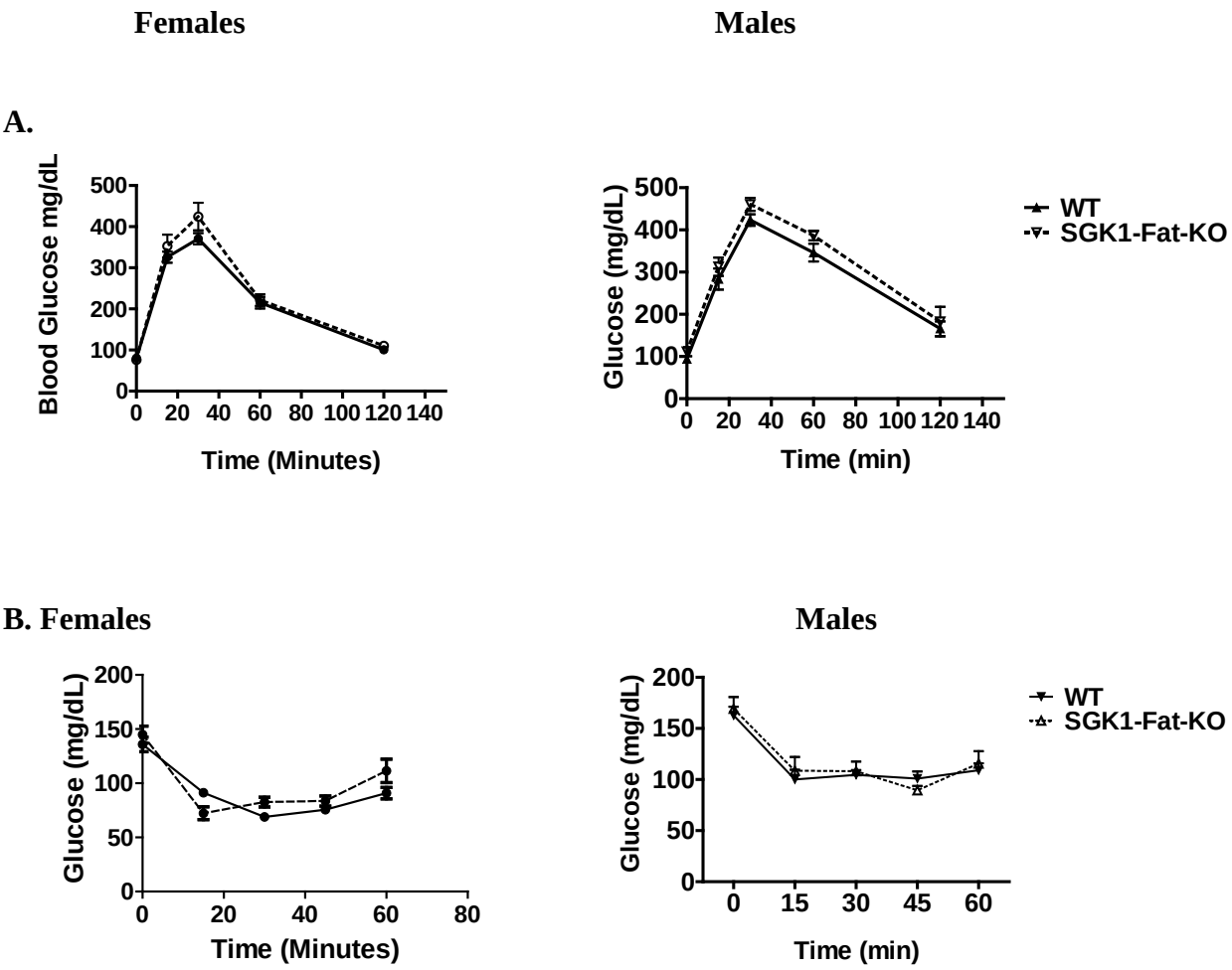

# CHAPTER FOUR

## Significance and Future Directions

### I. Conclusions and Significance

We have addressed the effects of adipose specific knockdown of ZNF638 in vivo and have determined that ZNF638 is a critical regulator of adipocyte differentiation. To better understand the role of NMC1, a novel isoform of ZNF638, in adipocyte biology, we identified SMIF as a novel regulator of PPARγ. Concurrently, we determined the role of SGK1 in adipocyte biology by characterizing a SGK1 fat specific knockout mouse.

We first sought to determine the effects of adipose specific knockdown of ZNF638 in the *in vivo* context to ascertain its true biologic effects within the host microenvironment. We found that Fat-ZNF638-KD mice had a lean phenotype and an intriguing potential to maintain this phenotype despite an 8 week high fat diet challenge and increased food consumption. Fat-ZNF638-KD mice had a significant decrease of white adipose tissue in the subcutaneous, visceral and perigondal fat depots. Histologic and morphometric analysis of visceral white adipose depots revealed that Fat-ZNF638-KD mice had smaller adipocytes. Fat-ZNF638-KD mice were also able to maintain a lean phenotype without the deleterious deposition of fat in the liver and muscle. Our results are particularly compelling because several lean mouse models generated by the manipulation of genes involved in adipocyte differentiation often have fatty livers and increased deposition of fat in the liver and muscle that often results in insulin resistance (Reue K). In a previous study we showed that in vitro, ZF638 is expressed during the early phases of adipogenesis prior to the expression of PPARγ. In the present work, we showed that white adipocytes from Fat-ZNF638-KD mice have decreased expression mRNA expression

of PPARγ and PPARγ target genes that are important in lipid uptake and storage. These findings are convincing that our model recapitulates the *in vitro* system and further confirms that ZNF638 regulates PPARγ expression. Overall our findings are significant because we have determined that ZNF638 has a true biologic role in adipocyte differentiation. Given the critical role of obesity in the development of insulin resistance and other chronic diseases, drugs that inhibit ZNF638 would be an important potential means to treat obesity and counteract the deleterious effects of this disease.

To better understand the mechanisms by which NMC1, a novel isoform of ZNF638, affects adipocyte differentiation, we sought to identify novel NMC1 interacting transcription factors. Ten transcription factors were identified as NMC1 protein interactors by a novel high throughput cell based screening strategy. All ten transcription factors were sequenced and confirmed by luciferase reporter assays to interact with NMC1. Candidate gene, Smad4-interacting factor (SMIF), was later confirmed in 3T3-L1 in vitro model system to be highly regulated during adipocyte differentiation with expression levels the highest in preadipocytes and markedly reduced in mature adipocytes. Given these results, we sought to determine whether SMIF interacted with PPARγ, the master regulator of adipogenesis. Using a luciferase reporter assay, we established that SMIF represses the transcriptional activity of PPARγ. To determine if SMIF interacts directly with PPARγ, we performed GST pulldown assays. Thus we determined that SMIF interacts directly with PPARγ. Although this study did not clarify a true biological role for SMIF in adipocyte differentiation, these findings are insightful because we have not only found a novel regulator of PPARγ but one that is a potent repressor of PPARγ's transcriptional activity. PPARγ activating ligands such as TZDs has been studied extensively in the treatment for insulin resistance and certain cancers (Tontonoz P). However, recent work has revealed that PPARγ

antagonist may be beneficial for the treatment of certain epithelial and hematopoietic cancers (Burton J). These results may suggest that an appropriate degree of pharmacological interference of PPARγ by SMIF agonists could possibly constitute an approach for treatments in other cells types.

Finally, we assessed the potential role of SGK1 in adipose tissue biology by generating a fat specific SGK1-KO mouse. Our results show that FAT-SGK1-KO female mice have an overall increase in visceral and inguinal fat mass under high fat diet conditions and increased serum leptin levels. These findings are notable because they are in contrast to mutations described in humans, indicating that SGK1 gene polymorphisms that result in SGK1 over activity lead to obesity (Dieter M). Female SGK1-fat-KO mice also showed a delayed decrease of plasma glucose concentration after glucose load which points to impaired cellular uptake of glucose. This is particularly significant because it confirms previous experiments that suggest a role of SGK1 in insulin-induced cellular uptake of glucose in liver, muscle and fat (Bioni K). Overall, these findings are substantial because there is growing, yet compelling evidence that SGK1 participates in the development of obesity and type II diabetes (Lang F). Many researchers have proposed pharmacologic SGK1 inhibitors as an attractive strategy to counteract obesity nevertheless; our data evokes a more complicated role of SGK1 in mature adipose tissue and may suggest that SGK1 inhibitors targeting the adipose tissue may not be beneficial.

## II. Future Directions

Future studies arising from this research should include: 1) the characterization of a fat specific ZNF638 knockout mouse and 2) to investigate of the role of glucocorticoids in obesity using the SGK1-fat-KO mouse model.

Since Fat-ZNF638-KD mice were generated by using the novel approach of Cre-LoxP induced RNA interference (RNAi), we will compare our findings to a more traditional one by generating a ZNF638 conditional knockout mouse. Transgenic mice were created in collaboration with inGenious Targeting Laboratories by placing two directly repeated loxP sites flanking the starting ATG (methionine) and exon 2 followed by a neomycin cassette located in intron 3 of the ZNF638 gene. Creation of the targeting vector, electroporation of C57BL/6 cells with targeting vector, screening of ES cells, microinfection of positive ES clones in blastocytes of mice, breeding of chimeras to generate F1 heterozygotes and the confirmation of germline transmission via genotyping were all performed at inGenious Targeting Laboratories. Prior to the completion of my dissertation work, F1 heterozygotes were bred to B6.Cg-Tg (ACTFLPe) 9205Dym/J or FLP mice to remove the neomycin cassette. F2 heterozygotes will later be screened by PCR using specific primers recognizing the neo deletion and the distal loxP site and later crossed to wild type mice to generate F3 heterozygotes. F3 progeny will be screened by PCR using specific primers the neomycin deletion, distal loxP site and FLP transgene absence. Male and female F3 heterozyotes can then be bred to generate homozygotes. Positive offspring will be bred to aP2 transgenic mice to achieve fat specific ZNF638 knockout mice.

We hypothesize that the anatomic and metabolic phenotype of the fat specific ZNF638 knockout mice (Fat-ZNF638-KO) would mimic our findings in the Fat-ZNF638-KD mice. In our previous approach in which ZNF638 was merely knocked down in the fat by RNAi, there was

increased lethality at weaning and throughout adulthood. Total ablation of ZNF638 in the adipose tissue could result in no surviving mice confirming our initial findings. If there is survival of the Fat-ZNF638-KO mice, similar to methods described to elucidate the phenotype of Fat-ZNF638-KD mice would be used to investigate if these mice are resistant to obesity and insulin resistance. If the phenotype is similar to the surviving Fat-ZNF638-KD mice, these findings would lend further support to the role of ZNF638 in adipocyte differentiation. Nevertheless, further investigation would be warranted to determine the cause of increased lethality in the knockdown mice.

We have previously shown that SGK1 mediates the early events of adipocyte differentiation controlled by glucocorticoids (Pietro N). To further elucidate the role of glucocorticoids in mature adipocytes, an important functional experiment would be to administer exogenous glucocorticoids to SGK-Fat-KO mice and characterize the resulting phenotype. It is well known that the chronic exogenous administration of glucocorticoids in humans and animals results in a syndrome of weight gain and fat deposition in the thorax and abdomen referred to as Cushing's (Bertagna X). This phenomenon has also been shown in rodents with intraperitoneal and intracerebroventricularly administration of glucocorticoids (Gounarides J) (Zakrzewska K). Slow release dexamethasone pellets inserted subcutaneously have also been shown to effectively increase adipose mass and corticosterone levels in mice (Spiegelman B). Furthermore, a dose dependent increase in fat mass was observed in mice containing subcutaneous pellets of up to 50 mg/animal, where epididymal fat pads were approximately twice as heavy as placebo controls (Spiegelman B). We would hypothesize that exogenous glucocorticoids administration would not result in weight gain in the SGK-Fat-KO mice. To test our hypothesis, a 50 mg dexamethasone or placebo slow release pellet (Innovative Research of America) would be placed in a

subcutaneous pocket on the lateral side of the neck of six week old SGK1-Fat-KO and wild type mice. Mice would be monitored throughout the treatment period to assess swelling or edema in the surgical area and potential toxicity due to drug release. During the treatment period, weights and body composition would be measured weekly. To test insulin sensitivity, insulin and glucose levels would be measured. Mice receiving the dexamethasone treatment and placebo will be euthanized 21 days after initial placement of the subcutaneous pellet. Following euthanasia, WAT depots, with primary interest in regions where fat is commonly deposited in Cushing's, (the dorsocervical, thoracic and visceral regions) would be collected and weighed. Additional tissues such as liver, kidney, spleen and BAT would be collected and weighed at that time. These experiments are already underway in our laboratory and results are forthcoming.

Appendix

# APPENDIX

## Serum- and Glucocorticoid-Inducible Kinase 1 (SGK1) Regulates Adipocyte Differentiation via Forkhead Box O1

Natalia Di Pietro,* Valentine Panel,* Schantel Hayes, Alessia Bagattin, Sunitha Meruvu, Assunta Pandolfi, Lynne Hugendubler, Geza Fejes-To´th, Aniko Naray-Fejes-To´th, and Elisabetta Mueller

**Abstract** The serum and glucocorticoid-inducible kinase 1 (SGK1) is an inducible kinase the physiological function of which has been characterized primarily in the kidney. Here we show that SGK1 is expressed in white adipose tissue and that its levels are induced in the conversion of preadipocytes into fat cells. Adipocyte differentiation is significantly diminished via small interfering RNA inhibition of endogenous SGK1 expression, whereas ectopic expression of SGK1 in mesenchymal precursor cells promotes adipogenesis. The SGK1-mediated phenotypic effects on differentiation parallel changes in the mRNA levels for critical regulators and markers of adipogenesis, such as peroxisome proliferator-activated receptor, CCAAT enhancer binding protein, and fatty acid binding protein aP2. We demonstrate that SGK1 affects differentiation by direct phosphorylation of Foxo1, thereby changing its cellular localization from the nucleus to the cytosol. In addition we show that SGK1-/-cells are unable to relocalize Foxo1 to the cytosol in response to dexamethasone. Together these results show that SGK1 influences adipocyte differentiation by regulating Foxo1 phosphorylation and reveal a potentially important function for this kinase in the control of fat mass and function. **(*Molecular Endocrinology* 24:2010)**

## Introduction

Imbalance between energy intake and its expenditure leads to obesity (Kahn B 2000, Spiegelman B 2001), which is a major risk factor for development of type 2 diabetes and

cardiovascular disease, part of a spectrum of diseases called “the metabolic syndrome” (Eriksson 1999, Vega G 2004). The efficient trafficking of calories instates of high or low food intake is orchestrated across multiple tissues by endocrine molecules and through signal transduction pathways that weaken or reinforce a number of key transcriptional effectors. Peroxisome proliferator-activated receptor (PPAR) γ and CCAAT enhancer binding protein (C/EBP)α are the principal regulators of the transcriptional development of adipose tissue and control the conversion of undifferentiated mesenchymal cells into adipocytes. Studies involving gain- or loss-of-function of these factors have definitively demonstrated their necessity in promoting full adipogenesis (Tontonoz P 1994, Rosen E 1999, Rosen E 2002, Linhart H 2001, Feytag S et al 1994). In addition to these two central players, a number of other factors have been described as contributing either positively or negatively to the adipogenic process (Farmer S 2006). Among these, several forkhead winged helix family members have been shown to be important transcriptional integrators of developmental and metabolic processes (Carlsson P 2002). In particular, Foxo1, Foxa1 and 2, and Foxc2 counter the conversion of preadipocytes into adipocytes through distinct mechanisms involving repression of PPARγ’s gene transcription, activation of Pref1, or inhibition of PPARγ’s ability to activate its target genes (Nakae 2003, Davis K 2004, Davis K 2004, Wolfrum C 2003, Armoni M 2006, Dowell P 2003).

The transcriptional regulation of adipogenesis is influenced by endocrine cues such as insulin and glucocorticoids, which activate intracellular pathways to increase messenger molecule levels, such as cAMP, or signaling kinases, such as those belonging to the AGC family. These kinases include arginine, serine kinase (RSK), ribosomal protein S6 kinase (S6K), MAPKs, protein kinase B/Akt, protein kinase C (PKC), and cAMP/GMP-dependent kinases and function to phosphorylate serine or threonine residues present at R-XRXXS/T consensus motifs. Gain- or

loss-of-function studies implicate a unique role in adipogenesis for several of these AGC kinases. In particular, Akt, when overexpressed, increases differentiation in 3T3-L1 cells, whereas its absence reduces adipogenesis in primary fibroblasts (Bae S 2003). Furthermore, PKC isoforms β-I and δ promote differentiation (Webb 2003), whereas PKC δ opposes the adipogenic process (Zhou Y 2006). The serum- and glucocorticoid-inducible protein kinase 1 (SGK1) is the newest member of the AGC kinases, initially characterized in rat mammary tumor cells as an immediate early gene induced by serum and glucocorticoids (Webster 1993). Although SGK1 expression is present in a variety of tissues, the physiological function of this kinase has been studied primarily in the kidney where it controls sodium reabsorption via regulation of the epithelial sodium channel ENaCα (Pearce D 2003, Naray-Fejes-Toth 2000). Mice lacking SGK1 are viable, confirming that this kinase is not required for survival (Wulff P 2002). However, SGK1-/- mice show a reduced ability to retain salt after challenge by a salt-deficient diet, highlighting a role for SGK1 in salt metabolism (Wulff P 2002, Fejes-Toth 2008). Dexamethasone priming of preadipocytes is necessary for their adipogenic commitment and differentiation (Pantoja C 2008), but the mechanisms through which glucocorticoids stimulate adipogenesis have not been fully elucidated. Therefore, we investigated the potential role of SGK1 as a mediator of glucocorticoid-initiated signals in adipocytes. Our results show that treatment with dexamethasone induces SGK1 during early adipogenesis. Ectopic expression of SGK1 enhances adipocyte differentiation, whereas its down-regulation via small interfering RNA (siRNA) reduces it. Furthermore, SGK1 directly phosphorylates Foxo1, leading to its relocalization to the cytosol. Dexamethasone promotion of adipogenesis appears to be mediated through SGK1 effects on Foxo1 because dexamethasone is unable to influence Foxo1's subcellular localization in SGK1-/-cells.

## Materials and Methods

### Materials and reagents

Antibodies against total and phospho-Foxo1 (T-24, S-256, or S-319), total and phospho-SGK1 (S-422), β-actin, GFP, Alexa Fluor 488 goat antirabbit, troglitazone, and rosiglitazone were purchased respectively from Santa Cruz Biotechnology, Inc. (Santa Cruz, CA), Cell Signaling Technology (Danvers, MA), Sigma (St. Louis, MO), Stressgen Biotech Corp. (Victoria, British Columbia, Canada), Invitrogen (Carlsbad, CA), and Cayman Chemical Co. (Ann Arbor, MI).

### Plasmids

Human GFP-Foxo1, GFP-Foxo1AAA, and GST-Foxo1 were purchased from Addgene, Inc. (Cambridge, MA). Mouse SGK1 cDNA was cloned into pCR2.1-TOPO vector (Invitrogen) after PCR amplification of a mouse kidney cDNA library using Triple Master Taq Polymerase (Eppendorf) with the following primers: mSGK1 forward (F), 5′- AACAGCCACCATGGCCG TCAAAGCCGAGGC- 3′; and mSGK1 reverse (R), 5′-GGCGAG ACTGCCAAGCTTCC-3′. The mSGK1 cDNA was subsequently subcloned into pCR3.1 (Invitrogen) using *Eco*RI.Constitutively active SGK1 (S422DSGK1) and inactive SGK1 (K127NSGK1) were generated according to Dieter *et al.* (33), using the QuikChange II XL Site-Directed Mutagenesis kit (Stratagene, La Jolla, CA) with the following primers: S422D F, 5′-GCCTTCCTCGGCTTC**GAT**TATGCACCTCCTGTGG- 3′, S422D R, 5′CCACAGGAGGTGC ATA**ATC**GAAGCCGAGGAAGGC- 3′, K127N F, 5′GAAGTATTCTATGCAGTC**AAC**GTTT

TACAGAAGAAAGCCATCCTG- 3′, K127NR, 5′-CAGGATGGCTTTCTTCTGTAAAAC**GT**

**T**GACTGCATAGAATACTTC- 3′(Mutagenesis site indicated by *bold*).

**Cell culture**

3T3-L1, 10T1/2, and U2OS cell lines (American Type Culture Collection, Manassas, VA) and PPAR-/-cells (kind gift of Dr. Rosen) were grown in DMEM (Mediatech, Inc., Manassas,VA) supplemented with 10% fetal bovine serum (FBS) (Hyclone Laboratories, Logan, UT) and 1% penicillin/streptomycin (Mediatech) in 5% CO2.

**Animals**

C57BL/6J male mice (6–8 wk of age) were housed in 12 h light, 12-h dark cycle (light on at 0700 h), at 22 C, and allowed *ad libitum* access to diet and water. Mice were fed a normal diet that contained 9% of calories as fat (Zeigler Bros, Gardners, PA). SGK1-loxP mice were generated as described elsewhere (24). Mice were killed for tissue collection by CO2 narcosis using an approved chamber receiving CO2 from a pressurized gas cylinder followed by cervical dislocation, according to National Institutes of Health ACUC animal study-approved procedures. Tissues were snap frozen in liquid nitrogen and stored at 80º C for subsequent analysis.

**Adipocyte differentiation**

3T3-L1 and 10T1/2 cells were induced to differentiate either with MDI medium consisting of 0.5 µM 3-isobutyl-1-methylxanthine, 1 µM dexamethasone, and 5 µg/ml insulin, in addition to DMEM with 10% FBS and penicillin/streptomycin or with 5 µg/ml insulin and PPARγ ligand troglitazone (10 µM) or rosiglitazone (100 nM). After 48 h of MDI induction, cells were grown

in maintenance medium consisting of DMEM supplemented with 10% FBS, 1% penicillin/streptomycin, and 5µg/ml insulin.

**Oil Red O staining**

To measure lipid accumulation, cells were washed twice with PBS and fixed with 10% buffered formalin (Electron Microscopy Sciences, Halfield, PA) for 30 min. The fixed cells were incubated for 1 h in freshly diluted Oil Red O solution (Sigma), prepared by mixing six parts of Oil Red O stock solution (0.5% Oil Red O in isopropanol) and four parts of distilled water and washed three times with distilled water.

**Transfection assays**

Cells ($3x10^5$) were transfected with Nucleofector or Shuttle devices (Amaxa) according to manufacturer's instructions. Cells were transfected with either 1 µg of cDNA or 100 nM of si-RNA (ON-TARGET*plus SMART* pool or individual si-RNAs; Dharmacon) and induced to differentiate. The sequences of the si-RNA are represented in supplemental Table I published as supplemental table data. All experiments were performed in duplicate, three to five times. The empty vector cDNA (pcDNA3.1) or the ON-TARGET*plus Non-targeting* pool were used as negative controls.

**Real-time PCR**

RNA was extracted from cultured cells or animal tissues using Trizol reagent (Invitrogen), according to the manufacturer's instructions. cDNA was obtained from 1 µg of total RNA using High-Capacity cDNA Archive Kit (Applied Biosystems, Foster City, CA). Real-time PCR was

performed using ABI Prism 9700HT Sequence Detection System Instrument (Applied Biosystems) connected to Sequence Detector Software (Applied Biosystems) for collection and analysis of data. According to the recommendations of the manufacturer, 25µl/96-well reactions were set up in a MicroAmp Optical 96-well reaction plate using FastStart SYBR Green (Roche, Indianapolis, IN), 5 µM reverse and forward primers (IDT DNA), and 20 ng of cDNA. Realtime PCR was performed according to the following protocol: 50 C for 2 min and 95 C for 15 min, and subsequently 40 cycles at 94 C for 15 sec, 59 C for 30 sec, and 72 C for 30 sec. 18S rRNA was used to normalize the data. For the analysis of SGK1, PPARγ, C/EBPα, aP2, and 18S the following primers were used: mSGK1 F, 5′-CTTGGGCTATCTGCACTCCC-3′; mSGK1 R, 5′-GCCCAAAGTCAGTGAGGACG-3′; mPPARγ F, 5′-AGTCTGCTGATCTGCGAGCC-3′; mPPARγ R 5′-CTTTCCTGTCAAGATCGCCC- 3′ ; mC/EBPα F, 5′-GAACAGCAACGAG TACCGGGTA- 3′; mC/EBPα R, 5′-GCCATGGCCTTGACCAAGGAG- 3′; maP2 F, 5′-TCGAT GAAATCACCGCAGAC- 3′; maP2 R, 5′-TGTGGTCGACTTTCCATCCC-3′; 18S F, ′5 - AGTCCCTGCCCTTTGTACACA; 18S R, 5′-CGATCCGAGGGCCTCACTA-3′.

***In vitro* kinase assay**

BL21 cells (Stratagene) were transformed with GST-Foxo1 or GST expression plasmids and GST or GST-Foxo1 fusion protein were purified. Briefly, BL21 bacteria were initially grown at 37 C overnight, and the following morning a starter culture was added to 200 ml LB broth containing 100 g/ml ampicillin (Sigma). Bacteria were grown at room temperature, induced with 1 mM isopropyl-β-δ-thio-galactopyranoside (Fisher Scientific, Pittsburgh, PA) for 2 h and

centrifuged at 7700 x *g* for 10 min at 4 C (Sorvall). Bacterial pellets were resuspended in cold PBS and lysed using a sonicator (Misonix) for 2 min with 30-sec intermittent bursts and 10-sec pauses. After sonication, 1% TritonX-100 was added to the solution, and lysates were rocked at room temperature for 30 min, followed by centrifugation at 20,000 x *g* for 20 min at 4 C. The GST fusion proteins were purified on glutathione-sepharose beads 4B (Amersham Pharmacia Biotech, Piscataway, NJ) and quantified on SDS-PAGE gels by Coomassie staining (Bio-Rad Laboratories, Inc., Hercules, CA) by comparison with BSA standards. *In vitro* kinase assays were performed by incubating 0.5 µg GST-Foxo1 protein, or GST alone, for 10 min at 30 C, in kinase buffer (Upstate Biotechnology, Inc., Lake Placid, NY), in the absence or presence of 0.5 µl of purified active S422DSGK1 and a cocktail containing inhibitor and MgAc/ATP (Upstate) and 1 µl of [γ-32P]ATP (PerkinElmer, Wellesley, MA). A thermomixer was used to keep the beads in suspension (Eppendorf). The reaction was stopped on ice, and samples were centrifuged at 800 x rpm for 10 min at 4 C. The proteins were resolved by SDS-12% PAGE, and protein phosphorylation was detected using Biomax MR Film (Eastman Kodak Co., Rochester, NY).

**Western blot analysis**

For protein analysis, cells were washed twice with cold PBS and harvested in lysis buffer containing 50 mM Tris/HCl (pH 7.4), 150 mM NaCl, 1 mM EDTA, 1% Triton X-100, 25 mM sodium pyrophosphate, and a protease inhibitor cocktail (Roche). Whole-cell extracts were obtained by three cycles of freezing and thawing followed by centrifugation at 14,000 rpm for 5 min at 4 C, to remove insoluble material. Protein (30 µg) was separated by SDS-PAGE and transferred to polyvinylidene difluoride membrane (Pierce Chemical Co., Rockford, IL). Blots were blocked for 1 h at room temperature in Tris-buffered saline-Tween 20 with 5% nonfat dry

milk and subsequently incubated with primary antibodies overnight at 4 C. After three washes with Tris-buffered saline-Tween 20, membranes were incubated at room temperature for 1 h with secondary antibodies. Immune complexes were visualized by ECL Plus detection reagent (Pierce) following the manufacturer's instructions.

**Generation of MEF cells**

WT and SGK1-loxP MEF cells were isolated from 13-d-old embryos derived from SGK1-loxP heterozygous pregnant females crossed with SGK1-loxP heterozygous males, using standard methods (24). DNA was obtained from each embryo's head and tail to confirm their genotype. MEF cells were maintained in DMEM, containing 10% FBS supplemented with penicillin and streptomycin, and grown in 5% CO2. The WT and SGK1-loxP genotypes were confirmed by PCR using the following primers: F, 5′-CTCATTCCAGACCGCTGACAA-3′; R, 5′-AAAGCTTATCTCAAACCCAAACCAA-3′.

**Immunofluorescence**

MEF cells ($5 \times 10^5$) were plated in four-chamber slides (Thermo Fisher) and infected with $2 \times 10^7$ PFU of Cre-GFP adenovirus (Vector BioLabs, Burlingame, CA) to obtain recombination at the SGK1 locus. Cells were treated 48 h after infection with 2 μM of dexamethasone or vehicle and 24 h later fixed and permeabilized following the manufacturer's instruction (Invitrogen). Fixed cells were treated for 1 h at room temperature with 3% BSA blocking solution and incubated for 1 h at room temperature with anti-mFoxo1 antibody at dilution of 1:200 in 3% BSA and visualized by red fluorescence with an antirabbit IgG secondary antibody Alexa Fluor.

To visualize nuclei, slides were mounted with ProLong Gold Antifade reagent containing 4′,6-diamidino-2-phenylindole (Invitrogen). To assess the overall number of cells with cytoplasmic or nuclear localization of Foxo1, each field was divided by a grid into 12 sections, and the number of cells with nuclear or cytoplasmic Foxo1 in each section was determined.

### Statistical analysis

All experiments were repeated at least three times. Results are presented as means ±SEM. Student's *t* test and ANOVA performed with Prism version 5.0 (GraphPad Software, Inc., San Diego, CA) were used as needed. $p < 0.05$ was considered statistically significant.

## Results

### SGK1 is induced during adipocyte differentiation

In the last few years it has been shown that SGK1 plays an important role in metabolism, specifically in the kidney (Pearce D 2003). Given the function of SGK1 as a downstream effector of glucocorticoid signaling (Lang F et al 2006), we assessed the potential function of this kinase in adipose tissue. To determine whether SGK1 is expressed in murine adipose tissues and to quantify its levels in this tissue relative to other organs, we analyzed the SGK1 mRNA levels by real-time PCR, in metabolic tissues. As shown in figure 16, the highest level of SGK1 expression was identified in the kidney. Interestingly, SGK1 RNA levels were detected also in adipose tissue, with white fat tissue expressing more than brown fat. To investigate whether SGK1 mRNA is regulated during adipogenesis *in vitro*, we analyzed SGK1 gene expression during different stages of differentiation in 3T3-L1 or 10T1/2 cells. The results shown in figure 16

indicate that SGK1 was induced during adipocyte differentiation in both cell lines. The levels of PPARγ, C/EBPα, and aP2 were measured to assess the extent of differentiation achieved in those cells (supplemental Fig. 1A published as supplemental data on The Endocrine Society's Journals Online web site at http:// mend.endojournals.org). Interestingly, SGK1 mRNA levels were increased within a few hours from the induction of preadipocytes with the standard differentiation cocktail containing dexamethasone, insulin, and isobutylmethylxanthine (MDI). Conversely, cells induced to differentiate in the presence of insulin and PPARγ ligands showed an increase of the expression of SGK1 only at late stages. To determine which component of the differentiation mixture was responsible for the early induction of mRNA SGK1, we analyzed SGK1 levels in preadipocytes treated only with one of the three inducers. As shown in figure 16C, SGK1mRNA levels were induced 3-fold by dexamethasone within 3 h of treatment. Insulin and 3-isobutyl-1-methylxanthine appeared to be able to increase SGK1 mRNA levels, but this induction occurred only after 6 h, in the case of insulin. Both dexamethasone and insulin increased the levels of total and phospho-SGK1 protein. Because it is known that PPARγ can induce SGK1 expression in human kidney cells (Hong G 2003), we assessed whether PPARγ plays a role also in dexamethasone-mediated induction of SGK1. We therefore measured the induction of SGK1 in PPAR-/- cells treated with MDI. Because dexamethasone has been shown to induce C/EBPδ during adipogenesis, we determined whether SGK1 could play a role in this process. As shown in supplemental figure 17, C/EBPδ was reduced when SGK1 is knocked down in differentiated 10T1/2, suggesting that SGK1 could play a potential role in mediating C/EBPδ induction during differentiation.

**SGK1 affects adipogenesis *in vitro***

To investigate the potential role of SGK1 in adipogenesis, we ectopically expressed or silenced SGK1 in preadipocytes and measured the effects of the modulation of SGK1 on differentiation, both at the phenotypical and molecular level. Constitutively active SGK1 ($^{S422D}$SGK1) ectopically expressed in 10T1/2 cells (Figure 17A) led to an increase in the number of lipid-storing cells, as shown by Oil RedO staining (Figure 17B). The mRNAlevels of markers of adipogenesis such as PPARγ, C/EBPα, and aP2 were significantly induced in $^{S422D}$SGK1-expressing cells, indicating that this kinase plays a positive role in differentiation (Figure 17C). In contrast, decreasing endogenous SGK1 levels by RNA interference (Figure 17D) led to diminished differentiation, as measured phenotypically by Oil Red O staining (Figure 17E). SGK1 knockdown in preadipocytes cells induced to differentiate with either MDI or rosiglitazone led to a significant decrease in mRNA levels for markers of adipogenesis (Figure 17). These data suggest that modulation of SGK1 levels can affect adipogenesis.

**SGK1 phosphorylates Foxo1 *in vitro* and *in vivo***

It has been shown that Foxo1 acts as a negative regulator of adipogenesis (Nakae J 2003, Kim J 2009). To determine the mechanisms through which SGK1 affects adipocyte differentiation, we tested whether SGK1 could phosphorylate Foxo1. The *in vitro* protein kinase assay (Figure 18A) shows that full-length glutathione-*S*-transferase (GST)-Foxo1 was directly phosphorylated by SGK1, whereas a GST control protein was not. To determine whether SGK1 phosphorylation of Foxo1 occurs *in vivo*, we cotransfected Foxo1 and SGK1 in U2OS cells and assessed the phosphorylation state of exogenously expressed Foxo1, using antibodies recognizing Foxo1 only when phosphorylated specifically at threonine 24 (T24), or serine 256 (S256) or serine 316

(S319) residues. As shown in figure 18B, in unstimulated conditions, Foxo1 showed a basal level of phosphorylation at all three sites (Figure 18B, lane 3). However, when constitutively activated $^{S422D}$SGK1 was cotransfected with Foxo1, phosphorylation was increased *in vivo* at these specific threonine and serine residues (Figure 18B lane 4). A triple alanine mutant of Foxo1 (Foxo1AAA) at T24, S256, and S316 sites could not be phosphorylated when coexpressed with the constitutively active form of $^{S422D}$SGK1 (Figure 18B, lane 6). Conversely, inactive SGK1 ($^{K127N}$SGK1) did not affect the phosphorylation levels of Foxo1 at any of these sites (Figure 18B, lane 8), further supporting the notion that SGK1 can directly phosphorylate these residues in Foxo1. To assess whether SGK1 is able to phosphorylate endogenous Foxo1 in 10T1/2 cells, the constitutively active or the inactive forms of SGK1 ($^{S422D}$SGK1 and $^{K127N}$SGK1) were transfected in this preadipocytic cell line, and the levels of phosphorylation of endogenous mouse Foxo1 were detected. As shown in Fig. 18C, Foxo1 phosphorylation at T24 and S253 (which corresponds to the human Foxo1 S256 residue) sites were increased, whereas the total level of Foxo1 remained unchanged. The level of phosphorylation at serine in position 319 could not be assesse due to the inability of the human Foxo1 phos-pho-specific antibody to cross-react with the mouse residue. To determine whether SGK1 is phosphorylated during adipogenesis and whether Foxo1 phosphorylation state is dependant on SGK1, we analyzed the levels of phosphorylation of both SGK1 and Foxo1 in 3T3-L1cells. As shown in figure 18D, both the levels of SGK1 and Foxo1 phosphorylation are increased during 3T3-L1differentiation. Taken all together, these data indicated that SGK1 is able to phosphorylate Foxo1 both *in vitro* and in cells.

**SGK1 affects Foxo1 subcellular localization**

To determine whether SGK1 can affect the subcellular localization of Foxo1 and cause the inhibition of its activity by leading to its nuclear exclusion, we expressed green fluorescent protein (GFP)-Foxo1 in the presence or in the absence of constitutively active $^{S422D}$SGK1 and monitored GFP localization in U2OS and in 10T1/2 cells. As shown in figure 19A, GFP-Foxo1 appeared to be predominantly localized in the cell nucleus in the absence of exogenous SGK1. In contrast, GFP-Foxo1 was excluded from the nucleus when the constitutive active $^{S422D}$SGK1 was ectopically coexpressed. To better quantify these effects, we assessed the overall number of cells with nuclear or cytoplasmic expression of GFP-Foxo1 in the presence or absence of ectopically expressed $^{S422D}$SGK1. To confirm the requirements of the Foxo1 phosphorylation sites for SGK1 action, we measured whether the cellular localization of the mutant Foxo1AAA, which cannot be phosphorylated, would be affected by SGK1. As shown in Fig. 19B, in the absence of SGK1, more than 60% of cells retained GFP-Foxo1 in the nucleus. Conversely, in the presence of SGK1, Foxo1 was localized in the nucleus in only 28% of the cells. Interestingly, GFP-Foxo1AAA appeared to be predominantly nuclear, independently of the presence or absence of SGK1. These data suggest that SGK1 limits the function of Foxo1 by secluding it to the cytoplasm. To determine whether dexamethasone affects Foxo1 localization and if this process is mediated by SGK1, we monitored GFP-Foxo1 subcellular localization in wild-type (WT) and SGK1 -/- mouse embryonic fibroblast (MEF) cells, in the presence or absence of dexamethasone. As shown in Fig. 4, C and D, in the presence of vehicle, Foxo1 was primarily localized in the nucleus in both WT MEF and SGK1 -/- cells. Conversely, in WT MEF cells treated with dexamethasone, the proportion of Foxo1 in the nucleus decreased whereas the

percentage of cells with cytosolic Foxo1 staining increased. No changes in Foxo1 subcellular distribution occurred in SGK1 -/- MEF treated with dexamethasone.

**SGK1 rescues the inhibitory effects of Foxo1 on differentiation**

Foxo1 gain- and loss-of-function studies performed in 3T3-F442A and 3T3-L1 cells have shown that this forkhead factor acts as a negative regulator of adipogenesis (Nakae J 2003, Kim J 2009). To assess whether Foxo1 affects adipocyte differentiation also in the mesenchymal cell system in which we observed SGK1 proadipogenic function, we ectopically expressed or knocked down Foxo1 in 10T1/2 cells. Expression of exogenous Foxo1 (or Foxo1AAA) inhibited adipogenesis, whereas its knockdown via siRNA caused increased differentiation, as shown by Oil Red O staining (Figure 20A and B) and by the changes in the levels of expression of markers of adipogenesis (Figure 20C and D). We next checked whether SGK1 affects differentiation in 10T1/2 cells through Foxo1 by determining whether expression of activated $^{S422D}$SGK1 could overcome Foxo1 inhibition of adipogenesis. As shown in Fig. 20 E, active $^{S422D}$SGK1, but not the kinase-dead $^{K127N}$SGK1, rescued the differentiation defects present in adipocytes ectopically expressing Foxo1, as demonstrated by the increase in PPARγ, C/EBPα, and aP2 mRNA levels in cells expressing $^{S422D}$SGK1 compared with the levels in control cells. This rescue effect of SGK1 does not occur when Foxo1AAA is expressed, further confirming that SGK1 effects on adipogenesis rely on its ability to phosphorylate Foxo1. Furthermore, Foxo1 had a greater inhibitory effect on adipogenesis in the absence of SGK1, as shown by the decreased mRNA levels of PPARγ, C/EBPα, and aP2 in cells expressing Foxo1 and small interfering SGK1 (si-SGK1) in comparison to cells expressing Foxo1 and small interfering control (si-control) (Figure

20 F). In contrast, Foxo1AAA affected differentiation independently of SGK1 expression. These results confirm that SGK1's positive action on adipogenesis is mediated through the inactivation of Foxo1 via its phosphorylation.

## Discussion

Adipogenesis has been amenable to detailed mechanistic studies because many of the features of fat cells can be reproduced *in vitro* and induced by a cocktail of hormones. In cells of mouse or human origin, *in vitro* differentiation is significantly enhanced by glucocorticoids. These molecules play a crucial role in the early phases of differentiation and are required for induction of preadipocytes to adipocytes (Pantoja C 2008, Bujalska 2008a, Bujalska I 2008b). *In vivo* effects of corticosteroids are well known as seen in patients with Cushing's syndrome or in those in whom glucocorticoids areused for medical therapy: they all exhibit significant weight gain as a result of increased adipogenesis and lipid storage. These tissue-specific effects have been elegantly studied in transgenic mice expressing the enzyme involved in cortisol production, 11β-hydroxyl steroid dehydrogenase type 1. Mice overexpressing 11β-hydroxyl steroid dehydrogenase type 1 in adipose tissue develop visceral obesity, presumably as a result of the direct action of cortisol on adipose tissue (Masuzaki H 2001, Masuzaki H 2003). Despite evidence for the direct role of corticosteroids in fat formation, their specific mechanism of action in this regard remains ill defined. In this paper, we investigated the potential role of SGK1 in the regulation of adipogenesis and its function as a possible mediator of glucocorticoids' effects on this tissue.

Our results demonstrate that dexamethasone treatment of preadipocytes rapidly induces SGK1 expression in the early inductive stages of adipogenesis. Early expression of SGK1 in differentiation appears to be critical because forced down-regulation of this kinase in preadipocytes, by siRNA knockdown studies, leads to inhibition of differentiation. Forced expression of SGK1 results in increased adipogenesis, phenocopying the effects of glucocorticoids both with regard to cell morphology and gene expression. Overall these results predict a role for SGK1 in adipocytes *in vivo*. In fact, in humans, SGK1 polymorphisms, which confer increased SGK1 activity, are associated with obesity in a Caucasian cohort (Dieter M 2004). Total ablation of SGK1 in mice does not reveal an immediately obvious adipose defect. Although this would imply that SGK1 is not absolutely necessary in normal development of adipose tissue, our results suggest that it is important to explore the possibility that SGK1 may yet contribute to an abnormal phenotype under certain metabolic conditions known to induce or require SGK1. This logic is supported by similar observations and approaches taken to demonstrate the importance of SGK1 in salt homeostasis in SGK1 -/- mice. These animals manifest deficiencies in salt metabolism only when exposed to a low salt diet, a known physiological stimulus that induces SGK1 mRNA levels (Wulff P 2002).

Our results show that Foxo1 is a direct target of SGK1 in adipocytes and provide a potential mechanistic explanation for the proadipogenic effects exerted by SGK1. SGK1 phosphorylates Foxo1 at threonine 24, serine 256, and serine 319 residues, leading to subcellular redistribution of Foxo1 from the nucleus to the cytosol. Interestingly, Akt phosphorylates Foxo1 at the same target sites, also leading to its nuclear exclusion (Kops G 1999). This suggests that different extracellular stimuli may converge on Foxo1 to achieve diverse effects through common mechanisms. Foxo1 has been clearly demonstrated to negatively influence adipocyte

differentiation (Nakae J 2003, Kim J 2009). Our observation, that dexamethasone-induced subcellular relocalization of Foxo1 is SGK1 dependent, argues strongly in favor of this pathway in mediating the proadipogenic properties of glucocorticoids. In this regard, SGK1 may serve as a critical nexus between glucocorticoids and Foxo1. We postulate that in pathological states characterized by high amounts of circulating glucocorticoids, SGK1 levels in adipose tissue may be increased leading to promotion of fat differentiation. This could be tested by assessing whether the obesity phenotype so characteristic of subjects with Cushing's syndrome is due to higher SGK1 expression in fat tissue. If so, it is possible that the use of SGK1-specific inhibitors may be potentially very useful therapeutic agents in the treatment of this type of obesity.

**Figure 16. SGK1 is expressed in fat tissue and induced during adipogenesis**. A) SGK1 mRNA levels in tissues obtained from C57BL/6J 8-wk-old male mice. Relative mRNA levels were determined by real-time PCR and normalized using 18S.(B) mRNA levels of SGK1 were evaluated during differentiation (0–6 d) after MDI induction or after treatment with rosiglitazone and insulin (3T3-L1 cells) or after MDI or troglitazone and insulin treatment (10T1/2 cells) (*p<0.05; **, p<0.01; ***, p<0.001; ns, nonsignificant). (C) SGK1 mRNA levels in 3T3-L1 after stimulation with a specific inducer (*, p<0.05; **, p<0.01, ***, p<0.001; ns, nonsignificant). BAT, Brown adipose tissue; IBMX, isobutylmethylxanthine;WAT, white adipose tissue.

**A.**

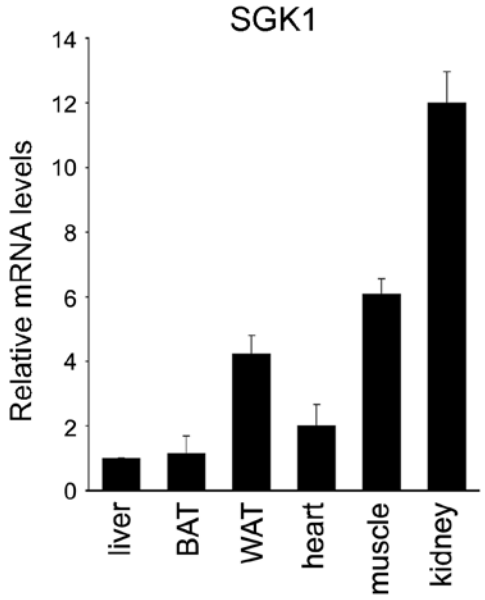

**Figure 16 (continued)**

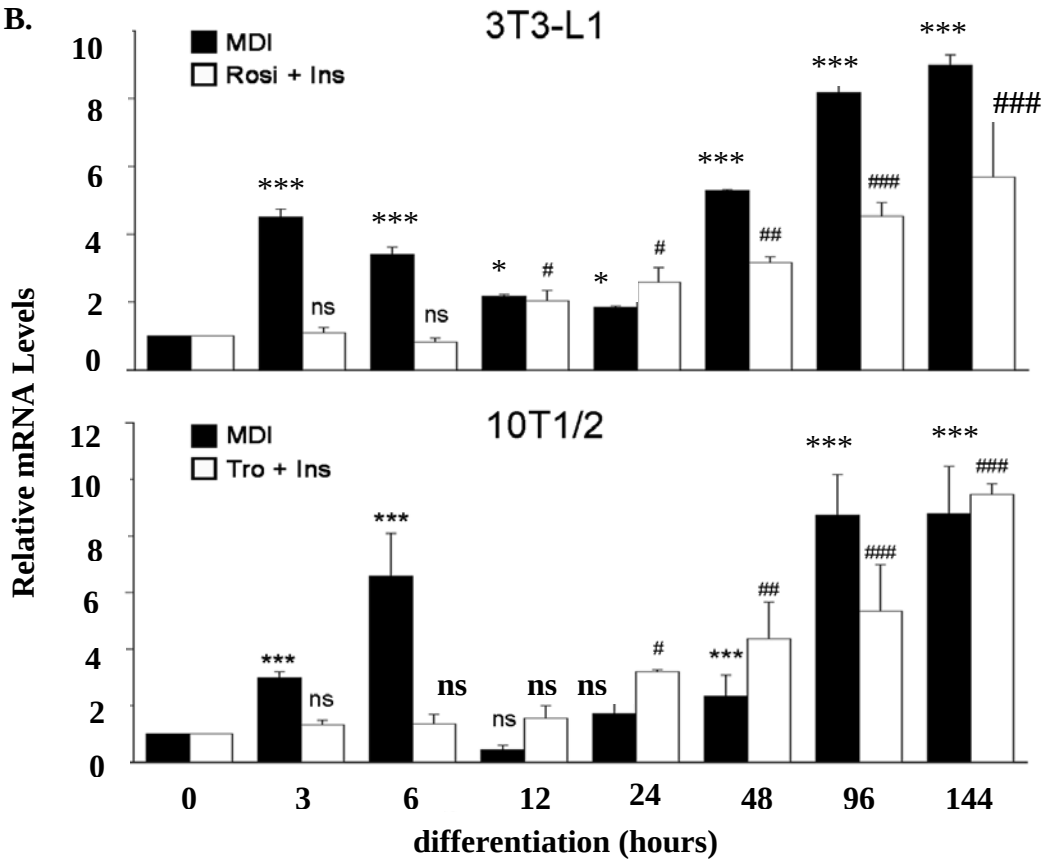

**Figure 16 (continued)**

**C.**

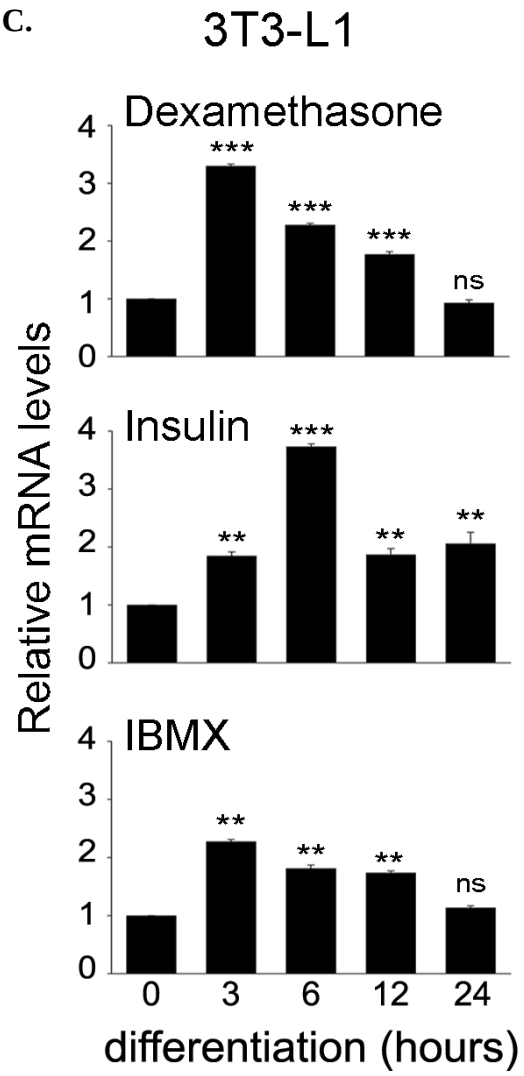

**Figure 17. SGK1 modulates adipogenesis**.(A) SGK1 mRNA levels were measured by RT-PCR in constitutively active SGK1 (S422DSGK1)-expressing cells and compared with control vector cells (***, *P* < 0.001). (B) Oil Red O staining of 10T1/2 ectopically expressing S422DSGK1 after 6 d of differentiation showed increased lipid accumulation. (C) Ectopic expression of S422DSGK1 in 10T1/2 enhanced PPARγ, CEBPα, and aP2 mRNA levels in comparison to vector during MDI-induced differentiation. (***, p <0.001). (D) Analysis of SGK1 mRNA levels in 10T1/2 cells expressing either control siRNA or si-SGK1 (***, p< 0.001). E, Oil Red O staining of 10T1/2 cells expressing si-SGK1 showed decreased lipid accumulation compared with si-ctl expressing cells at d 6 of differentiation. F, PPARγ, CEBPα, and aP2 mRNA levels were reduced in SGK1 knockdown 10T1/2 cells compared with control-expressing cells induced to differentiate with MDI (***, p <0.001). si-ctl, Small interfering control.

**A**

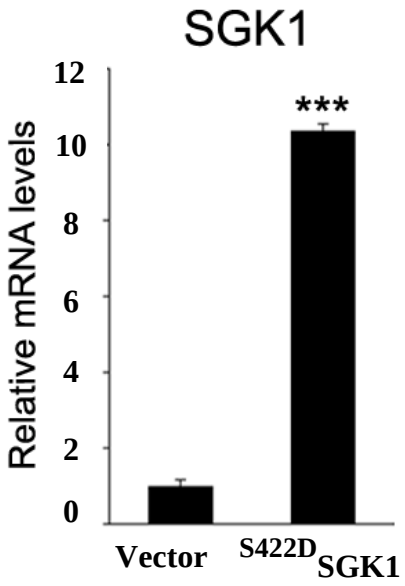


**B.**

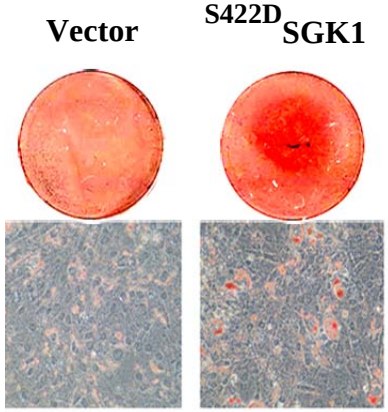

**Figure 17 (continued)**

**C.**

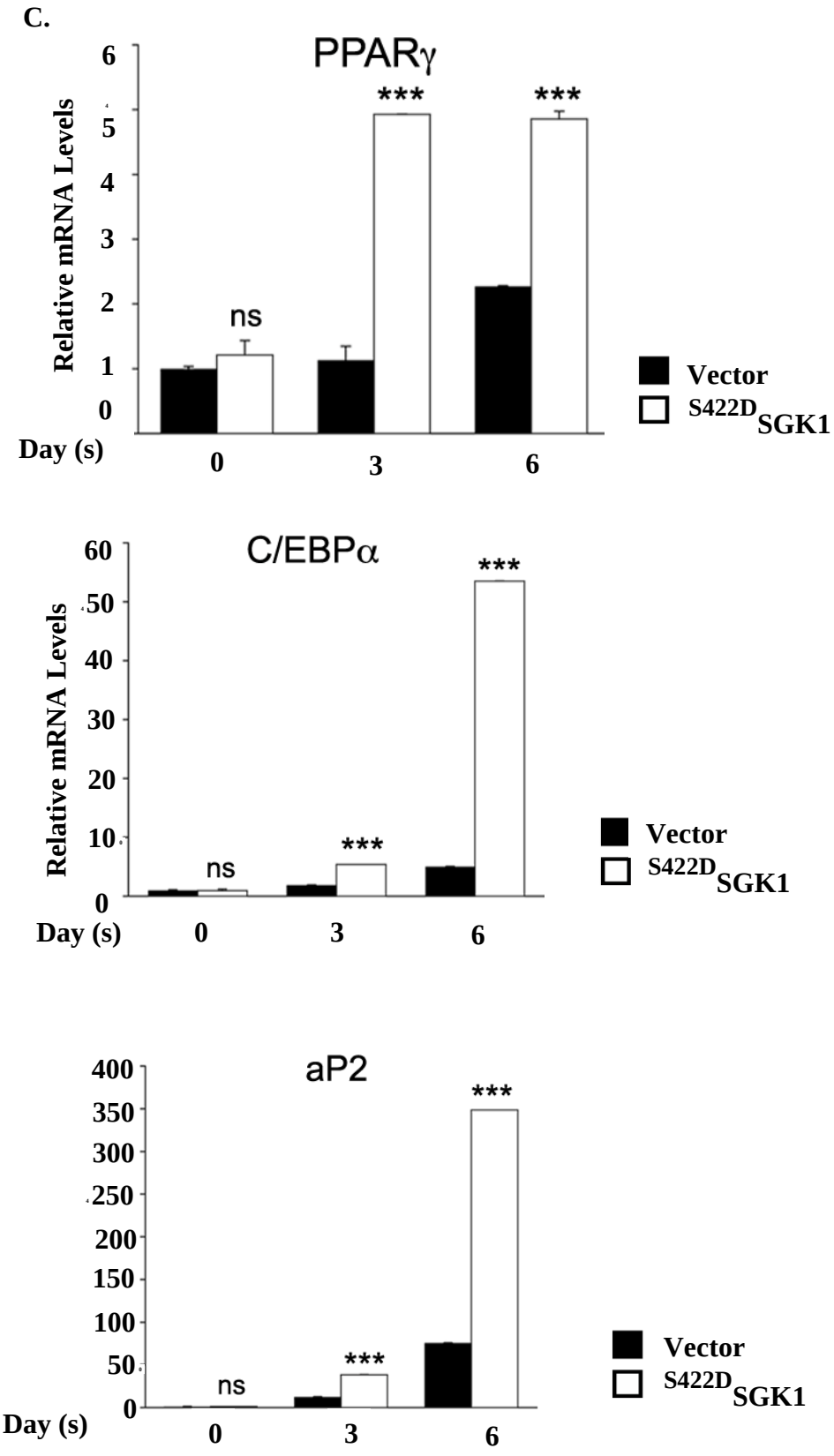

**Figure 17 (continued)**

**D.**

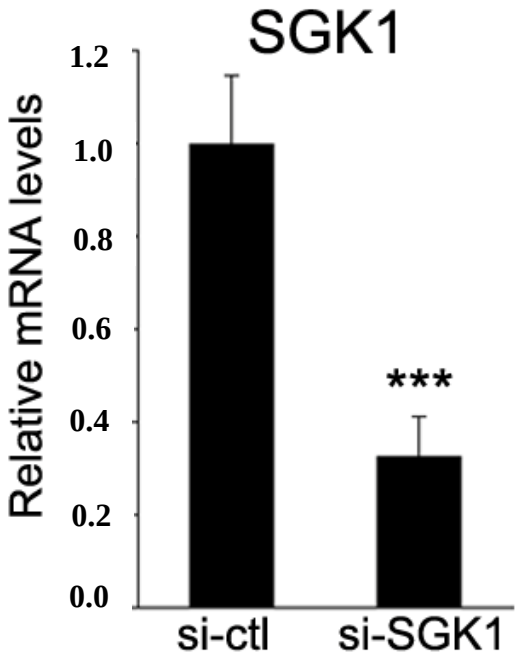


**E.**

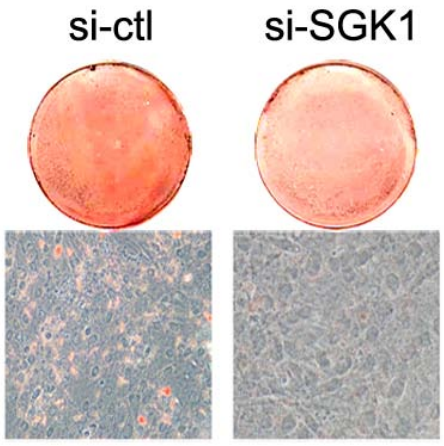

**Figure 17 (continued)**

**F.**

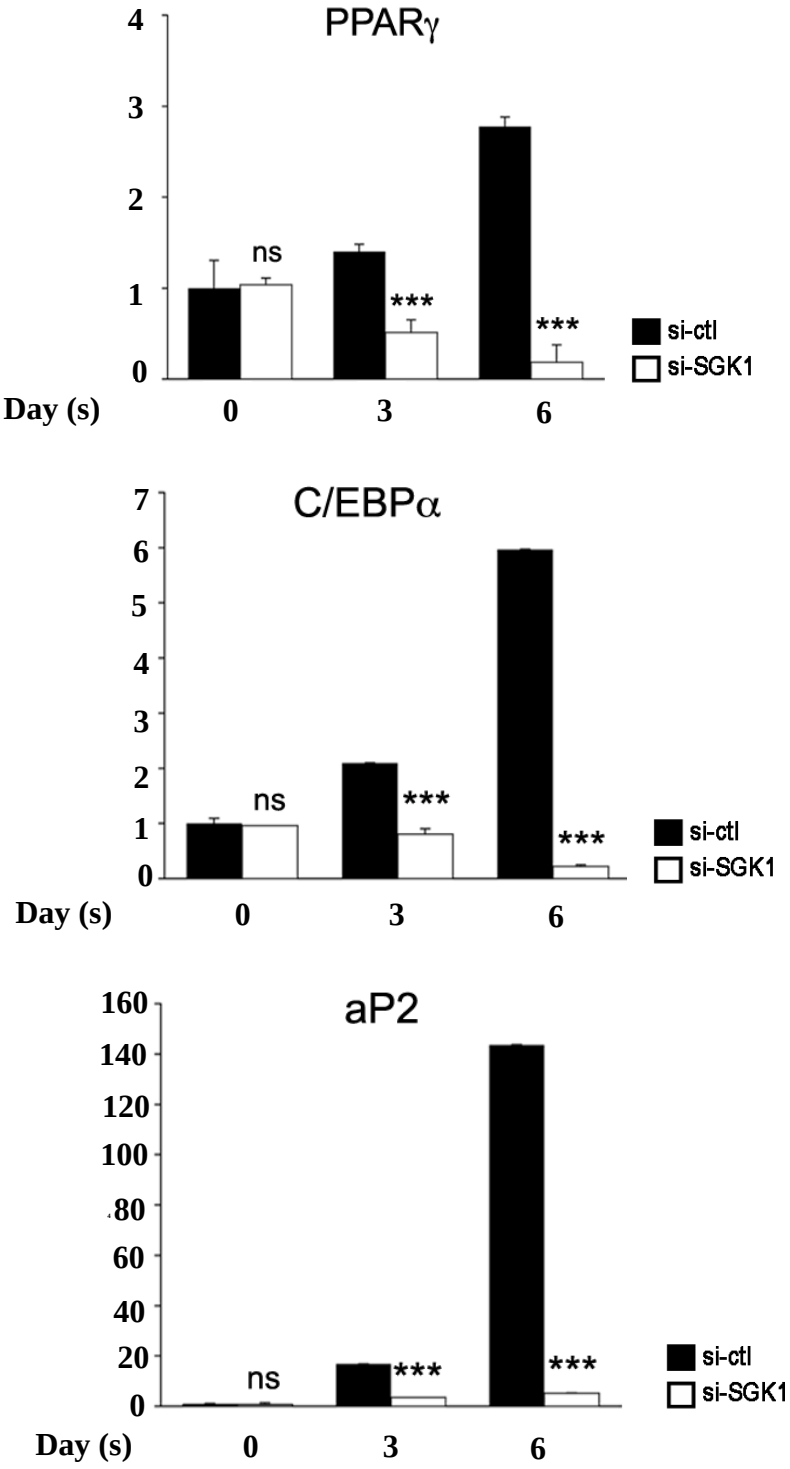

**Figure 18. SGK1 phosphorylates Foxo1**. (A) *In vitro* kinase assays performed in the presence of [$\gamma^{32}$P]ATP and purified GST-Foxo1 or GST proteins. (B) Western blot analysis of U2OS cells cotransfected with GFP-Foxo1 WT, GFP-Foxo1AAA, or control vector, in the presence or absence of either constitutively active SGK1 (S422DSGK1) or SGK1 kinase-dead (K127NSGK1). Phospho-specific antibodies recognizing phosphorylated Foxo1 protein at residues T-24, S-256, and S-319 were used to visualize phosphorylation. GFP and β-actin antibodies were used as controls. (C) Phosphorylation levels of endogenous Foxo1 in 10T1/2 cells expressing constitutively active S422DSGK1 or kinase-dead K127NSGK1 or vector, using phospho-specific antibodies. (D) Total and phosphoryated levels of endogenous SGK1 (P-SGK1) and Foxo1 (P-Foxo1) proteins during a time course of 3T3-L1 differentiation.

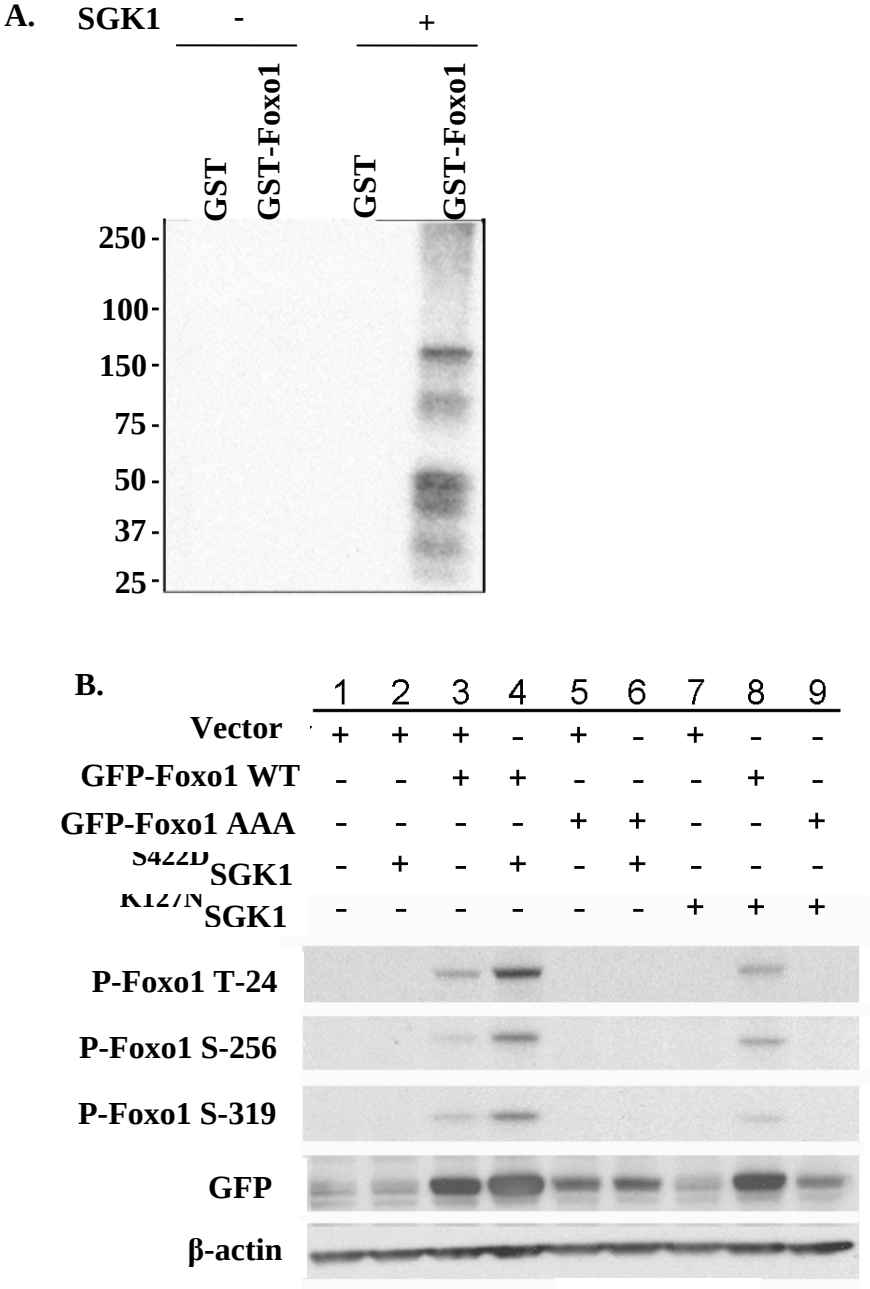

**Figure 18 (continued)**

**C.**

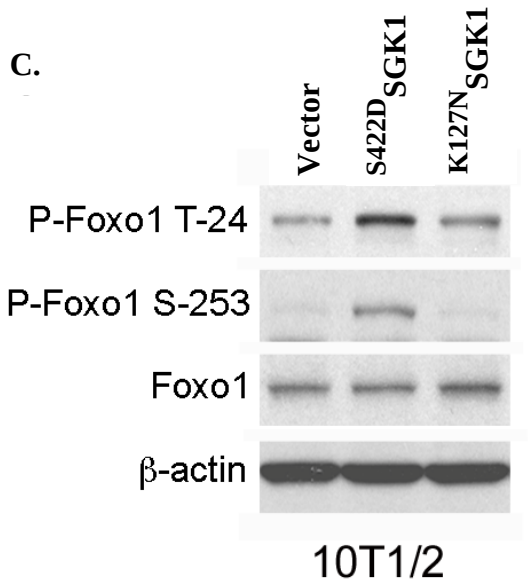


**D.**

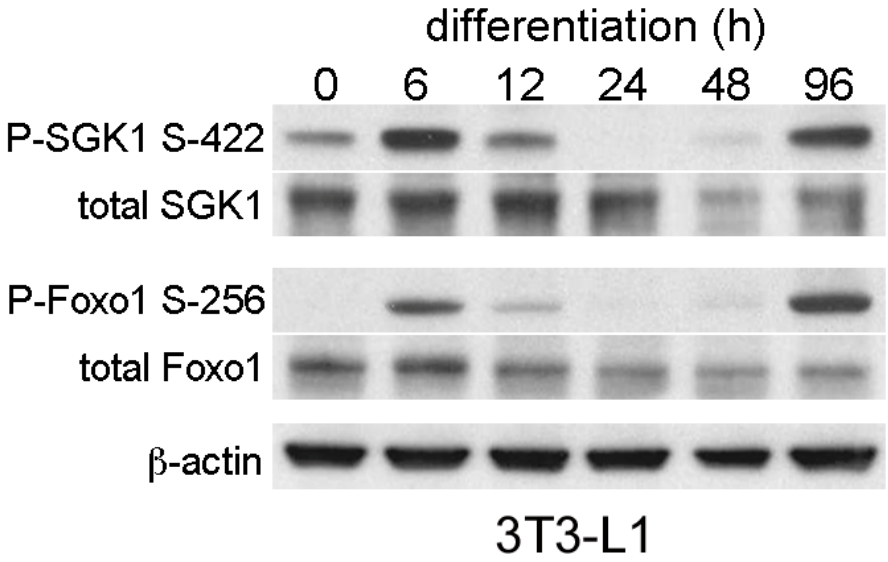

**Figure. 19. Foxo1 subcellular localization is SGK1 dependent.** Panel A, U2OS and 10T1/2 cells were transfected with GFP-Foxo1 in combination with constitutively active S422DSGK1 or vector and nuclear /cytoplasmic localization monitored by fluorescence. Panel B, GFP-Foxo1 WT or GFPFoxo1AAA (T24A, S256A, S319A) were cotransfected in U2OS cells with constitutively active S422DSGK1 or vector. Quantification of the number of cells expressing GFP-Foxo1 WT or GFP-Foxo1AAA in the nucleus or in the cytoplasm were expressed as percentage relative to the total number of cells counted per subcellular compartment (***, $p < 0.001$; ns, not significant; N, nuclear localization; (C) cytoplasmic localization). Panel C, Quantification of the number of cells showing endogenous Foxo1 localized either in the nucleus or in the cytoplasm, in WT or in SGK1-/- MEF cells in the presence of dexamethasone or vehicle alone. The values are expressed as percentage of number of cells with nuclear or cytoplasmic Foxo1 *vs.* total number of cells counted per field (***, $p<0.001$; ns, not significant; N, nuclear localization; C, cytoplasmic localization; Dex, dexamethasone). Panel D, Subcellular localization of endogenous Foxo1 in WT or SGK1-/-MEF cells. Endogenous Foxo1 is visualized in *red* and nuclei with 4′,6-diamidino-2-phenylindole staining.

**A.**

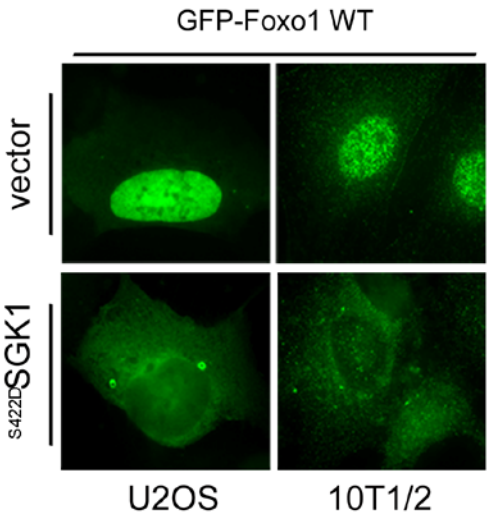

**Figure 19 (continued)**

**B.**

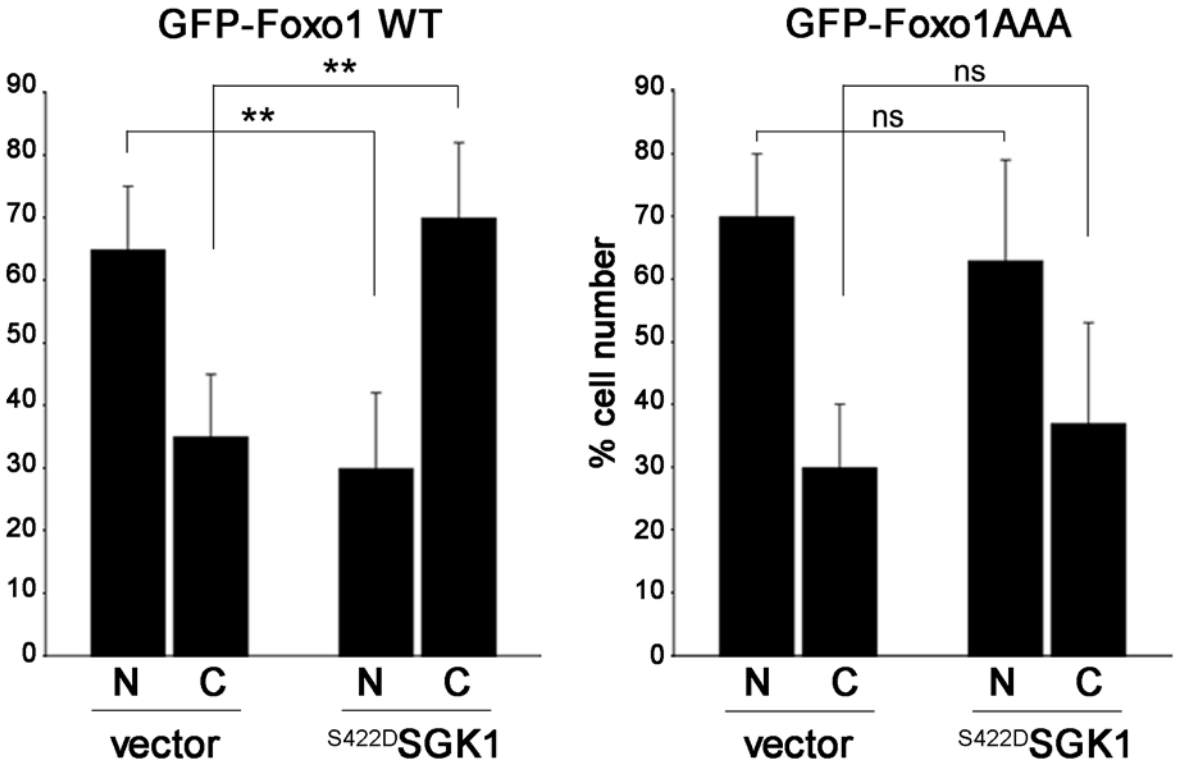

**Figure 19 (continued)**

**C.**

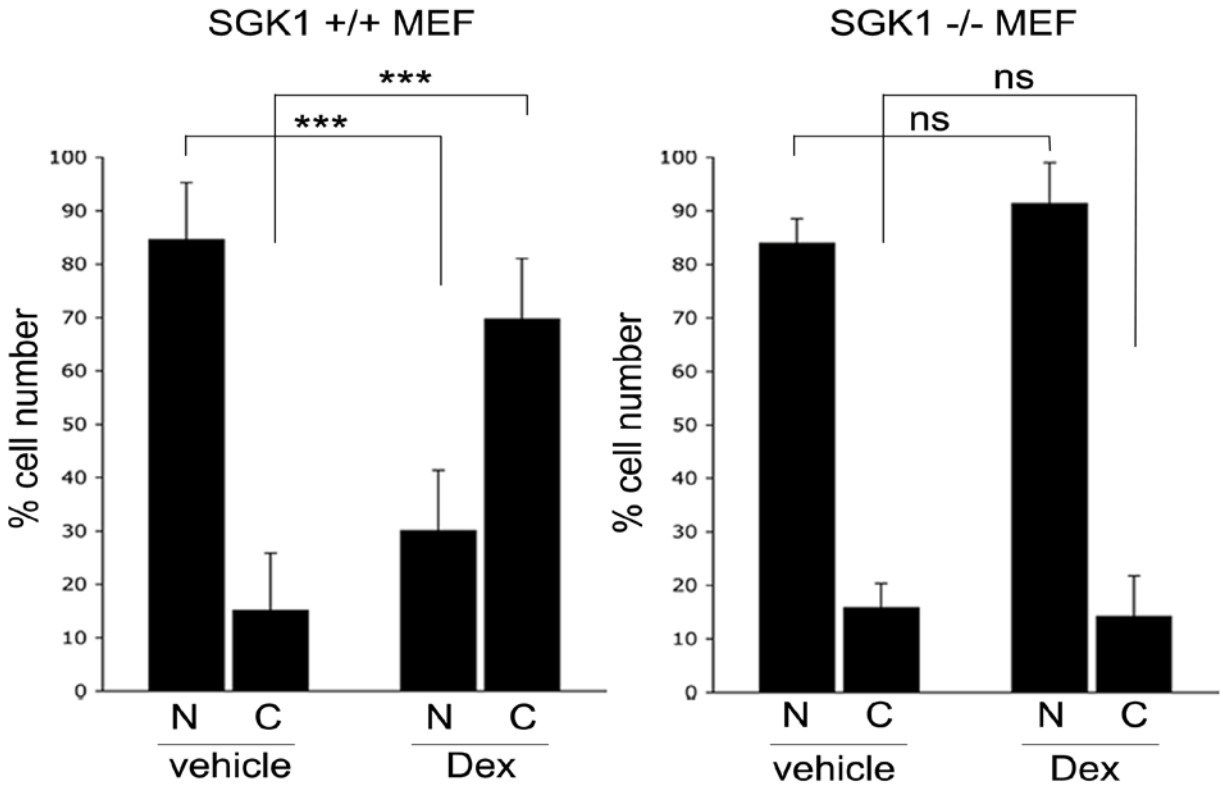

**Figure 19 (continued)**

**D.**

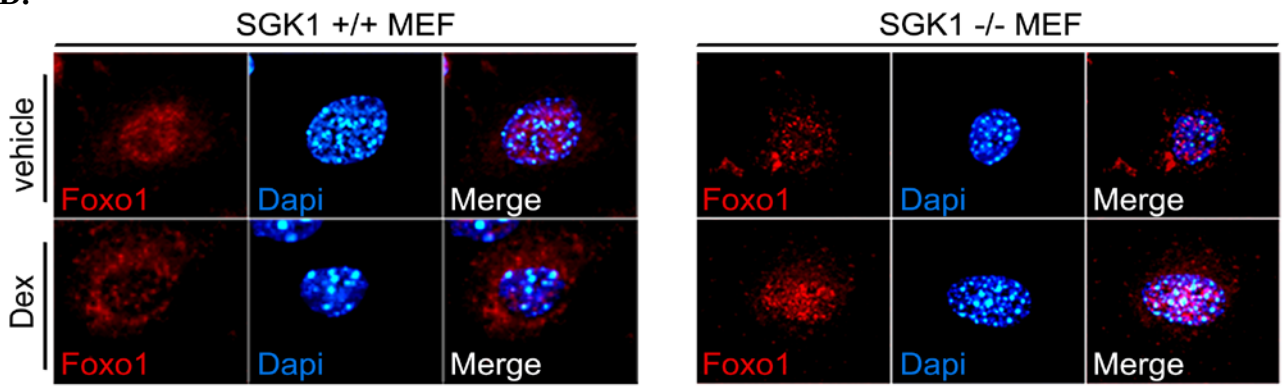

**Fig. 20. SGK1 rescues Foxo1 inhibitory effect on adipogenesis.** Oil red O staining of 10T1/2 cells expressing (A) vector, Foxo1 WT or Foxo1AAA or (B) si-control versus si-Foxo1. (C) PPARγ, C/EBPα and aP2 levels in 10T1/2 cells expressing Foxo1 WT, Foxo1AAA or control vector, at 3 days of differentiation. (***p<0.001). (D) aP2 mRNA levels in 10T1/2 cells expressing si-Foxo1 or si-control. (E) PPARγ, C/EBPα and aP2 mRNA levels in 10T1/2 expressing Foxo1 WT or Foxo1AAA andconstitutively active S422DSGK1 or inactive K127NSGK1 (***p<0.001; ns: nonsignificant). (F) PPARγ, C/EBPα and aP2 mRNA levels determined after 3 days of differentiation in 10T1/2 cells expressing sicontrol or si-SGK1 in the presence of vector, GFP-Foxo1 WT or GFP-Foxo1AAA. (***p<0.001; ns: nonsignificant).

**A.**

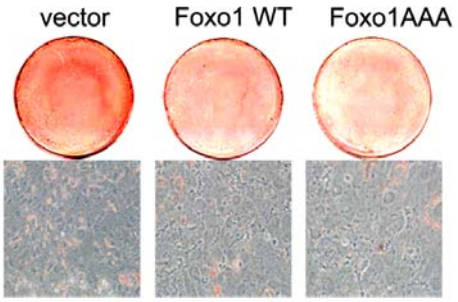


**B.**

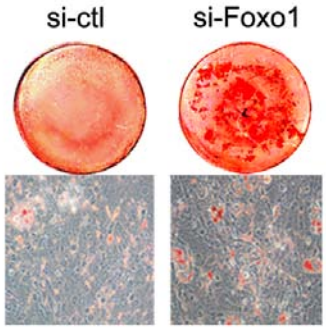


C.

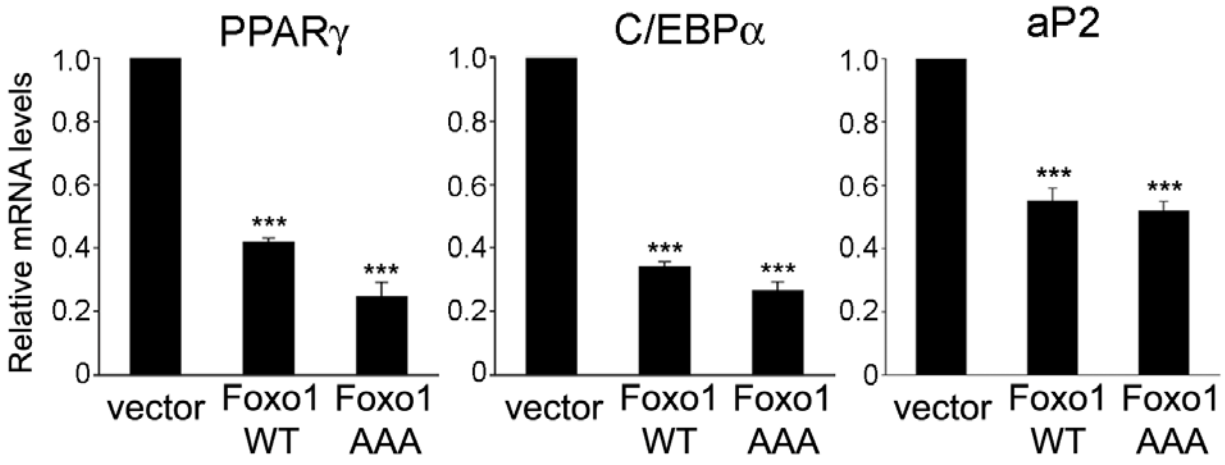

**Figure 20 (continued)**

**D.**

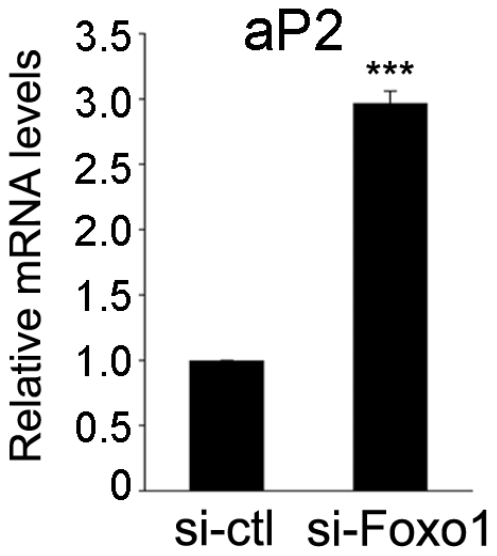

**Figure 20 (continued)**

**E.**

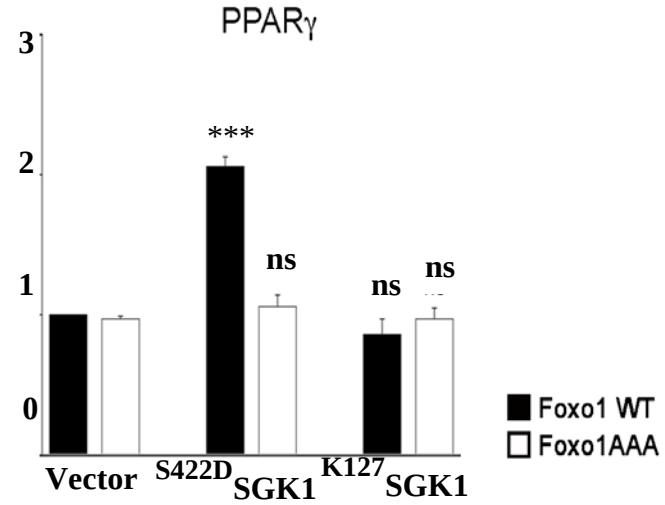


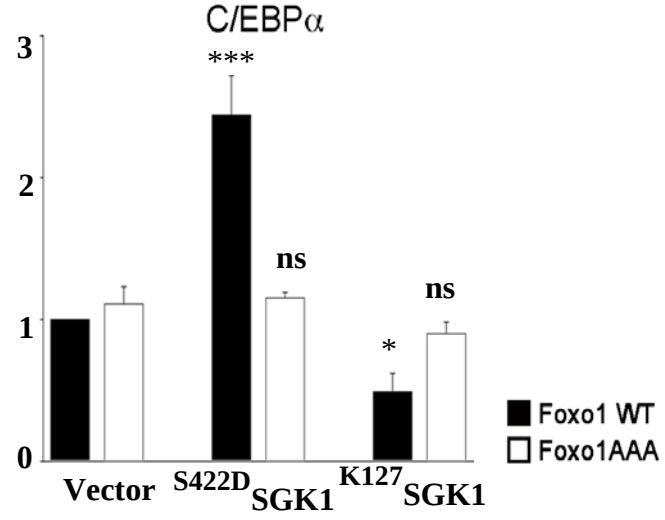


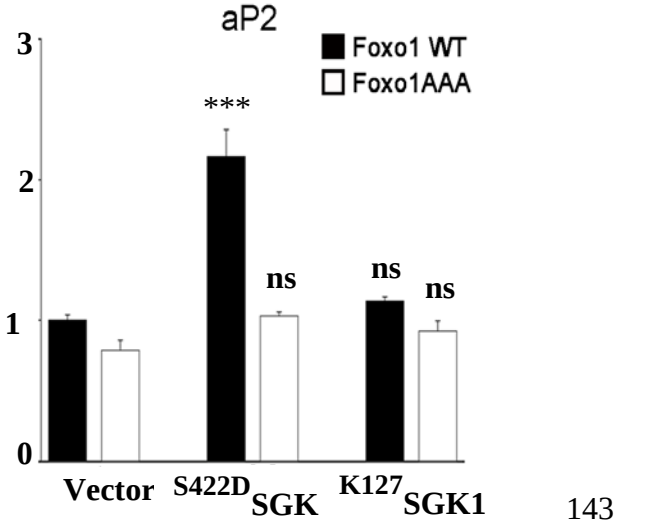

**Figure 20 (continued)**

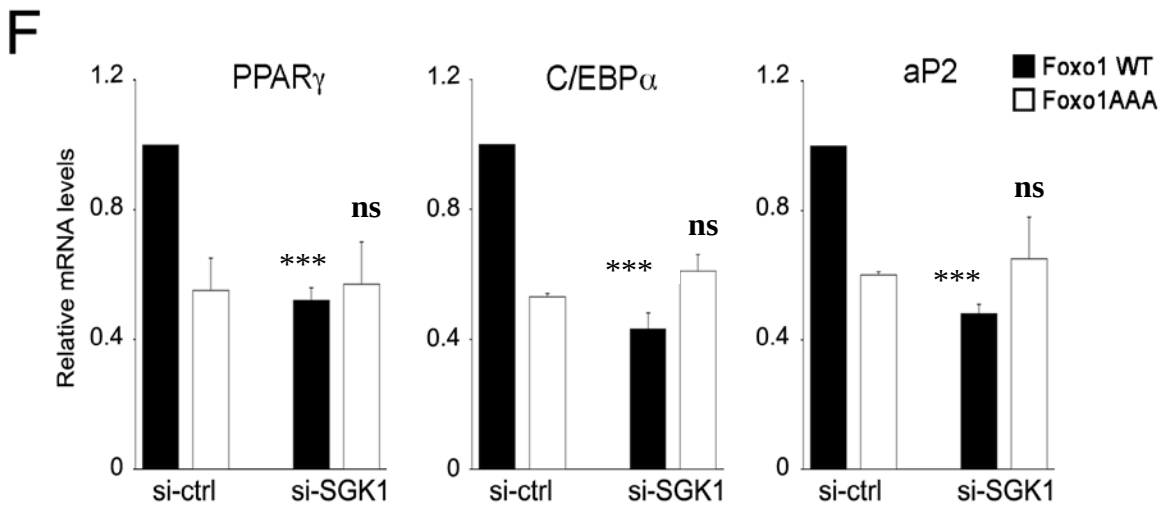

References

## REFERENCES


Ahima R. "Adipose Tissue as an Enodcrine Organ." Obesity (2006): 242S-249S.

Akerbald P, Lind U, Liber D et al. "Early B-cell Factor (O/E-1) is a Promoter of Adipogenesis and Involved in Control of Genes Important for Terminal Adipocyte Differentiation." Molecular and Cellular Biology (2002): 8015-8025.

Alihaud G, Grimaldi P, Negrel R,. "Cellular and Molecular Aspects of Adipose Tissue Development." Annu. Rev. Nutr. (1992): 207-233.

Amelio A, Miraglia L, Conkright J, Mercer B et al. "A Coactivator Trap Identifies NONO (p54nrb) as a Component of the cAMP-signaling Pathway." PNAS (2007): 20314-20319.

Anderson J. "Identification of a Human Decapping Complex Associated with hUpf Proteins in Nonsense-Mediated Decay." Molecular and Cellular Biology (2002): 8114-8121.

Armoni M, Harel C, Karni S, Chen H, Bar-Yoseph F, Ver M, Quon M, Karnieli E. "FOXO1 Represses Peroxisome Proliferator-Activated Receptor-gamma1 and gamma 2 Gene Promoters in Primary Adipocytes. A Novel Paradigm to Increase Insulin Sensitivity." J Biol chem (2006): 19881-19891.

Bai R, Koester C, Ouyang T, Hahn S et al. "SMIF, a Smad4-interacting protein that functions as a co-activator in TGFB signalling." Nature Cell Biology (2003): 181-190.

Banerjee S, Feinberg M, Watanabe M, Gray S, Haspel R et al. "The Krüppel-like Factor KLF2 Inhibits Peroxisome Proliferator-activated Receptor-γ Expression and Adipogenesis." The Journal of Biochemical Chemistry (2003): 2581-2584.

Barak Y, Nelson M, Ong E, et. al. "PPARγ is Required for Placental, Cardiac, and Adipose Tissue Development." Molecular Cell (1999): 585-595.

Barbatelli G, Murano I, Madsen. "The Emergence of Cold-induced Brown Adipocytes in Mouse White Fat Depots is Determined Predominantly by White to Brown Adipocyte Transdifferentiation." American Journal of Physiology-Endocrinology and Metabolism (2010): E1244-E1253.

Barbera M, Schluter A, Pedraza N. "Peroxisome Proliferator-activated Receptor α Activates Transcription of the Brown Fat Uncoupling Protein-1 Gene." The Journal of Biologial Chemistry (2001): 1486-1493.

Bell C, Walley A. "The Genetics of Obesity." Nat Rev Genetics (2005): 221-234.

Bertagna X, Guignat L, Groussin L. "Cushing's Disease." Best Practice & Research Clinical Endocrinology & Metabolism (2009): 607-623.

Bieker J. "Kruppel-Like Factors: Three Fingers in Many Pies." The Journal of Biological Chemistry (2001): 34355-34358.

Bioni K, Hennige A, Huang D et al. "Serum-and Glucocorticoid-Inducible Kinase 1 Mediates Salt Sensitivity of Glucose Tolerace." Diabetes (2006): 2059-2066.

Birsoy K, Chen Z, Friedman J. "Transcriptional Regulation of Adipogenesis by KLF4." Cell Metabolism 7 (2008): 339-347.

Boyle K, Hadaschik D, Virtue S, Cawthorn W et al. "The Transcription Factor Egr1 and Egr2 Have Opposing Influences on Adipocyte Differentiation." Cell Death and Differentiation (2009): 782-789.

Brayer K, Kulshreshtha S, Segal D,. "The Protein-Binding Potential of CH2H Zinc Finger Domains ." Cell Biochem Biophys (2008): 9-19.

Bujalska, I, hewitt K, Hauton D, Lavery G, Tomlinson J et al. "Lack of Hexose-6-Phospate Dehydrogenase Impairs Lipid Mobilization from Mosue Adipose Tissue ." Endocrinology (2008): 2584-2591.

Burton J, Goldenburg D, Blumenthal D. "Potential of Peroxisome Proliferator-Activated Receptor Gamma Antagonist Compounds as Therapeutic Agents for a Wide Range of Cancer Types." PPAR Res (2008): 1-7.

Calle E, Rodriguez C et al. "Overweight, Obesity, and Mortality from Cancer in a Prospectively Studied Cohort of U.S Adults." N Engl J Med (2003): 1625-1638.

Cannon B, Nedergaard J. "Brown Adipose Tissue: Function and Physiological Significance." Physiol Rev (2004): 277-359.

Carlson P, Mahlapu M. "Forhead Transcriptional FActors: key Players in Development and Metabolism." Dev Biol (2002): 1-23.

Carnevalli L, Masuda K, Frigerio F, Bacquer O et al. "S6K1 Plays a Critical Role in Early Adipocyte Differentiation." Developmental Cell (2010): 763-774.

Chen M, Chen H, Nguyen A, Gupta D et al. "G2α Deficiency in Adipose Tissue Leads to a lean Phenotype with Divergent Effects on Cold Tolerance and Diet-Induced Thermogenesis." Cell Metabolism (2010): 320-330.

Chen Z, Torrens J, Anand A, Spiegelman B. "Krox 20 Stimulates Adipogenesis via C/EBPB-dependent and independent Mechanisms." Cell Metabolism (2005): 93-106.

Cheng L, Zhang J, Reed R. "The Transcription Factor Zfp423/OAZ is Required for Cerebellar Development and CNS Midline Patterning." Developmental Biology (2007): 43-52.

Choi W, Jeon B, Yun C, Kim P, et al. "Proto-oncogene FBI-1 Represses Transcription of p21CIP1 by Inhibition of Transcription Activation by p53 & Sp1." Journal of Biological Chemistry (2009): 12633-12644.

Choy L, Derynck R. "Transforming Growth Factor-Beta Inhibits Adipocyte Differentiation by Smad3 Interacting with CCAAT/Enhancer-binding Protein (C/EBP) and Repressing C/EBP Transactivation Function." The Journal of Biological Chemistry (2003): 9609-9619.

Choy L, Skillinton J, Derynck R. "Roles of Autocrine TGF-B Receptor and Smad Signaling in Adipocyte Differentiation." The Journal of Cell Biology (2000): 667-681.

Cinti S. "Transdifferentiation Properties of Adipocytes in the Adipose Organ." Am J Physiol Endocrinol Metab (2009): E977-E986.

Collins S, Kuhn CM, Petro AE, Swick AG, Chrunyk BA. "Role of Leptin in Fat Regulation." Nature (1996): 677.

Coumoul X, Shukla V, Li Cuiling, Wang R, Deng C. "Conditional Knockdown of Fgfr2 in Mice Using Cre-LoxP Induced RNA Interference." Nucleic Acids Research (2005): 1-8.

Dai H, Hogan C, Gopalakrishnan B, et. al. "The Zinc Finger Protein Schnurri Acts as a Smad Partner in Mediating the Transcriptional Response to Decapentaplegic." Developmental Biology (2000): 373-387.

Das S, Raj L, Zhao B, et. al. "Hzf Determines Cell Survival upon Genotoxic Stress by Modulating p53 Transactivation." Cell (2007): 624-637.

Davis K, Moldes M, Farmer S. "The Forkhead Transcription Factor FoxC2 Inhibits White Adipocyte Differentiation ." J Biol Chem (2004): 42453-42461.

Dieter M, Palmada M, Rajamanickam J. "Regulation of Glucose Transporter SGLT1 by Ubiquitin Ligase Nedd4-2 and Kinases SGK1, SGK3, and PKB." Obesity Research (2004): 862-870.

Dixon J. "The Effect of Obesity on Health Outcomes." Molecular and Cellular Endocrinology (2010): 104-108.

Dowll P, Otto T, Adi S, Lane. "Convergenence of Peroxisome Proliferator-Actiavated Receptor gamma and fOXO1 Signaling Pathways." J Biol chem (2003): 45485-45491.

Eriksson J, Simith U, Waagstein F, Wysocki M, Jansson P. "Glucose Turnover and Adipose Tissue Lipolyssis are Insulin-Resistant in Healthy Relatives of Type 2 Diabets Patients: Is Cellular Insulin Resistance a Secondary Phenomenon?" Diabetes (1999): 47-54.

Farmer S. "Molecular Determinants of Brown Adipocyte Formation and Function." Genes & Development (2008): 1269-1275.

Farmer S. "Transcriptional Control of Adipocyte Formation ." Cell Metabolism (2006): 263-273.

Fejes-Toth G, Frindt G, Naray-Fejes-Toth A, Palmer L. "Epithelial Na+ Channel Activation and Processing in Mice Lacking SGK1." Am J Physiol Renal Physiol (2008): F1298-F1305.

Filhol O, Benitez M, Cochet C,. "A Zinc Ribbon Motif Is Essential for the Formation of Functional Tetrameric Protein Kinase CK2." Madame Curie Bioscience Database. (2010).

Fraser J, Schreiber R, Strem B, Zhu M. "Plasticity of Human Adipose Stem Cells Toward Enodthelial Cells and Cardiomyocytes." Nat. Clin Pract. Cardiovasc. Med 3 (2006): S33-S37.

French S, Story M. "Environmental Influences on Eating and Physical Activity ." Annu Rev Public Health (2001): 309-335.

Freytag S, Paielli D, Gilbert J. "Ectopic Expression of the CCAT/enhancer-binding Protein alpha Promotes the Adipogneic Program in a Varieity of Mouse Fibroblastic Cells." Genes Dev (1994): 1654-1663.

Galic S, Oakshill J, Steinberg G,. "Adipose Tissue as an Endocrine Organ ." Molecular and Cellular Endocrinology (2010): 129-139.

Geer S, Wei E. "Gender Differences in Insulin Resistance, Body Composition, and Energy Balance." Gender Medicine (2009): 60-75.

Geisler JG, Zawalich K, Lakey JR, Stukenbrok H. "Estrogen Can Prevent or Reverse Obesity and Diabetes in Mice Expressing Human Islet Amyloid Polypeptide." Diabetes (2002): 2158-2169.

Gelman L, Zhou G, Fajas L, et. al. "p300 Interacts with the N- and C- Terminal Part of PPARγ 2 in a Ligand-Independent and -Dependent Manner, Respectivley." The Journal of Biological Chemistry (1999): 7681-7688.

Gesta S, Yu-Hua T, Kahn C. "Developmental Origin of Fat: Tracking Obesity to its Source." Cell (2007): 242-256.

Goodman R, Smolik S. "CBP/p300 in Cell Growth, Transformation, and Development ." Genes & Development (2000): 1553-1577.

Gounarides J, Korunch-Andre M, Killary, K. "Effect of Dexamethasone on Glucose Tolerance and Fat Metabolism in a Diet-Induced Obesity Mouse Model." Endocrinology (2008): 758-766.

Gray S, Feinberg M, Hall S, Kuo C et al. "The Kruppel-like Factor KLF15 Regulates the Insulin Sensitive Glucose Transporter GLUT4." The Journal of Biological Chemistry (2002): 3422-34328.

Gregoire F, Smas C, Sul H. "Understanding Adipocyte Differentiation." Physiol Rev (1998): 783-809.
Gronenborn A. "The DNA-Binding Domain of GATA Transcription Factors - A Prototypical Type IV Cys2 -Cys2 Zinc Finger." Iuchi S, Kudell N Zinc Finger Proteins: From Atomic Contact to Cellular Function. Landes Bioscience/Eurekah.com and Kluwer Academic/Plenium Publishers, 2005.

Gupta R, Arany Z, Seale P, mepani P et al. "Transcriptional Control of Preadipocyte Determination by Zfp 423." Nature (2010): 619-625.

Hagman J, Belanger C, Travis A, et. al. "Cloning and Functional Characterization of Early B-cell Factor, a Regulator of Lymphocyte-Specific Gene Expression." Genes & Development (1993): 760-773.

Haigis M, Sinclair D. "Mammalian Sirtuins: Biological Insights and Disease Relevance." Annu Rev Pathol (2010): 253-295.

He W, Barak Y, Hevener A, Olson P. "Adipose-specific Peroxisome Proliferator-Activated REceptor Gamma Knockout Causes Insulin Resistance in Fat and Liver but not in Muscle." Proc. Natl. Acad. Sci (2003): 15712-15717.

Hong G, Lockhart a, Davis B, Rahmoune H, Baker S, Ye L et al. "PPAR gamma Acitvation Enhances Cell Surface EnaC alpha via Up-regulation of SGK1 in Human Collecting Duct Cells." FASEB (2003): 1966-1968.

Huang D, Boini K, Osswald H, Friedrich B et al. "Resistance of Mice lacking the Serum-and Glucocorticoid-inducible Kinase SGK1 Against Salt-Sensitive Hypertenstion Induced by a High-Fat Diet." Am J Physiol Renal Physiol (2006): F1264-F1273.

Jin Q, Zhang F, Yan T et al. "C/EBP alpha Regulates SIRT1 Expression During Adipogenesis." Cell Res (2010 ): 470-479.

Jin W, Takagi T, Kanesashi S, Kurahashi T et al. "Schnurri-2 Controls BMP-Dependent Adipogenesis via Interaction with Smad Proteins." Developmental Cell (2006): 461-471.

Jing E, Gesta S, Kahn R. "SIRT2 Regulates Adipoctye Differentiation Involving FoxO1 Acetylation/Deacetylation." Cell Metabolism (2007): 105-114.

Jones K, Greer E, Pearce, Ashrafi K. "Rictor/TORC2 Regulates Caenorhabditis elegans Fat Storage, Body Size, and Development Through sgk-1." PLoS Biology (2009): 0604-0614.

Kaczynski J, Cook T, Urrutia R,. "Sp 1 - and Krupel-Like Transcription Factors." Genome Biology (2003): 1-8.

Kahn B, Flier J. "Obesity and Insuliin Resistance." J Clin Invest (2000): 473-481.

Kajimura S, Seale P, Tomaru T. "Regulation of the Brown and White Fat Gene Program Through a PRDM16/CtBP Transcriptional Complex." Genes and Dev (2008): 1397-1409.

Kanazawa A, Kawamura Y, Sekine A, Iida A. "Single Nucleotide Polymorphisms in the Gene Encoding Kruppel-like Factor 7 are Associated with type 2 Diabetes." Diabetologia (2005): 1315-1322.

Kawagish H, Takeshi W, Hatsume U et al. "HZF Regulates Adipogenesis Through Translational Control of C/EBP alpha." EMBO (2008): 1481-1490.

Kawamura Y, Tanaka Y, Kawamor R, Maeda S. "Overexpression of Kruppel-like Factor 7 Regulates Adipocytokine Gene Expression in Human Adipocytes and Inhibits Glucose-Induced Insulin Secretion in Pancreatic B-Cell Line." Molecular Endocrinology (2006): 844-856.

Kim J, Huntley J, chang J, Arden K, Olefsky J. "FoxO1 Haploinsufficiency Protects Against High-fat diet-induced Inslin Restance with enhanced Peroxisome Proliferator-Activated Receptor gamma Activation in Adipose Tissue." Diabetes (2009): 1275-1282.

Kim S, Ha J, Yun S, Kim E et al. "Transcriptional Activation of Peroxisome Proliferator-activated receptor-gamma Requires Activation of Both Protein Kinase A and Akt During Adipocyte Differentiation." Biochemical and Biophysical Research Communications (2010): 55-59.

Kimura Y, Hart A, Masanori H, et. al. "Zinc Finger Protein, Hzf, Is Required for Megakaryocyte Development and Hemostasis. ." J. Exp. Med. (2002): 941-952.

Klaus S, Casteilla L, Bouillaud F, Ricquier D. "The Uncoupling Protein UCP: A Membranous Mitochondrial Ion Carrier Exclusively Expressed in the Brown Adipose Tissue." Int. J. Biochem (1991): 791-801.

Klug A, Schwabe J,. "Zinc Fingers." Serial Review (1995): 597-604.

Kops G, Burgering B. "Forhead Transcription Factors: New Insights into Protein Kinase b (c-akt) Signaling." J Mol Med (1999): 656-665.

Lang F, Bohmer C, Palmada M, Seebohm G, Strutz-Seebohm N, Vallon V. "(Patho)physiological significance of teh Serum-and Glucocorticoid-Inducible Kinase Isoforms." Physiol Rev (2006): 1151-1178.

Lang F, Görlach A, and Vallon V. "Targeting SGK1 in diabetes." Expert Opin Ther Targets (2009): 1303-1311.

Laudes M, Bilkovski R, Uberhauser F et al. "Transcription Factor FBI-1 Acts as a Dual Regulator in Adipogenesis by Coordinated Regulation of cyclin A and E2F-4." Journal of Molec Med (2008): 597-608.

Laudes M, Christodolides C, Sewter C et al. "Adipogenesis, Role of the POZ Zinc Finger Transcription Factor FBI-1 in Human and Murine Adipogenesis." The Journal of Biochemistry (2004): 11711-11718.

Li D, Yea S, chen Z, Goutham M. "Kruppel-like Factor 6 Promotes Preadipocyte Differentiation Through Histone Deacetylase 3-Dependent Repression of DKL1." The Journal of Biological Chemistry (2005): 26941-26952.

Lin J, Wu P, Lindenburg K. "Defects in Adaptive Energy Metabolism with CNS-linked Hyperactivity in PGC-1alpha Null Mice." Cell (2004): 121-135.

Lutterbach B, Westendorf J, Linggi B, et. al. "ETO, a Target of t(8;21) in Acute Leukemia, Interacts with the N-CoR and mSin3 Corepressors." Molecular and Cellular Biology (1998): 7176-7184.

Mao J, Yang T, Gu Z, Heird WC, Finegold MJ. "aP2-Cre-Mediated Inactivation of Acetyl-CoA Carboxylase 1 Causes Growth Retardation and Reduced Lipid Accumulation in Adipose Tissues." PNAS (2009): 17576-17581.

Masuzaki H, Paterson J, Shinyama H, Morton N, Mullins J et al. "A Transgenic Model of Visceral Obesity and the Metabolic Syndrome." Science (2001): 2166-2170.

Matsushima Y, Ohshima M, Sonoda M and Kitagawa Y. "A Family of Novel DNA-Binding Nuclear Proteins Having Polypyrimidine Tract-Binding Motif and Arginie/Serine-Rich Motif." Biochemical and Biophysical Research (1996): 427-433.

Matthews J, Bhati M, Lehtomaki E, et. al. "It Takes Two to Tango: The Structure and Function of LIM, RING, PHD, and MYND Domains." Current Pharmaceutical Design (2009): 3681-3696.

Moitra J, Mason M, Olive M, et. al. "Life Without White Fat: a Transgenic Mouse." Genes & Development (1998): 3168-3181.

Mori T, Sakaue H, Iguchi H, Okada G et al. "Role of Kruppel-like Factor 15 (KLF15) in Transcriptional Regulation of Adipogensis." Journal of Biological Chemistry (2005): 12867-12875.

Morrison D, Pendergrast P, Starropoulos P et al. "FBI-1, a factor that binds to the HIV-1 Inducer of Short Transcripts (IST), is a POZ Domain Protein ." Nucleic Acids Research (1999): 1251-1262.

Mueller E, Drori S, Aiyer A, et. al. "Genetic Analysis of Adipogenises through Peroxisome Proliferator-Activated Receptor y Isoforms." The Journal of Biological Chemistry (2002): 41925-41930.

Must A, Spadano J. "The Disease Burden Associated with Overweight and Obesity." JAMA (1999): 1523-1529.

Musuzaki H, Flier J. "Tissue-specific Glucocorticoid Reactivating enzyme, 11B-hydroxysteroid Dehydrogenase type 1 (11B-HSD1)-A Promising Drug Taret for the Treatment of Metabolic Syndrome." Curr Drug Targets Immune Endocr Metab Disord (2003): 255-262.

Nakai J, Kitamura T, Ktamura Y, Biggs 3rd W, Arden K, Accili D. "The Forhead Transcription Factro Foxo1 Regulates Adipocyte Differntiation." Dev Cell (2003): 119-129.

Naray-Fejes-Toth A, Fejes-Toth G. "The SGK, an Aldosterone-induced Gene in Mineralcorticoid Target Cells, Regulates the Epithelial soidum channel." Kidney Int (2000): 1290-1294.

Nieto M. "The Snail Superfamily of Zinc-Finger Transcription Factors." Nature Reviews (2002): 155-166.

Oishi Y, Manabe I, Tobe K, Tsushima K et al. "Kruppel-like transcription factor KLF5 is a Key Regulator of Adipocyte Differentiation." Cell Metabolism (2005): 27-39.

Pantoja C, Huff J, Yamamoto K. "Glucocorticoid Signaling Defines a NOvel Commitment State Druing Adipogenesis in vitro." Mol Biol Cell (2008): 4032-4041.

Pearce D. "SGK1 Regulation of Epithelial Sodium Transport." Cell Physiol Biochem (2003): 13-20.

Pei H, Yao Y, Yang Y et al. "Kruppel-like Factor KLF9 Regulates PPAR gamma." Cell Death and Differentiation (2010): 1-13.

Penny D, Emerson c. "10T1/2 cells: an in vitro Model for Molecular Genetic Analysis of Mesodermal Determination and Differentiation." Eviron Health Perspect (1989): 221-227.

Perez-Mancera P, Bermejo-Rodriguez C, Gonzalez-Herrero I, Herranz M et al. "Adipose Tissue Mass is Modulated by SLUG (SNAI2)." Human Molecular Genetics (2007): 2971-2986.

Perrotti N, He RA, Phillips SA, Haft CR, Taylor SI. "Activation of Serum- and Glucocorticoid-Induced Protein kinase (Sgk) by Cyclic AMP and Insulin." The Journal of Biological Chemistry (2001): 9406-9412.

Picard F, Kurter M, Chung N et al. "Sirt1 Promotes Fat Mobilization in White Adipocyte by Repressing PPARγ." Nature (2004): 771-776.

Pietro N, Panel V, Hayes S, Bagattin A et al. "Serum-and-Glucocorticoid-Inducible Kinase 1 (SGK1) Regulates Adipocyte Differentiation via Forkhead Box O1." (2010).

Planat-Benard V, Silvestre J, Cousin B. "Plasticity of Human Adipose Lineage Cells Toward Endothelial Cells: Physiological and Therapeutic perspectives." Circulation (2004): 656-663.

Remy I, Montmarquette. "PKB/Akt Modulates TGF-β Signalling Through a Direct Interaction with Smad 3." Nature Cell Biology (2004): 358-365.

Reue K, Phan J. "Metabolic Consequences of Lipodystrophy in Mouse Models." Curr Opin Clin Nutr Metab Care (2006): 436-441.

Reznikoff K, Brankow D, Heidelberger C. "Establishment and Characterization of a Cloned Line of C3H Mouse Embryo Cells Sensitive to Postconfluence Inhibition of Division." Cancer Res (1973): 3231-3238.

Rochford J, Laudes S, Laudes M, Boyle K et al. "ETO/MTG is an Inhibitor of C/EBPβ Activity andn a Regulator of Early Adipognenesis." Molecular Cellular Biololgy (2004): 9863-9872.

Rosen E, Hsu C, Wang X, Sakai S, Freeman M, Gonzalez F, Spiegelman B. "C/EBP alpha is required for Differntiation of White, but not Brown, Adipose Tissue ." Proc natl Acad Sci USA (2002): 12532-12437.

Rosen E, MacDougald O. "Adipocyte Differentiation From the Inside Out." Nature Reviews (2006): 885-896.

Rosen E, Sarraf P, Troy A, et. al. "PPARy is Required for the Differentiation of Adipose Tissue In Vivo and In Vitro ." Molecular Cell (1999): 611-617.

Rosen E, Walkey C, Puigserver P, Spiegelman. "Transcriptional Regulation of Adipogenesis." Genes & Development (2000): 1293-1307.

Ross S, Graves R, Spiegelman. "Targeted Expression of a Toxin Gene to Adipose Tissue: Transgenic Mice Resistent to Obesity." Genes & Development (1993): 1318-1324.

Sauer B. "Inducible Gene Targeting in Mice Using the Cre/lox System." Methods: A Companion to Methods in Enzymology (1998): 381-392.

Seale P, Kajimura S, Yang W, Chin S. "Transcriptional Control of Brown Fat Determination by PRDM16." Cell Metab (2007): 38-54.

Skruk T, Alberti-Huber C, Herder C, et. al. "Relationship Between Adipocyte Size and Adipokine Expression and Secretion." The Journal of Clinical Endocrinology & Metabolism (2006): 1023-1033.

Soukas A, Kane E, Carr C, Melo J, Ruvkun G. "Rictor/TORC2 Regulates Fat Metabolism, Feeding, Growth, and Life Span in Caenorhabditis elegans." Genes and Development (2009): 496-510.

Spiegelman B, Flier J. "Obesity and the Regulation of Energy." Cell (2001): 531-543.

Spiegelman B, Lowell B, Antonella A. "Adrenal Glucocorticoids Regulate Adipsin Gene Expression in Mice." The Journal of Biological Chemistry (1989): 1811-1815.

Sue N, Jack B, Eaton S, Perason R et al. "Targeted Disruption of the Basic Kruppel-Like Factor Gene (Klf3) Reveals a Role in Adipogenesis." Molecular and Cellular Biology (2008): 3967-3078.

Takahashi N, Kawada T, Yamamoto T, et. al. "Overexpression and Ribozyme-meditated Targeting of Transcriptional Coactivators CREB-binding Protein and p300 Revealed Their Indespensable Roles in Adipocyte Differentiation through the Regulation of Peroxisome Profilerator-activated Receptor y." The Journal of Biological Chemistry (2002): 16906-16912.

Tan N, Khachigian L,. "Sp 1 Phosphorylation and Its Regulation of Gene Transcription." Molecular and Cellular Biology (2009): 2483-2488.

Tanaka T, Yoshida N, Kishimoto T, Akira S. "Defective Adipocyte Differentiation in Mice Lacking C/EBPβ and/or C/EBPδ Gene." The EMBO Journal (1997): 7432-7443.

Tang Q, Jian M, Lane M. "Repression Effect of Sp1 on the C/EBP alpha Gene Promoter: Role in Adipocyte Differentiation." Molecular and Cellular Bio (1999): 4855-4868.

Tansey J, Sztalyrd C, Grucia-Grey J. "Perilipin Ablation Results in a Lean Mouse with Aberrant Adipocyte Lipolysis, Enhanced Leptin Production, and Resistance to Diet Induced Obesity." PNAS (2001): 6494-6499.

Timmons J, Wennmalm K, Larsson O. "Myogenic Gene Expression Signature Establishes that Brown and White Adipocytes Originate from Distinct Cell Llineages." Proc. Natl. Acad. Sci (2007): 4401-4406.

Tong Q, Dalgin G, Xu H, Tin C, Leiden J, Hotamisligil G. "Function of GATA Transcription Factors in Preadipocyte-Adipocyte Transition." Science (2000): 134-138.

Tontonoz P Hu E, Graves R, Budavari A, Spiegelman BM. "PPARγ 2: Tissue-specific Regulator of an Adipocyte Enhancer." Genes Dev (1994): 1224-1234.

Tontonoz P, Hu E, Spiegelman B. "Simulation of Adipognesis in Fibroblasts by PPARγ, a Lipid Activiated Transcription Factor." Cell (1994): 1147-1156.

Tontonoz P, Spiegelman B. "Fat and Beyond: The Diverse Biology of PPARγ." Annual Reviews of Biochemistry (2008): 289-312.

Tsai R, Reed R. "Cloning and Functional Characterization of Roaz, a Zinc Finger Protein that Interacts with O/E-1 to Regulate Gene Expression: Implications for Olfactory Neuronal Development." The Journal of Neuroscience (1997): 4159-4169.

Tvrdik P, Asadi A, Kozak L. "Cig30, a Mouse Member of a Novel Membrane Protein Gene Family, Is Involved in the Recruitment of Brown Adipose Tissue." Journal of Biological Chemistry (1997): 31738-31746.

Uldry M, Yang W, St-Pierre J. "Complementary Action of the PGC-1 Coactivators in Mitochondrial Biogenesis and Brown Fat Differentiation." Cell Metabolism (2006): 331-341.

Um H, Frigerio F, Watanabe M, Picard F, Joaquin M. "Absence of S6K1 Protects Against Age- and Diet-Induced Obesity While Enhancing Insulin Sensitivity." Nature (2004): 2000-2005.

Um S, Frigerio F, Watanabe, Picard F et al. "Absence of S6K1 Protects Against Age-and Diet Induced Obesity While Enhanceing Insulin Sensitivity." Nature (2004): 200-205.

Vega G. "Obesity and the Metabolic Syndrome." Minerva Endocrinol (2004): 47-54.

Wang F, Tong Q. "SIRT2 Suppresses Adipocyte Differentiation by Deacetylating FoxO1 and Enhancing FoxO1's Repression Interaction with PPAR gamma." Molecular Biology of the Cell (2009): 801-808.

Wang S, Tsai R, Reed R,. "The Characterization of the Olf-1/EBF-Like HLH Transcription Factor Family: Implication in Olfactory Gene Regulation and Nueronal Development." The Journal of Neuroscience (1997): 4149-4158.

Webb P, Doyle C, Anderson N. "Protein Kinase C-ε Promotes Adipogenic Commitment and is Essential for Terminal Differentiation of 3T3-F422A Preadipocytes." Cellular and Molecular Life Sciences (2003): 1504-1512.

Webster, M, Goya L, Ge y, Maiyar A, Firestone G. "Characterization of sgk, a Novel member of the Serine/Threonine Protein Kanase Gene Family Which is Transcriptionally Induced by Glucocorticoids and Serum." Mol Cell biol (2006): 2151-2163.

Weis B, Schmidt J, Lyko F, Linhart HG. "Analysis of Conditional Gene Deletion Using Probe based Real-Time PCR." BMC Biotechnology (2010): 75.

Wolfrum C, Shih D, Kuwajima S, Norris A, Kahn C, Stoffel M. "Role of Foxa-2 in Adipocyte metabolism and Differentatioin ." J Clin Invest (2003): 345-356.

Wu J, Srinivasan V, Neumann J, Lingrel J. "The KLF2 Transcription Factor Does Not Affect the Formation of Preadipocytes but Inhibits Their Differentiaton into Adipocytes." Biochemistry (2005): 11098-11105.

Wulff P, Vallon V, Huang D, Volkl H, Richter K et al. "Impaired Renal Na+ Retention in the SGK1-knockout Mouse." J Clin Invest (2002): 1263-1268.

Yeh W, Cao Z, Classon M, Mcknight SL. "Cascade Regulation of Terminal Adipocyte Differentiation by Three Members of the C/EBP Family of Leucine Zipper Proteins. Genes & Development." Genes and Development (1995): 168-181.

Younce C, Azfer A, Kolattukedy P et al. "MCP-1 (Monocyte Chemotatic Protein-1) Induced Protein, a Recently Identified Zinc Finger Protein, Induces Adipogenesis in 3T3-L1 Pre-adipocytes without Peroxisosme Proliferator-Activated Receptor gamma." The Journal of Biological Chemistry (2009): 27620-27628.

Yu C, Marken K et al. "The Nuclear Receptor Corepressors NCoR and SMRT Decreases Peroxisome Proliferator Acitvated Receptor Gamma 2." Journal of Biological Chemistry (2005): 13600-13605.

Yu S, Reddy J. "Transcription Coactivators for Peroxisome Proliforator-Activated Receptors." Science Direct (2007): 936-951.

Zakrzewska K, Cusin I, Stricker-Krongrad A. "Induction of Obesity and Hyperleptinemia by Central Glucocorticoid Infusion in the Rat." Diabetes (1999): 365-370.

Zhang J, Fu M, Cui T, et. al. "Selective Disruption of PPARγ 2 Impairs the Development of Adipose Tissue and Insulin Sensitivity ." PNAS (2004): 10703-10708.

Zhang Y, Leung D, Nordeen S, and Goleva E. "Estrogen Inhibits Glucocorticoid Action via Protein Phosphatase 5 (PP5)-mediated Glucocorticoid Receptor Dephosphorylation." The Journal of Biological Chemistry (2009): 24342-24552.

Zhou Y, Wang D, Fuqiang L, Shi J, Song J. "Differentiation of Protein Kinase C-βI and δ In the Regulation of Adipocyte Differentiation." The International Journal of Biochemistry & Cell Biology (2006): 2151-2163.

Zhou Z, Toh S, Guo K, Ng C. "Cidea-Deficient Mice Have Lean Phenotype and are Resistant to Obesity." Nature Genetics (2003): 49-56.